Essays in Environmental, Climate, and Public Health Impacts of Freight Transportation

Submitted in partial fulfillment of the requirements for

the degree of

Doctor of Philosophy

in

Engineering and Public Policy

Priyank Lathwal

B.Tech. Electrical Engineering, National Institute of Technology Kurukshetra M.S. Management Science and Engineering, Columbia University M.S. Engineering and Public Policy, Carnegie Mellon University

Carnegie Mellon University Pittsburgh, PA August, 2021 © Priyank Lathwal, 2021 All Rights Reserved

Dedication

To my parents: Thank you for instilling the value of hard work, honesty, and perseverance from early on in my life. Everything I am today is because of your blessings, the foundation you provided, and the sacrifices you made.

To my sister: Thank you for staying by my side all these years and for motivating me when the chips were down. Your love and support made this possible.

To Bruno: who unfortunately passed away in 2017. You brought so much joy to our lives, and I miss you every day.

Committee Members

1. Prof. Parth Vaishnav (Chair)

Assistant Professor, School for Environment and Sustainability, University of Michigan

Adjunct Assistant Professor, Department of Engineering and Public Policy, Carnegie Mellon

University

2. Prof. Granger Morgan (Co-Chair)

Professor, Department of Engineering and Public Policy, Carnegie Mellon University

3. Prof. Constantine Samaras

Associate Professor, Department of Civil and Environmental Engineering, Carnegie Mellon University

4. Prof. Eric Williams

Professor, Department of Sustainability, Golisano Institute for Sustainability, Rochester Institute of Technology

Acknowledgements

First and foremost, I would like to express my deepest and heartfelt gratitude to my PhD advisors, Prof. Parth Vaishnav and Prof. M. Granger Morgan, for their excellent guidance and encouragement during my doctoral studies in the Department of Engineering and Public Policy (EPP) at Carnegie Mellon University (CMU). Both Parth and Granger took me on as a graduate student when I was looking for a new problem to solve and was undergoing a host of other challenges. Despite being an unplanned need to supply support, my advisors arranged graduate funding for my research, and not even once in my doctoral studies did they make me feel stressed about funding. For this, among other reasons, I am eternally indebted to them for their role in providing me the necessary resources to complete my doctoral studies.

I consider it to be my good karma to have Parth as my academic advisor. Besides being an excellent researcher, he has been a role model for me in his ability to be trustworthy and respectful to everyone he engages with on a day-to-day basis. Parth taught me to be bold in exploring new areas and not necessarily be tied to the limitations of one's background. I attribute this constant encouragement as one of the primary reasons I quickly picked up working in a new field and found decarbonization research interesting. He has been generous with his time for troubleshooting when things got stuck on the research front and always motivated me to put my intellectual curiosity to productive use. His patience, guidance, and constructive input have materially improved the quality of this dissertation and have undoubtedly influenced my growth as an independent researcher. Moreover, he continually urged me to stress-test my assumptions and, in the process, allowed me to recognize the inherent limitations of our work. This attitude of trying to do the best possible with available information but bending backward is essential for

scientists today, and I hope to carry this attitude with me in my future endeavors. Thank you, Parth, for everything and for leading by example in so many ways.

Granger has been a legendary figure in my life. I have great respect and admiration for him and have been in awe of his work since I first read his climate policy paper during my master's degree. It was a major contributing factor in my decision to apply to CMU EPP. He provided strategic guidance that was invaluably helpful in shaping the direction of my research and contributed significantly to shaping my path to become a researcher. Besides research, I took numerous invaluable life lessons in the simplest of his actions, even if he didn't intend them all to be that way. One, in particular, comes to mind. In one of the research seminars in my second year, I was lost in connecting the dots between my then research and future career goals. He took note and inquired after the seminar as to what was bothering me. On sharing my dilemma, he recounted the story of his doctoral advisor, Professor Kenneth Bowles, who pursued his varied interests despite being trained in engineering science and retiring moving on to computer science. I found great comfort in this approach and at once felt reassured as it unburdened me from trying to learning everything that interested me during my doctoral studies. The personal takeaway was that the flow of life would continue to offer learning opportunities and what is more important is to be a lifelong student. Thank you, Granger, for being an excellent mentor and founding a program as unique as EPP.

I would like to thank my thesis committee members, Prof. Constantine Samaras and Prof. Eric Williams, for their collaboration, research guidance, and constructive feedback on the chapters included in this dissertation.

Thanks to my instructors at CMU: Prof. Alex Davis, Prof. Brian Kovak, Prof. Albert Presto, Prof. Baruch Fischhoff, Prof. Jay Apt, Prof. Nick Muller, Prof. Peter Adams, and many others. I thoroughly enjoyed taking their courses and attending research seminars during my time at EPP.

I would also like to thank my advisors and collaborators during my master's degree at Columbia University. I would like to acknowledge Prof. Geoffrey Heal, Prof. Garud Iyengar, and Prof. Upmanu Lall for supporting my interests in energy and environment and for introducing me to CMU EPP.

I am grateful to my undergraduate advisor, Prof. Sathans Suhag, for getting me started with research in electric power systems and, more importantly, for always believing in me.

Thanks to the EPP administrative staff, Vicki, Debbie, Patti, Adam, Peter, Deb, and Kim, for making sure that things ran on time, and I didn't get kicked out of the country for missing a deadline. It is because of your expertise and patience that I felt comfortable in the warm and intellectual environment at CMU EPP.

Pittsburgh would not have been as enjoyable had it not been for the great company of my current and former housemates, Sushil Lathwal, Sai Yerneni, Bijit Singha, Vikesh Sidhu, Mike Andrews, and Anup Prakashan, who helped maintain a pleasant atmosphere at home.

In addition, special thanks to Shreya Ahuja, Aman Tyagi, Prithvi Acharya, Ana Caceres, Nyla Khan, and Anirudh Mohan for introducing me to new things to try in and around Pittsburgh. I am sure that I would not have grown as much without these experiences.

Thanks to fellow EPP'ers and the wonderful community of friends who always made time to grab a coffee, chat, give me a ride, and play table tennis. In this respect, I am very grateful to Anjalie Field, Angelena Bohman, Ankush Das, Bhuwan Dhingra, Carlos Hernandez, Chaitanya Ahuja, Charles Van-Hein Sackey, Christophe Combemale, Devendra Singh Chaplot, Dian Yu, Emily Grayek, Evan Sherwin, Gopaljee Atulya, Jaison Desai, Ji Hoon Shin, Joan Nkiriki, Jorge Izar Tenorio, Kam Mongkolsinh, Kanthashree Mysore, Kate McMahon, Katie Jordan, Kristen Allen, Liza Reed, Luke Dennin, Lynn Kaack, Matthew Bruchon, Nikki Ritsch, Peter Tschofen, Priya Donti, Quay, Rohit Singh, Rolly Mantri, Sam Jones, Sarah Troise, Shayak Sengupta, Shrimai Prabhumoye, Shuchen Cong, and Tracey Ziev.

Thanks to Noa Goodman for keeping me in good physical condition.

Above all, I'd like to thank my parents, Prem Lathwal and Major General Ranbir Singh Lathwal, for their encouragement and support all these years. I would not have been where I am today had they not taken great care in ensuring that I got a good education during my formative years, many at times even at the expense of sacrificing personal comfort and staying in different places for my schooling. Thank you, papa, for motivating me by sharing your war stories when the doctoral process seemed rough, and referees had harsh feedback on my work. I owe a great deal of gratitude to my mother, who would often stay up late for many of my advisor meetings for a

post-meeting debrief, attempting (or pretending) to understand my research, and for making me realize that it's important to succeed in failure before one can succeed in success. Thanks to my sister, Prachika Lathwal, who held the fort back in India, helping our parents settle (in my absence) in their post-retirement life. Thank you, Prachika, for always being a phone call away and seeing my passion for science and technology long before I saw it in myself. You are so brave and independent at such a young age, and I am incredibly fortunate to have a sibling like you.

Thanks to the Center for Climate and Energy Decision Making (SES-0949710) for supporting my work through a cooperative agreement between the National Science Foundation (NSF) and CMU; the Philips and Huang Family Fellowship in Energy; the EPP Department for support through academic funds at CMU.

- Priyank Lathwal, August 2021

Abstract

The freight transportation sector is a growing contributor to global greenhouse gas emissions, and successful emissions mitigation requires studying its impacts in different contexts. However, an evaluation of different decarbonizing strategies across nations is missing in the literature. This dissertation consists of two methodologically distinct but related studies looking at the environmental, climate, and public health impacts of freight transportation.

In the second chapter, I look at these impacts in the context of ocean shipping in India and explore the emissions reduction potential of shore power in India. However, given how dirty and emissions-intensive India's electricity generation currently is, I show that shore power is not a cost-effective strategy to reduce air pollutants and greenhouse gas emissions in India.

In the third chapter, I evaluate freight trucking pollution impacts across the contiguous United States and the implications of trucking pollution on minority group populations. Based on my analysis, I find that the environmental and climate social costs due to freight trucking in the US result in ~\$17B in environmental damages and ~\$25B in climate damages, respectively. Further, more trucking pollution occurs in counties and census tracts with a higher proportion of Black and Hispanic populations.

In a final chapter, I conclude with further discussion of the findings of this work, explain how they are broadly valuable for policymakers, some more general conclusions.

Table of Contents

D	ICATION	III
A	NOWLEDGEMENTS	V
A]	TRACT	X
1	CHAPTER 1. BACKGROUND AND INTRODUCTION	1
2 V	CHAPTER 2. ENVIRONMENTAL AND HEALTH CONSEQUENCES OF SHORE POWE SELS CALLING AT MAJOR PORTS IN INDIA	K FOK
V		
	Introduction	
	PRIOR WORK	
	MATERIALS AND METHODS	
	2.3.1 Study Area and Scope	
	2.3.3 Emissions Calculation.	
	2.3.4 Auxiliary Engine Power	
	2.3.5 India's State Grid Emission Factors	
	2.3.6 Energy Costs and Savings	
	2.3.7 Comparison with Total Emissions in the Area	
	2.3.8 Health Effects of Pollution Reduction	
	2.3.9 Cost of Grid Extension, Shore Infrastructure, and Vessel Retrofitting	21
	RESULTS AND DISCUSSION	
	2.4.1 Environmental Consequences	
	2.4.2 Annual Fuel Cost Savings due to Switching from Fuel Oil to Shore Power	
	2.4.3 Health Consequences	
	2.4.4 Cost Effectiveness of Shore Power in India	
	2.4.5 Effect of Renewable Electricity Generation	
	ACKNOWLEDGEMENTS	
3 DI	CHAPTER 3. POLLUTION FROM FREIGHT TRUCKS IN THE CONTIGUOUS UNITED	
PU	LIC HEALTH DAMAGES AND IMPLICATIONS FOR ENVIRONMENTAL JUSTICE	35
	Introduction	36
	MATERIALS AND METHODS	39
	3.2.1 Study Area and Scope	
	3.2.2 Data	
	3.2.3 Estimating freight trucking VMT	
	3.2.4 Estimating spatially resolved emissions arising from freight trucking	
	3.2.5 Estimating public health and climate damages due to freight trucking	
	3.2.6 Emissions reduction due to modal shift to rail	
	RESULTS	
	3.3.1 Freight Trucking Emissions in the US	
	3.3.2 Environmental Impacts of Freight Trucking	
	3.3.3 Spatially Resolved Public Health Impacts of Freight Trucking	
	3.3.4 Modal shift from freight trucks to Class-1 railroads	
	3.3.5 Environmental Justice Implications	
	CONCLUSIONS AND POLICY IMPLICATIONS	
	ACKNOWLEDGEMENTS	
4	CHAPTER 4: CONCLUSIONS AND POLICY IMPLICATIONS	60
5	APPENDIX A: SUPPLEMENTARY INFORMATION FOR CHAPTER 2	62
	IMO MARPOL HISTORY AND POPULATION DENSITIES OF MAJOR PORT CITIES	
	5.1.1 IMO International Convention for the Prevention of Pollution from Ships (MARPOI)	62

5.1.	2 Population densities of cities near major ports in India	63
5.2	MATERIALS AND METHODS	
5.2.	1 Study Area and Scope	63
5.2.		
5.3	DETERMINING AUXILIARY ENGINE LOADS	
5.4	INDIA'S GRID ELECTRICITY EMISSION FACTORS	91
5.5	ENERGY COST AND SAVINGS	
5.6	GLOBAL EMISSIONS INVENTORY COMPARISON	
5.7	HEALTH EFFECTS OF POLLUTION REDUCTION	
5.8	Cost of Grid Extension, Shore Infrastructure and Vessel Retrofitting	
5.9	EXTENDED RESULTS AND DISCUSSION	
5.9.	I = I	
5.9.	, 0	
5.9.		
5.9.	- · · · · · · · · · · · · · · · · · · ·	
5.9.	0 0	
<i>5.9</i> .		
5.10	SENSITIVITY ANALYSIS	
5.10		
5.10	· · · · · · · · · · · · · · · · · · ·	
5.10	······································	
5.10		
6 AP	PENDIX B: SUPPLEMENTARY INFORMATION FOR CHAPTER 3	139
6.1	EXTRACTING FREIGHT TRUCKING EMISSIONS FROM THE NATIONAL EMISSIONS INVENTORY (NEI 139), 2017
6.2	Freight Analysis Framework 4 (FAF4) Road Network	140
6.3	EMISSION FACTORS FOR SINGLE UNIT AND COMBINATION TRUCKS	
6.4	COMPARISON OF FREIGHT TRUCKING AIR POLLUTION RELATED PUBLIC HEALTH DAMAGES FROM	
DIFFER	RENT MODELS	142
6.5	MODAL SHIFT: SHIFTING TONNAGE FROM FREIGHT TRUCKS TO RAILROADS	
6.5.	1 Emission factors for Class-1 railroad	144
6.6	DISTRIBUTIONAL EFFECTS OF FREIGHT TRUCKING AIR POLLUTION	147
6.6.	- ~ · · · · · · · · · · · · · · · · · ·	147
6.6.	2 Distribution of dependent variables	148
6.6.		
6.6.	4 Studentized Regression Residual Plots	152
	PENDIX C: ENVIRONMENTAL IMPACTS OF ELECTRIFICATION AND AUTOMATI	
FREIGH	IT TRUCKING IN THE UNITED STATES (FUTURE WORK CHAPTER)	154
7.1	Introduction	155
7.2	Methods	156
8 CH	APTER 8: REFERENCES	160

List of Tables

Table 2.1 Summary statistics of ships calling at major ports in India 2017-2018. 5,732 unique
ships visited major ports during the year.
Table 3.1 Freight trucking emissions comparison between FAF4 and NEI for 2017. NO _x and CO ₂
constitute a non-trivial share of US emissions. The difference in estimates column provides the
percentage difference of FAF4, 2017 diesel truck emission estimates from NEI, 2017 diesel truck
emission values. The estimates in the last two columns provide percentage contribution of freight
trucking emissions to total US emissions from FAF4 and NEI data. These are obtained by
dividing the FAF4 and NEI freight trucking emissions by emissions from all sources in NEI,
2017
Table 3.2 Effect of freight trucking PM _{2.5} , SO ₂ , and NO _x emissions on racial and ethnic
subgroups at the county level. The dependent variable is the log of PM _{2.5} , SO ₂ , and NO _x
emissions emitted by freight trucks in counties. For predictor variables that are log values, the
relationship can be estimated as $\%\Delta Y_p = \%\beta \times \Delta X_c$. For predictors that are not log values, the
relationship is estimated as $\%\Delta Y_p = 100 \times (e^{\beta}-1)$. These numbers are statistically significant and
the numbers in the parenthesis show 99% confidence intervals. 56
Table 3.3 Effect of freight trucking PM _{2.5} , SO ₂ , and NO _x emissions on racial and ethnic
subgroups at the census tract level. The dependent variable is the log of PM _{2.5} , SO ₂ , and NO _x
emissions emitted by freight trucks in census tracts. For predictor variables that are log values,
the relationship can be estimated as $\%\Delta Y_p = \%\beta \times \Delta X_t$. For predictors that are not log values, the
relationship is estimated as $\%\Delta Y_p = 100 \times (e^{\beta}-1)$. These numbers are statistically significant and
the numbers in the parenthesis show 99% confidence intervals
Table 3.4 Odds ratios of a county being an importer. These numbers are statistically significant
and the numbers in the parenthesis show 99% confidence intervals.
Table 5.1 List of ECAs adoption, their entry into force, and the effective date of implementation.
The table has been adapted from IMO website. 160
Table 5.2 Population density of cities located near major ports in India
Table 5.3 Indian Major Ports with their latitude, longitude and state information
Table 5.4 Summary statistics of non-major ports in India. This data is collated from Government
of India (GoI's) annual report on ports' statistics (page XIV) for the year 2017-2018. 173
Table 5.5 Emissions burden (in tons) for marine vessels in the city of Mumbai for the year
2010. ¹⁷⁴
Table 5.6 Date and time windows for vessel activity data shared by major ports of India. Chennai
and Kamarajar ports shared vessel activity data which spanned >1 year. HDC shared data from
April 2018 to March 2019.
Table 5.7 Classification used for grouping different vessel types
Table 5.8 Quantile distributions of port call duration (in hours) in ports' vessel data. We also
observe that there is a long tail of port call duration for some vessel categories in the raw dataset
which can induce bias in our results, if we assume that vessels connect to shore power in the
remaining time spent at port. So, we delete all vessel calls which have port call duration > 98 th
percentile of call duration (~ 228 hours) in the dataset
Table 5.9 Snapshot of vessel calls at each point of the cleaning process. Indian major ports
received 24,202 vessel calls in 2017-2018 out of which 21,937 were relevant for our study 71
Table 5.10 Port call distribution of different vessel types across major ports in India. Deendayal
port had the highest energy consumption of ~77 GWh at berth. Additionally, JNPT had the
port had the ingliest energy consumption or 1/10 Will at being. Additionally, 111 I had the

shortest port call duration (~28 hours) compared to Kolkata where the port call duration was the
longest (~77 hours)
Table 5.11 Port call distribution and unique vessels across individual major ports. Port of
Deendayal received highest number of vessel calls (2,654 calls) compared to Kamarajar port
which received the least number of vessel calls (794 calls)
Table 5.12 Comparison of ships mentioned in the Chennai Annual Administration Report 2017-
2018 ¹⁸³ with vessel details in authors' cleaned dataset
Table 5.13 Comparison of vessel categories between cleaned data with those mentioned in
Paradip Annual Administration Report 2017-2018. 189
Table 5.14 Ships' auxiliary engine emission factors (in g/kWh) for different pollutant types.
These are taken from US EPA's report. ⁷⁴ 80
Table 5.15 AE power defaults (in kW) by vessel category at berth. For passenger ships, we use
PAX instead of DWT to linearly interpolate their hoteling loads. The values in Min. DWT and
Max. DWT column for passenger ships denote the capacity of the passenger ships denote the
capacity of the passenger ship in the table below. For categories which didn't have a range of
auxiliary power information available, we used a constant linear function
Table 5.16 Auxiliary capacity information of passenger ships in our dataset. We collated
passenger capacities of respective ships from online sources such as the manufacturers of these
ships and government records
Table 5.17 State level emission factors from previous figure for PM _{2.5} , SO ₂ , NO _x and CO ₂ . All
values are in g/kWh and reported up to two significant digits. Baseline emission factors are for
the state's electricity grid. The ranges in parenthesis signify minimum and maximum values of
emission factors for the region (east, west, north, and south). SO ₂ emission factor for Tamil Nadu
and Odisha are an order of magnitude higher than other states
Table 5.18 Electricity grid emission factors used for coal fired power plants for the year 2017
and 2030. For 2030, we assume that retrofits to curb PM2.5, SO2, and NOx would be introduced
at coal power plants as per GoI's directives and thus we scale the emission factors accordingly.
We scale NO _x emission factor by 10, SO ₂ emission factor by 20, and PM _{2.5} emission factor by
250 when considering the emissions from coal power generation between 2017 and 2030.92 95
Table 5.19 Electricity tariffs for supplying shore power electricity to major ports
Table 5.20 Sector classification that we used in estimating EDGAR city emissions from various
sources in port cities
Table 5.21 Port latitude and longitude considered for EDGAR city level emissions estimation.
The latitude and longitude ranges show the city rectangle area which was considered for
calculating contributions of major ports' emissions in the city. The area ranges included major
sources of pollution in the city such as airports, oil refineries and industrial areas
Table 5.22 2019 population of cities located near major ports in India
Table 5.23 Port-wise hourly peak berthing load, hourly excess solar generation, transformer
ratings, number of circuit breakers and cables needed
Table 5.24 Distance from the port to the nearest distribution substation
Table 5.25 Major ports' contribution to city emissions in 2017 and 2030 when berthed ships burn
RO. Growth rate in shipping is assumed to be 3% annually from 2017-2030.89,90 100
Table 5.26 Major ports' contribution to city emissions in 2017 and 2030 when berthed ships burn
MGO. Growth rate in shipping is assumed to be 3% annually from 2017-2030. ^{89,90} 101
Table 5.27 Major ports' contribution to city emissions in 2017 and 2030 when berthed ships burn
RO. Growth rate in shipping is assumed to be 18% annually from 2017-2030. ^{57,58}

Table 5.28 Major ports' contribution to city emissions in 2017 and 2030 when berthed ships burn
MGO. Growth rate in shipping is assumed to be 18% annually from 2017-2030. ^{57,58}
Table 5.29 Annual emissions from berthed ships for PM2.5, SO2, NOx, CO2, port's electricity
load, fuel cost and savings
Table 5.30 Annual emissions from shore power to meet berthing load requirement at ports. The
2030 scenario assumes that air pollution control technologies for PM _{2.5} , SO ₂ , and NO _x have been
installed on coal power plants
Table 5.31 % change in emissions by switching from RO and MGO to shore power at major
ports in 2017- 2018
Table 5.32 Total emissions change (in tonnes) by switching from RO and MGO to shore power
at major ports in 2017- 2018.
Table 5.33 Fuel cost savings and lifetime savings (in US \$) by switching from RO and MGO to
shore power at major ports. For both fuel types, the savings are highest for bulk carriers, tanker
and general cargo ships. The useful life of the vessel is assumed to be 27 years which is the 96 th
percentile of vessel age in our dataset
Table 5.34 Port-wise annual savings, average savings per call and median savings per call 111
Table 5.35 Avoided premature mortality by switching from RO to shore power in 2017-2018.
The growth in shipping is assumed to be 3% each year. 89,90 Also, we assume that no emissions
control has been enforced on power generation and road transportation. All values are reported
up to 2 significant digits and the parentheses show 95% confidence interval (CI)
Table 5.36 Avoided premature mortality by switching from MGO to shore power in 2017-2018.
The growth in shipping is assumed to be 3% each year. 89,90 Also, we assume that no emissions
control has been enforced on power generation and road transportation. All values are reported
up to 2 significant digits and the parentheses show 95% confidence interval (CI)
Table 5.37 Avoided premature mortality by switching from RO to shore power in 2030. The
growth in shipping is assumed to be 3% each year. 89,90 Also, this is under the assumption that
power generation and road transportation have become cleaner. All values are reported up to 2
significant digits and the parentheses show 95% confidence interval (CI)
Table 5.38 Avoided premature mortality by switching from MGO to shore power in 2030. The
growth in shipping is assumed to be 3% each year. 89,90 Also, this is under the assumption that
power generation and road transportation have become cleaner. All values are reported up to 2
significant digits and the parentheses show 95% confidence interval (CI)
Table 5.39 Avoided premature mortality by switching from RO to shore power in 2030. The
growth in shipping is assumed to be 18% each year. 57,58 Also, this is under the assumption that
power generation and road transportation have become cleaner. All values are reported up to 2
significant digits and the parentheses show 95% confidence interval (CI)
Table 5.40 Avoided premature mortality by switching from MGO to shore power in 2030. The
growth in shipping is assumed to be 18% each year. ^{57,58} Also, this is under the assumption that
power generation and road transportation have become cleaner. All values are reported up to 2
significant digits and the parentheses show 95% confidence interval (CI)
Table 5.41 Sources of uncertainty and uncertainty analysis conducted by the authors
Table 5.42 Specifications for the PV panels used in the solar PV system. These were used to
estimate hourly annual solar generation at the respective ports
Table 5.43 Annual port energy requirement and solar PV system capacity
Table 5.44 Port-wise cost of electricity purchase, solar PV system and maintenance cost, solar
feed-in revenue

Table 5.45 Avoided premature mortality by switching from RO to shore power. We assume that
electricity in this case is supplied through solar panels and is emissions free. The growth in
shipping is assumed to be 3% each year. 89,90
Table 5.46 Avoided premature mortality by switching from MGO to shore power. We assume
that electricity in this case is supplied through solar panels and is emissions free. The growth in
shipping is assumed to be 3% each year. 89,90
Table 5.47 % difference in emission factors at which the vessel operator becomes indifferent in
burning diesel oil in ships' on-board generator versus using grid-electricity. The <i>green</i> values
show that the electricity grid is cleaner. The value in the cell indicates the percentage change in
the grid emission factor for in-situ electricity generation using ships' on-board generators to be
the cleaner option. The <i>red</i> values show that in-situ electricity generation using ships' on-board
generators is cleaner. The numbers indicate the proportional change in grid electricity emission
factors needed for shore power to be the cleaner alternative
Table 6.1 Freight trucking emissions from the NEI, 2017 data. 127
Table 6.2 VMT by single unit and combination trucks by type of road in the FAF4 dataset. A
major share of combination truck VMT is traversed on the interstate highways whereas the VMT
is more distributed for SU trucks
Table 6.3 Lifetime mileage weighted emission factors (in g/mile) for single unit and combination
trailer freight diesel trucks for model year (MY) 2017. The values are from Table A16 and Table
A22 as reported in the GREET study. 141
Table 6.4 Comparison of long-haul freight trucking emissions (in tons) using lifetime mileage
weighted emission factors reported in Tong et al. ²⁴⁰ and GREET model. ¹⁴¹
Table 6.5 Emission factors for class-1 railroad expressed in g/ton-mile for 2017 146
Table 6.6 Description of independent variables used in the regression analysis

List of Figures

Figure 2.1 Geographic location of India's 12 Major Ports ~7,500 km coastline. HDC (shown Haldia Port in the map) is governed by the Kolkata Port Trust; ⁷⁰ but is considered a separate in this analysis	ht h h h h h h h h h h h h h h h h h h
rate in (a, b) is assumed to be 3% per year (2007-2017 Indian shipping annual growth rate) ⁸⁵	25
Figure 2.3 Change in total emissions (in tonnes) for (a) PM2.5, (b) SO2, (c) NOx, and (d) C major ports, if ships were to use shore power instead of burning MGO for meeting their electricity requirement. Baseline emission factors are based on the grids of the state in which port is located. However, the high and low estimates (indicated by the yellow whiskers) are based on East, West, North, and South regional grids	26 (a, c) ell 29 39 niles ural
Figure 3.3 (A-C) Public health damages from PM _{2.5} , SO ₂ , and NO _x due to freight trucking aggregated at the source counties. The source county damage shows total air pollution damage that occurs across all other counties due to the freight trucking activity originating from the source county. It includes the air pollution damage that occurs from the county within itself. F) Public health damages from PM _{2.5} , SO ₂ , and NO _x due to freight trucking aggregated at the receptor counties. The receptor damage at a county includes total air pollution damage due to freight trucking activity occurring in other counties. It includes the damage that occurs within receptor county due to freight trucking activity within the receptor county	(D-e o in the
major ports in India. There were 21,937 vessel calls in 2017- 2018 with a median vessel call duration of ~39 hours and mean vessel call duration of ~50 hours.	l 72.

Figure 5.2 Scatterplot of linear regression relationship between TEU and DWT for 577 container
ships. The red line shows the least squares fit ($R^2=0.9747$ and p-value~0)
Figure 5.3 (a) distribution of vessel sizes. The vast majority of vessels calling at the Indian ports
are smaller than the ones calling at California. (b) Distribution of ages of vessels calling at
Californian and Indian major ports. The data suggests that the that the vessels calling at the ports
have similar ages
Figure 5.4 Frequency plot of port call duration of Indian major ports. We only consider vessels
which stayed in the port greater than or equal to 5 hours and less than or equal to 228 hours 90
Figure 5.5 India's power generation mix in 2017 by different fuel sources. The total electricity
generation as of 03/31/2018 was ~1,300,000 GWh. ²⁰⁵
Figure 5.6 Regional emission factors for PM _{2.5} , SO ₂ , NO _x and CO ₂ Indian States. Red color
denotes the mean value of emission factor in each region. We use state data on generation from
the Central Electricity Authority (CEA) ⁸² and combine it with peer reviewed data on annual coal
generation at the state level in India in 2012 ^{81,207} to estimate these values
Figure 5.7 Hourly SO ₂ emissions from berthed ships at Chennai and Kochi from 01/01/2017
00:00 hours to $01/01/2018$ $00:00$ hours. The emissions of PM _{2.5} and NO _x approximately follow
identical hourly profiles for other major ports
Figure 5.8 (a) Monthly AE load requirement (in GWh) for all berthed ships at major ports from
01/01/2017 00:00 hours to $01/01/2018$ 00:00 hours. (b) Daily AE load requirement (in GWh) for
all berthed ships at major ports
Figure 5.9 Change in total emissions (in tonnes) at major ports, if ships were to use shore power
instead of burning RO for meeting their electricity requirement
Figure 5.10 SO ₂ emission hotspots in India. Paradip, Chennai, Kamarajar and VOC are located
near thermal power plants which use low grade coal for power generation. Hence, their emission
factors are higher compared to other major ports. The base map has been adapted from the global
SO ₂ hotspots tracker and is publicly available. 222
Figure 5.11 (a) Distribution of annual fuel cost savings for switching from RO and MGO to
shore power across major ports. (b) Distribution of lifetime fuel cost savings for switching from
RO and MGO to shore power across major ports. Median savings were higher for MGO
compared to RO in both cases.
Figure 5.12 (a-b) Avoided premature mortality in 2030 by switching from RO (left) and MGO
(right) to shore power. The growth in shipping is assumed to be 18% each year. ^{57,58} Also, this is
under the assumption that power generation and road transportation become cleaner
Figure 5.13 Change in premature mortality with % change in grid desulphurization for 2020.
Positive values indicate premature mortality avoided and negative values indicate premature
mortality across port cities. We assume that ships use MGO in 2020 and the shipping growth is
assumed to be 3% each year from 2017-2020. 89,90 We find that the switch over occurs roughly
around ~70% of grid desulphurization
Figure 5.14 Map showing the location of the port and city of Kochi, as well as the population
densities of the adjoining areas. The location of the powerplants was obtained from Carbon
Brief's coal plant tracker, ²²³ and the population densities were obtained from Socioeconomic
Data and Applications Center (SEDAC). ²²⁴ The reader can refer to the wind rose for Kochi
here. 225
Figure 5.15 Map showing the location of ports and the city of Chennai, as well as the population
densities of the adjoining areas. The location of the powerplants was obtained from Carbon
Brief's coal plant tracker. ²²³ and the population densities were obtained from Socioeconomic
DUCES COMEDIANE HACKEL. FAND THE DODINATION DENSINES WERE ODIAINED FROM SOCIOECONOMIC

here. 226
Figure 5.16 Map showing the location of Deendayal Port and the city of Gandhidham, as well as the population densities of the adjoining areas. The location of the powerplant was obtained from Carbon Brief's coal plant tracker, ²²³ and the population densities were obtained from Socioeconomic Data and Applications Center (SEDAC). ²²⁴ The reader can refer to the wind rose for Kandla here. ²²⁷
Figure 5.17 Map showing the location of Mumbai and JNPT Port and parts of Mumbai, along with population densities of the adjoining areas. The location of the powerplant was obtained from Carbon Brief's coal plant tracker, ²²³ and the population densities were obtained from Socioeconomic Data and Applications Center (SEDAC). ²²⁴ Wind rose for the city of Mumbai in 2017-2018. ²²⁸
Figure 5.18 Map showing the location of the port and city of Kolkata, along with population densities of the adjoining areas. The location of the powerplant was obtained from Carbon Brief's coal plant tracker, ²²³ and the population densities were obtained from Socioeconomic Data and Applications Center (SEDAC). Wind rose for the city of Kolkata in 2017-2018. ²²⁸
Figure 5.19 Map showing the location of HDC and the city of Haldia, along with population densities of the adjoining areas. The location of the powerplant was obtained from Carbon Brief's coal plant tracker, ²²³ and the population densities were obtained from Socioeconomic Data and Applications Center (SEDAC). ²²⁴ The reader can refer to the wind rose for Haldia here. ²²⁹
Figure 5.20 Map showing the location of New Mangalore port and city of Mangalore, along with population densities of the adjoining areas. The location of the powerplant was obtained from CarbonBrief's coal plant tracker, ²²³ and the population densities were obtained from Socioeconomic Data and Applications Center (SEDAC). Windrose for the city of Mangalore in 2017-2018. ²²⁸
Figure 5.21 Map showing the location of Paradip port and city of Paradip, along with population densities of the adjoining areas. The location of the powerplant was obtained from Carbon Brief's coal plant tracker, ²²³ and the population densities were obtained from Socioeconomic Data and Applications Center (SEDAC). The reader can refer to the wind rose for Paradip here. ²³⁰
Figure 5.22 Map showing the location of VOC port and the city of Tuticorin and its population density. The location of the powerplant was obtained from Carbon Brief's coal plant tracker, ²²³ and the population densities were obtained from Socioeconomic Data and Applications Center (SEDAC). ²²⁴ Windrose for the city of Tuticorin in 2017-2018. ²²⁸
Figure 5.23 Map showing the location of Vizag port and the city of Visakhapatnam and its population density. The location of the powerplant was obtained from Carbon Brief's coal plant tracker, ²²³ and the population densities were obtained from Socioeconomic Data and Applications Center (SEDAC). ²²⁴ Windrose for the city of Visakhapatnam in 2017-2018. ²²⁸ 132 Figure 6.1 Comparison of freight trucking air pollution related public health social costs (in log10 tons) from EASIUR and AP3. We observe that social costs from both the models roughly
lie on the y=x line

related health damages whereas red indicates counties that are net importers of trucking polluti	ion
related health damages. The map indicates damages in arcsinh scale, and the unit is US \$ 1	143
Figure 6.3 Freight rail fuel efficiency of freight railroads from 1980-2019. The figure is from	
AAR report. 146	145
Figure 6.4 % change in PM _{2.5} , SO ₂ , NO _x , and CO ₂ emissions if a percentage of the total freigh	
ton-miles are shifted from diesel freight trucks to Class-1 railroads.	146
Figure 6.5 Q-Q plot of untransformed dependent variables (PM _{2.5} , SO ₂ , and NO _x emissions). T	The
untransformed variables are non-linear (a,c,e; left panel) whereas the log transformed depende	nt
variables, i.e., log(PM _{2.5}), log(SO ₂), and log (NO _x) emissions (b,d,f; right panel) are distributed	b
normally 1	149
Figure 6.6 Distribution of independent variables that are included in the model specification.	152
Figure 6.7 Regression residual plots for the three model specifications.	153
Figure 7.1 Flow chart showing datasets and methods to estimate emissions from short-haul and	b
long-haul freight trucking.	156
Figure 7.2 Percentage share of freight ton-miles by distance range in miles	157
Figure 7.3 Schematic of the transfer hub model for autonomous long-haul trucking. From	
Viscelli (2020). ²⁴⁸	158

1 Chapter 1. Background and Introduction

1.1 Greenhouse gas (GHG) emissions from international transportation

Article 2 of the Paris Agreement establishes the goal of limiting the increase in average global temperature since pre-industrial levels to "well below 2°C" and to pursue "efforts to limit the temperature increase to 1.5°C". Meeting these goals will require a rapid and massive reduction in GHG emissions by transitioning existing fossil fuel-reliant energy infrastructure to low-carbon sources. Despite the role that access to low-cost fossil fuels has played in modernizing our lives, the negative environmental, climate, and human health costs of relying on fossil fuels to society are enormous.^{2,3} Projected future increases of GHG emissions such as carbon dioxide (CO₂) through human activity are a big concern. Presently, CO₂ emissions from transportation are roughly 25% of global CO₂ emissions, with road transport accounting for ~72% of those emissions.⁴ Further, CO₂ emissions from transport are growing the fastest of any sector, and globally, transportation may become the highest-emitting sector by 2040.⁵ Despite existing regulations to limit them, emissions from transportation are expected to increase in the coming decades (Figure 1.1). According to the International Transport Forum (ITF), global freight transport accounts for ~7% of global CO₂ emissions. 6 Compared to rail, ocean and inland shipping, and aviation, road freight transportation is the most emission-intensive per ton-mile of freight transported and accounted for ~30% of the global transport CO₂ emissions in 2020 (Figure 1.2). Since the 2000s, heavy-duty vehicles' energy consumption and tailpipe CO₂ emissions grew ~2.6% each year, with trucks accounting for ~80% of that growth.8

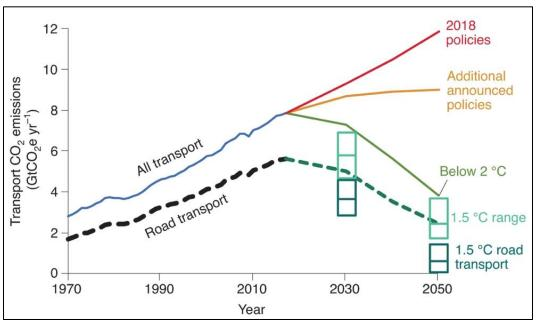


Figure 1.1 Global transport emissions from all modes (rail, road, aviation, shipping, etc.). Historical values are shown as black and blue. Emissions resulting from 2018 policies are shown in red; emissions after accounting for additionally announced policies are shown in orange; emissions to limit average global temperature rise to below 2° C are shown in green. The light green box shows ranges of global transport emissions across all modes to be compatible with 1.5° C whereas the dark green box shows only road transport emissions that are agreeable with 1.5° C temperature rise scenario. The figure is from Axsen et al.⁴

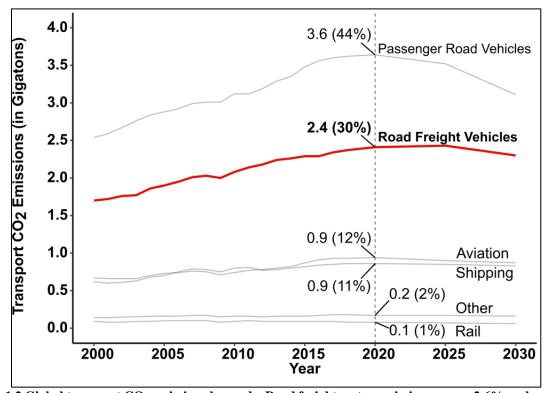


Figure 1.2 Global transport CO_2 emissions by mode. Road freight sector emissions grew ~2.6% each year from 2000 to 2020. The plot was produced by the author using International Energy Agency data.⁷

1.2 Why focus on freight transportation?

Even though the freight sector is a growing contributor to global GHG emissions, more than half of all countries do not collect any national road freight activity information⁹ and the sector is largely unregulated in many countries across the globe. Although passenger vehicles contribute the most GHG emissions from transport, they are probably also easier to decarbonize.¹⁰ Accordingly, in this thesis, we choose to focus exclusively on freight transportation. There are a few other reasons for this. First, road freight vehicles rely almost exclusively on petroleumderived fuels¹ and account for ~40% of directly emitted CO₂ from transport.¹¹ Due to growth in international trade and the expansion of global supply chains, global freight activity is expected to grow 2.6-fold between 2015 and 2050. 12 Thus, no matter the mitigation strategy under consideration, evaluating freight transportation emissions is going to be an important discussion for any nation trying to formulate a decarbonization policy for the coming decades. Another reason for the focus on freight transportation is that historically, there has been relatively less focus and research on freight vehicles compared to passenger vehicles. 4,13 In the context of lightduty vehicles (LDVs), cost-effective strategies exist such as vehicle electrification, fuel switching, and improving vehicle efficiency. However, the situation is more complicated for freight vehicles as optimal fuel choices and subsequent emissions reduction strategies depend upon the category of freight mode (ship, car, train, airplane), type of load being shipped (long distance versus short distance), energy density of storage or alternative fuel, and the vehicle performance in different geographic terrains and weather conditions. Because of these factors, today no simple pathway exists to smoothly decarbonize freight transportation, especially for

-

¹ According to the International Energy Agency (IEA), road freight transportation is the primary end-user of diesel fuel and accounts for roughly half of the global diesel demand. Gasoline as a fuel plays a much smaller role in freight transportation and is used mainly by light commercial vehicles.¹¹

hard to decarbonize modes such as long-distance road transportation, marine shipping, and aviation. 10 Also, it remains to be seen whether technology choices such as electric batteries and hydrogen or ammonia are long-term practical solutions for one or more of the long-distance freight modes. Third, vehicles miles traveled (VMT) due to freight activity are projected to increase in the coming decades, faster in developing countries (India and China) than in developed countries in the European Union and North America. 14 With the stringency of air pollution control and fuel standards in other transport sectors, the proportion of emissions attributable to freight is likely to gain more importance in the coming decades. Much like climate policy, designing an effective transportation policy for the long-term requires more than just "muddling through." Getting locked in on a technology pathway or investing in a particular strategy that does not scale well with future technological and socio-economic developments is a significant risk for achieving decarbonization objectives. Therefore, understanding the pathways to emissions mitigation and their interactions with projected increases in freight traffic across modes (rail, ships, trucks), choice and cost-effectiveness of sustainable freight infrastructure projects to pursue while evaluating the impacts of freight

1.3 Air quality impacts of freight transportation emissions

policymakers.

Freight transportation is dominated by diesel engines that are a significant source of air pollutants such as oxides of nitrogen (NO_x), sulfur dioxide (SO₂), and fine particulate matter (PM_{2.5}, includes elemental carbon). NO_x is a highly reactive group of gasses that include nitrous oxide (NO₂) and nitric oxide (NO) among other compounds. Exposure to high NO₂ concentration causes human respiratory airway inflammation and prolonged exposure leads to

transportation emissions in an economy are vital questions to answer for researchers and

the development of asthma. 18 In addition, it reacts with ammonia (NH₃) and volatile organic compounds (VOCs) to form secondary PM_{2.5} and ground-level ozone (O₃), both of which aggravate lung diseases and cause health complications in humans. ¹⁹ SO₂ is released in the ambient environment through electricity generation from power plants along with other industrial and mobile emission sources. It causes acid rain and has adverse impacts on human respiratory system.²⁰ Additionally, it leads to the formation of other particles that contribute to particulate matter (PM) pollution. PM is a mixture of solid particles and aerosols and includes PM_{10} (particles with an aerodynamic diameter of $\leq 10 \mu m$) and $PM_{2.5}$ (particles with an aerodynamic diameter of ≤2.5 µm).²¹ Primary PM_{2.5} occurs in the direct emissions from mobile sources, industrial activity, coal-based electric power generation and other stationary sources. Secondary PM_{2.5} formation occurs when criteria air pollutants (CAPs) like SO₂ and NO_x react chemically with other atmospheric pollutants and gases to form small particles. Exposure to PM_{2.5}, has deleterious impact on the environment (acid rain, damage to sensitive ecosystems)²² and on human health (heart and lung disease, asthma, aggravated respiratory function). ^{23–25} Ambient PM_{2.5} is a major risk factor for public health² and resulted in ~4.1M premature deaths globally in 2019 mostly in India (980,000 premature deaths) and China (1.4M premature deaths). 26,27 Although measures have been taken to reduce PM_{2.5} emissions in developing and developed countries, exposure to PM_{2.5} continues to be a public health risk. Thus, from both a decarbonization and an air quality perspective, it is imperative to reduce the emissions intensity of the freight sector. According to a framework proposed by McKinnon, ²⁸ transport emissions can be curtailed by five strategies: (1) reducing freight transportation demand by restructuring supply chains, (2) increasing fuel efficiency, and (3) reducing the carbon intensity of transportation fuel, (4) modal shift (i.e., shifting to a lower carbon-intensity mode),

and (5) improving vehicle utilization through capacity expansion of the vehicles and loading rates. A combination of one or more of these strategies can be used to help achieve the Paris agreement targets.

1.4 Thesis Outline

This dissertation contributes to filling knowledge gaps in contexts where freight sector emissions are significant but have been historically understudied due to the unavailability of data and/or lack of methods. Through this work, I explore technologies and mitigation strategies that allow us to reduce CAPs and GHG emissions. The original work in the thesis consists of two distinct but related research studies to reduce freight sector emissions in India and the United States (US).

Chapter 2 conducts a rigorous environmental benefit-cost analysis (BCA) of using shore power in India to reduce emissions by supplying electricity from the shore to cargo vessels docked in major ports in India, instead of having those vessels produce their own electricity by burning relatively high-sulfur diesel in on-board generators. Based on a unique vessel activity dataset I was able to compile from the Government of India (GoI), my co-authors and I find that shore power is not a cost-effective strategy to cut air pollution in India and does not reduce premature mortality significantly. This result is timely because the GoI has begun investing in deploying shore power infrastructure at ports in India. While electrification may have benefits in the long term, given how dirty electricity generation is today in India, we believe that the government is better off using its resources to clean up power generation in India.

Chapter 3 focuses on developing a method to spatially resolve the environmental, climate, and public health impacts of freight trucking in the contiguous United States. We use data from the US federal government and estimate the environmental, climate, and public health air pollution

damages at the county level for all contiguous states. We also quantify the extent of imports of air pollution damages due to freight trucking at the county level while evaluating the environmental justice implications of these damages for different demographic groups. My colleagues and I find that freight trucking NO_x and CO₂ emissions form a non-trivial share of total US emissions. We also observe that air pollution due to freight trucking disproportionately impacts people of color: more freight pollution occurs in census tracts with a higher proportion of Black residents and areas with a higher proportion of Black and Hispanic residents are more likely to experience higher pollution from other counties.

Finally, in **Chapter 4**, I synthesize the findings of the previous chapters and discuss additional possibilities for extending aspects of this work in the future.

Building on the data and tools developed for the work in **Chapter 3**, I include a future work chapter in the Appendix that describes work that will be completed in the near future. It explores the environmental effects of two technological revolutions (automation and vehicle electrification) on the freight trucking industry. Using the most recent commodities flow survey (CFS) data for the year 2017, I plan to evaluate the impacts of electrification and automation in the long-haul trucking segment.

2 Chapter 2. Environmental and Health Consequences of Shore Power for Vessels Calling at Major Ports in India

Abstract

To reduce local air pollution, many ports in developed countries require berthed ships to use shore-based electricity instead of burning diesel to meet their electricity requirement for loads such as lights, cargo-handling equipment, and air conditioning. The benefits of this strategy in developing countries remain understudied. Based on government data for all major ports in India, we find that switching from high-sulfur fuel to shore power reduces hoteling emissions of PM_{2.5} by 88%; SO₂ by 39%; NO_x by 85%; but increases CO₂ emissions by 12%. Switching from low-sulfur fuel reduces hoteling emissions of PM_{2.5} by 46% and NO_x by 84% but increases SO₂ emissions by 240% and CO₂ emissions by 17%. The lifetime cost savings from the switch to electricity are \$73M for high-sulfur fuel and \$370M for low-sulfur fuel. We estimate that switching from high-sulfur fuel to shore power might avoid at most a couple of dozen premature deaths each year, whereas switching from low-sulfur fuel could lead to a slight increase in premature mortality. Therefore, policymakers must first clean up power generation for shore power to be a viable strategy to improve air quality in Indian port cities.

This chapter has been published as: Lathwal P, Vaishnav P and Morgan M G 2021 Environmental and health consequences of shore power for vessels calling at major ports in India *Environmental Research Letters* **16** 064042 Online: https://doi.org/10.1088/1748-9326/abfd5b²⁹}

2.1 Introduction

The electrification of applications that currently involve the combustion of fossil fuels has been widely promoted as a strategy to achieve decarbonization and to reduce local air pollution. However, the effectiveness of this strategy depends on the local electricity generation mix over the lifetime of the product or infrastructure that is electrified. Indeed, scholars have raised grave concerns about the conventional wisdom that electrification by itself produces an environmental benefit. For example, in much of the eastern United States, electric vehicles do more damage to human health and the environment than do gas-electric hybrids. In this analysis, we ask whether the benefits of electrification exceed the costs in a sector and context that has drawn relatively little attention: ocean shipping in India.

The combustion of shipping fuels emits criteria pollutants such as fine particulate matter (PM2.5), oxides of nitrogen (NO_x), sulfur dioxide (SO₂)^{33–36}, that damage the environment^{34,37}, and human health.^{38,39} Criteria pollutants from ships caused ~60,000 premature deaths world-wide in 2015.⁴⁰ That number is expected to increase to ~250,000 premature deaths in 2020.³⁹ Global shipping accounted for 2.6% of the global carbon dioxide (CO₂) emissions in 2012.⁴¹ If left unregulated, CO₂ emissions from international shipping are expected to grow between 50% and 250% by 2050.⁴¹ While electrified ocean shipping remains elusive, there is great interest in the electrification of various port operations,^{42–44} and in the electrification of a ship's operations when it is in port.^{45–48} The second strategy has been shown to produce a net benefit in many ports in the United States and Europe to the extent that some ports have started to mandate it.⁴⁹ In this paper, we test a hypothesis that would seem to follow logically from these findings: given that ships that berth at Indian ports are allowed to burn far dirtier fuel than ships in Europe and North America are, and given that Indian cities are far more densely populated than those in Europe

and North America, the electrification of a ship's operations in port might be expected to produce a large benefit. Indeed, the logic of this hypothesis is so compelling that the Government of India has begun to invest in the provision of electricity to ships in port.⁵⁰ Our results suggest that this strategy is unlikely to be of much value for cargo vessels docked in major Indian ports until such time as the electricity generation that provides shore power is outfitted with much better pollution controls.

The International Maritime Organization (IMO) regulates pollution from ocean shipping. IMO's revised Maritime Agreement Regarding Oil Pollution (MARPOL) Annex VI, effective from January 1, 2020 (see Appendix A 5.1.1) seeks to reduce SO₂ emissions from ocean shipping. Before this regulation came into effect, ships could burn fuel with up to 3.5% sulfur. Under this regulation, ocean-going vessels (OGVs) are permitted to use fuel with up to 0.5% sulfur (5,000 ppm) outside the emission control areas (ECAs). The IMO has designated four ECAs (the North Sea, the Baltic Sea, the US Caribbean, and the coastal waters of Canada and the US), where permissible sulfur content of the fuel being used is 0.1% sulfur (1,000 ppm).⁵¹ India is not a part of an IMO ECA and hence ships at the Indian coast burn 0.5% sulfur fuel.

Asia had the largest share⁵² of world seaborne trade in 2018 with the continent accounting for 41% of total loaded and 61% of total unloaded goods.⁵³ Emissions from seaborne trade in East Asia have been estimated to result in between 14,500 and 37,500 premature deaths globally each year.³⁶ To address this, countries such as China have capped sulfur content in marine fuels to 0.5% sulfur (5,000 ppm) by designating domestic emission control areas (DECAs) across its national coastline and installing shore power at Chinese ports. In 2020, 493 berths in Chinese ports are expected to be equipped with shore power infrastructure.⁵⁴

Similar steps are being taken by the Government of India (GoI) to curtail air pollution. Beginning in 2020, new regulations tightened the standard for the sulfur content of on-road diesel from 350 ppm⁵⁵ to 10ppm.⁵⁶ Also, ocean freight through Indian ports is expected to grow at 18% per annum^{57,58} and GoI is building shore power infrastructure at Indian ports as part of their "Green Ports Initiative". ^{59,60} There are Indian ports such as the V.O. Chidambaranar (VOC) Port in Tamil Nadu (southern India) that already use shore power. Finally, the cities adjacent to India's ports are more densely populated than those in Europe and North America. For example, Mumbai has a population density of 31,000/km² and Gandhidham, which adjoins India's largest major port (Deendayal Port), has a population density of 8,000/km² (see Appendix A 5.1.2). By comparison, the Los Angeles region, home to the two largest U.S. ports, has a population density of <3000/km².⁶¹ For all these reasons, we anticipate that because the relative share of local SO₂ emissions from shipping in Indian port cities is likely to increase, shore power could potentially benefit air quality at major ports in India. Despite these developments, we are not aware of a rigorous environmental benefit-cost analysis of shore power in India. Literature on shipping impacts for India is sparse, presumably because of a lack of public data on Indian ports. Our study fills this gap.

In this analysis, we explore the potential of shore power as a strategy for India's 12 major ports. We assume an electricity system where the dominant source of load-following electricity is coal over the entire lifetime of any vessel that is switched to shore power. We report the results for 2017, the base year of the analysis when there is virtually no post-combustion scrubbing of emissions from coal-fired power plants. We also repeat the analysis for 2030 and assume that by then the emissions intensity of coal-fired plants is substantially reduced through the installation of air pollution control technology. In each case, we assume that the system remains static over

the period of the analysis. Furthermore, we (1) quantify the annual emissions of ships berthed at major ports in India in 2017-2018, (2) assess the contribution of berthed ship emissions as a proportion of total emissions in cities near major ports, (3) develop bottom-up hourly emission inventories for all major ports on the basis of vessel activity and fuel consumption calculations and use those results to estimate the change in emissions that would be achieved if ships were instead supplied with electricity generated on the shore, (4) estimate the change in vessel operator's fuel costs if they were to switch to shore power instead of burning Marine Gas Oil (MGO, 0.5% S), or Residual Oil (RO, 2.7% S) for meeting their load requirement, (5) estimate the net health and environmental consequences of switching to shore power in port cities. We assess these questions under two fuel use scenarios: first, assuming that ships burn lower-sulfur MGO to generate electricity, as required by international law from January 1, 2020, onwards, and second assuming that they continue to burn high-sulfur RO in their on-board generators as in the past. Finally, we evaluate the environmental and human health impacts from fuel switching only for PM_{2.5}, SO₂, NO_x, and CO₂, although we acknowledge that there are other pollutants such as mercury (Hg) from coal burning that may pose severe human health risks.⁶²

2.2 Prior Work

Many studies have shown that, in North America, Europe and Asia, the environmental and health benefits of shore power exceed the costs. Vaishnav and colleagues conducted a study on US ports and calculated an estimated social benefit of \$70-\$150 million per year by retrofitting one-fourth to two-thirds of all vessels calling at US ports.⁴⁷

Winkel et. al quantified the economic and environmental benefits of shore power in Europe while accounting for barriers in its implementation.⁴⁸ The health benefits of shore power in the study were estimated to be $\{0.63 \text{ billion and } \{0.93 \text{ billion for } 2010 \text{ and } 2020 \text{ respectively.}\}$ In

2010, a UK study estimated that using shore power reduced the emissions from berthed vessels by 91.6% for NO_x; 75.6% for carbon monoxide (CO); 45.8% for SO₂; and 24.5% for CO₂. ⁴⁵ The authors of the study also looked at the potential of shore power to reduce at-berth CO₂ emissions across countries and found it to be most effective in Norway (99.5% reduction), France (85% reduction), Japan (35.8% reduction), UK (24.5% reduction), and Italy (27.3% reduction). 45 Wang et al. found that the adoption of shore power at the port of Shenzhen in 2020 would reduce SO₂ by 88%, nitrogen dioxide (NO₂) by 94%, particulate matter (PM) by 95% and CO₂ by 37% but it seems to be a more expensive strategy compared to fuel switching. 46 If 80% of the container ships docking at the port of Shenzhen were to use shore power in 2020, then the per-tonne costs of reducing NO₂, PM, SO₂, and CO₂ were estimated to be \$56K, \$1.4M, \$290K and \$2,300 respectively. 46 While recent shipping studies in Asia focus on East Asia 36,63 and China, 64-66, very few studies^{67,68} address the problem of air pollution from ocean shipping in India. We are aware of two studies that systematically assessed emissions from ships in major ports in India. The first study by Joseph et al.⁶⁷ relies on assumptions from the late 1990s for estimating auxiliary engine load factors. The analysis was conducted for the Jawaharlal Nehru Port (JNPT) for the year 2006 and the authors determine the emissions contribution of total suspended particulate (TSP) matter, respirable particulate matter (PM₁₀), SO₂ for different port activities (port operations, construction, road transport) and find that TSP contributions dominated accounting for 68.5% of the total pollutant load and the minimum contribution was from SO₂ (5.3%). The paper found that maximum NO_x was emitted by the road transport sector and maximum SO₂ emissions in the port were from the maritime sector. The second study looked at emissions during 2013-2014 in the port of Kolkata (eastern coast of India).⁶⁸ The authors estimated annual emissions for Kolkata port for NO_x, SO_x, PM₁₀, PM_{2.5}, CO, hydrocarbons (HC)

and CO₂ during ships' different activity modes (reduced speed zone, maneuvering and hoteling) and found NO_x, SO₂ emissions to be the dominant among pollutant species. The authors attributed the high emissions to the longer length of the shipping channel, use of bunker fuel, non-compliance of vessels with IMO's emission standards and long turnaround time at berth. The study is limited in that the authors studied the emissions only at this one port for 2013-2014. Kolkata Port's shipping activity has increased to ~32%⁶⁹ by 2017-2018 and the emissions at the port are likely higher than what is reported in the paper. Finally, there are two big facilities under the jurisdiction of the Kolkata Port Trust, namely, (1) Kolkata Docking System (KDS) and, (2) Haldia Dock Complex (HDC), (located about 104 km away from KDS).⁶⁸ Mandal et al. appears not to have included HDC, which may also have resulted in an underestimate of emissions. In our analysis, we have estimated emissions at both KDS and HDC.

2.3 Materials and Methods

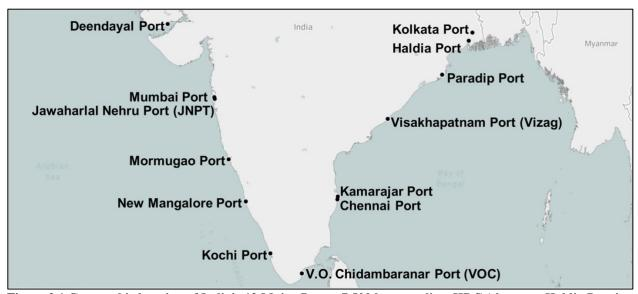


Figure 2.1 Geographic location of India's 12 Major Ports \sim 7,500 km coastline. HDC (shown as Haldia Port in the map) is governed by the Kolkata Port Trust; 70 but is considered a separate port in this analysis.

2.3.1 Study Area and Scope

Figure 2.1 shows the 12 major ports in India which are governed by the Ministry of Shipping (MoS) through respective Port Trusts (geographic details in Appendix A 5.2.1).⁷¹ These are the ports primarily visited by the large cargo vessels that are the focus of this paper. They handled ~680 million tonnes (MT) of cargo from April 2017 to March 2018.⁷² By comparison, the Port of Los Angeles (POLA) handled ~195 million metric revenue tonnes (MMRT) of cargo from July 2017 to June 2018.⁷³

In addition to the major ports there are over 200 non-major ports, many of which are not equipped to handle large cargo vessels. Many fishing vessels call at small and unofficial ports and undoubtedly contribute to pollution near these ports. However, it is not clear that they produce a significant amount of electricity for hoteling loads or that they could be profitably switched to shore power. As explained in Appendix A 5.2.1, since the focus of our analysis is on reducing pollution by switching to shore power at major ports, small fishing vessels and non-major ports are not included in the analysis.

2.3.2 Vessel Call Information

Through correspondence and meetings with stakeholders at various levels in the MoS, GoI, Port Trusts, Indian Ports Association (IPA), the Indian Coast Guard (ICG) and the Indian Army, we obtained vessel activity data for all 12 major ports in India. Our vessel call dataset consists of detailed information on ships, including each ship's IMO registration number, Maritime Mobile Service Identity (MMSI), a unique 9-digit number which identifies each ship's Automatic Identification System (AIS) station, Vessel Name, Vessel Type, Deadweight Tonnage (DWT), Gross Register Tonnage (GRT), Flag, Cargo information (for some ports), pilotage time, berth arrival and berth departure time.

These data are all for the same one-year time window: March 2017-March 2018. In the raw data, there were some vessel calls at ports for which the IMO registration number and MMSI information was missing. To obtain this information from online data at MarineTraffic, we developed a web scraper in the Python programming language to find the vessel IMO number, MMSI number, vessel age, and vessel type based on vessel name, GRT and DWT. In our analysis, we consider only vessels that remain in port for longer than 5 hours, and less than 230 hours, which is the 98th percentile of the durations of all port calls. The lower limit excludes vessels that do not spend sufficient time in port to be connected to shore power; the upper limit excludes vessels that may be in port, but not active. The details of how we processed the raw data obtained from port authorities for analysis are in Appendix A 5.2.2.

2.3.3 Emissions Calculation

The emissions for OGVs for each vessel call were estimated according to the following equation:

$$E_{i,j} = EF_i \times A_j \times t_j$$

Where:

 $E_{i,j}$ = Total emissions, in tonnes, for pollutant i (PM_{2.5}, SO₂, NO_x and CO₂) for vessel call j EF_i = Emission factor for pollutant i expressed in g/kWh of electricity generated by the auxiliary engine

 A_j = Auxiliary engine's actual operating load for vessel call j (in kW) based on the vessel type and its size

 $oldsymbol{t_j}=$ the time (in hours) the vessel spent hoteling during vessel call $oldsymbol{j}$

The emission factors for PM_{2.5}, NO_x, SO₂ and CO₂ were obtained from EPA guidelines for compiling mobile emissions inventories.⁷⁴ A similar approach was used by Mandal et al.⁶⁸ and Joseph et al.⁶⁷

The total time spent by a vessel hoteling at the port was determined by subtracting berth arrival time from the berth departure time in our datasets. Finally, we multiplied the emission factors by estimates of the hoteling load (expressed in kWh) for different vessel types and sizes to get emissions of respective vessel calls. While we calculated emissions for each vessel call, the results reported below are aggregated by vessel, vessel type, and as annual totals. The emission calculations were performed both for RO and MGO.

2.3.4 Auxiliary Engine Power

The auxiliary hoteling loads were estimated by multiplying the total berthing time (in hours) and the auxiliary engine load under operation (in kW) of the vessel of a given type and size. Our calculation is based on the approximation that the auxiliary hoteling load of a vessel scales linearly with its capacity in deadweight tonnes. In addition to using Goldsworthy et al.,⁷⁵ auxiliary engine load estimates, we compared the vessel sizes and ages in our dataset, against those that called at POLA and Port of Long Beach (POLB) (see Appendix A Figure 5.3). We found that the vessels in our dataset are of a comparable vintage to the ones in those ports. As such, we assumed that applying the relationship between vessel size and auxiliary loads observed in POLA⁷⁶ and POLB's⁷⁷ 2017 emissions inventory is appropriate (see Appendix A 5.3).

2.3.5 India's State Grid Emission Factors

We assumed that a vessel would require at maximum the same amount of electricity from shore power as it gets from running its on-board generator. The World Bank reports transmission and distribution (T&D) losses for India as ~19% ⁷⁸, including theft ⁷⁹. The actual technical losses are unknown. We assume T&D losses to be 10%. Coal contributed ~76% to aggregate electricity generation in India during 2017-2018. ⁸⁰ In our analysis, we assume that 76% of India's electricity in 2017 came from coal based electric power generation, but all of its load-following

electricity —which is what is relevant to the discussion of shore power—comes from coal.

Besides coal, gas generates ~4%; the rest is generated by non-emitting sources.⁸⁰ We neglect air emissions from natural gas-fired power generation. Since all other sources of power used in India produce no emissions from combustion, we assume that all power sector emissions come from the combustion of coal.

For shore-based electricity, we use the dataset from Oberschelp et al.⁸¹, which provides annual coal based PM_{2.5}, SO₂, NO_x and CO₂ emissions of coal power plants at the generating unit level for the year 2012. Using the latitude and longitude of coal powered generating units from Oberschelp et al.⁸¹, we aggregated the coal power plant emissions at the state level for India. We use Central Electricity Authority's (CEA) data to determine total electricity generation in Indian states in 2012.⁸² To calculate the emission factor, we divide emissions from coal-fired electricity generation in each state by the total electricity generation in the same state to arrive at state level PM_{2.5}, SO₂, NO_x and CO₂ emission factors (in g/kWh) for electricity generation. The estimates of state and regional level emission factors for India's grid electricity generation are reported in Appendix A 5.4.

2.3.6 Energy Costs and Savings

To estimate the mass of fuel used, our analysis assumes that auxiliary engines produce ~720g of CO₂ per kWh for RO and ~680g of CO₂ per kWh for MGO.^{83,84} We assume an emission intensity of ~3.1 kg CO₂ per kg⁸³ of fuel burnt for marine fuel.⁸³ Thus, RO produces ~4.3 kWh/kg fuel and MGO produces ~4.5 kWh/kg fuel. In combination, these numbers allowed us to estimate the mass of bunker fuel needed to produce the required energy. We obtained the price per ton (December 19, 2018) of both RO (\$445 per metric ton) and MGO (\$725 per metric ton) from Petrol Bunkering Group in Colombo Port, Sri Lanka⁸⁵ and multiplied this by the mass of

fuel consumed during a vessel call to calculate the fuel cost. The attractiveness of shore power depends on the local price of electricity. Therefore, we used the state-average price of electricity for the industrial and high-voltage consumers from their respective electricity regulatory commissions and converted from rupees to dollars per kWh using the market exchange rate on November 30, 2018. Finese tariffs were used to calculate the fuel cost for supplying shore power to the vessels and are reported in Appendix A 5.5. For each vessel call, we subtracted the cost of electricity from the cost of RO or MGO to calculate the net savings and estimated the total savings from shore power that would accrue to the vessel over its remaining lifetime.

Because 96% of the vessels in our dataset are less than 27 years old, we choose 27 years as the vessel lifetime and calculated the net present value of annual savings using a discount rate of 7%. Assuming that shoreside facilities to supply power exist, if the present value of these savings exceeds the cost of retrofitting the vessel, a vessel operator would reduce costs by retrofitting to receive shore power.

2.3.7 Comparison with Total Emissions in the Area

We used the Emission Database for Global Atmospheric Research (EDGAR) 2015 emissions inventory⁸⁷ to estimate the proportion of the pollution in the major port cities that is caused by OGVs. We selected 0.1 deg. × 0.1 deg. cells to include the port cities we were studying. We ensured that the selected cells included the international and domestic airports, oil refinery, and the industrial areas of those cities. Specific information on the geographical extent of selected areas is in Appendix A 5.6. The most recent year for which the EDGAR emissions inventory is available is 2010. To project emissions to 2017 and beyond, we assumed that those emissions would grow in line with the economy and with the volume of trade in goods through Indian ports. We assumed that, between 2020 and 2030, emissions of all pollutants from international

and domestic air transport, industrial and residential sectors grow at 6% per year⁸⁸, in line with Organisation for Economic Co-operation and Development's (OECD) projections for India's gross domestic product (GDP) growth in 2020-2030. From 2007-2017, the volume of seaborne trade through Indian ports grew at 3%. 89,90 We assume a 3% growth rate each year for Indian shipping and run a sensitivity analysis for the 18% growth rate projected by GoI^{57,58} during 2017-2025. We conducted the analysis for both RO and MGO at both growth rates and assumed that these growth rates remain constant until 2030. We assumed that the non-marine transportation sector grows by 9.7% per year⁹¹ until 2032, in accordance with the projections of the erstwhile Indian Planning Commission, as noted in Kaack et al.⁹ Finally, we assumed that the power generation sector grows by 5% per year from 2017-2030 based on projections for 2015-2030 from a study of Indian thermal power plants⁹² and Brookings India electricity demand estimates for 2030.93 In our results, we account for the effect of cleaning up of the coal power generation sector between 2017 and 2030 by scaling the coal power plant emission factors. We reduce the NO_x emission index by a factor of 10 (i.e., to 10% of its current value), SO₂ emission index by a factor of 20, and the PM_{2.5} emission index by a factor of 250 when considering the emissions from coal power generation during 2017 and 2030. These factors were derived from the new power plant emissions standards promulgated by the Government of India and summarized in Table 1 of Center for Study of Science Technology and Policy (CSTEP) report. 92

2.3.8 Health Effects of Pollution Reduction

We estimate the percentage contribution of shipping emissions to the total city emissions in 2017 relative to EDGAR emissions inventory.⁸⁷ We multiply the percentage share of shipping in the city (in 2017) and the percentage change in emissions at each port after switching from RO and MGO to shore power to estimate the percentage of pollution reduced in each city. We use the

estimated reduction in city pollution for PM_{2.5}, SO₂, and NO_x to approximate potential health benefits. Table 2. of Lee et al. ⁹⁴ provides estimates of absolute change in mortality across each of the Global Burden of Disease (GBD) regions for a 10% change in local PM_{2.5} precursor emissions. From this, we estimated the change in mortality in South Asia, per unit change in emissions of PM_{2.5} precursor pollutants. As described in 5.7 and 5.9.6.1 of Appendix A, we obtain a regional estimate of the change in premature mortality given a percentage increase in emissions of different particulate matter precursor pollutants (black carbon (BC), SO₂ and NO_x). After accounting for population in cities located near Indian major ports, we were able to make a very rough estimate of the annually avoided premature mortality in major port cities (see Appendix A 5.9.6.1).

2.3.9 Cost of Grid Extension, Shore Infrastructure, and Vessel Retrofitting

We estimate the cost of extending the distribution line from the nearest substation to the port to provide grid electricity supply at berth. We obtained the sub-station data from Power System Operation Corporation Limited. The distribution network is assumed to be connected to a 3-phase distribution transformer and a 33-kV line is sufficient to meet the hourly peak loads of auxiliary engines at each major port (details in Appendix A 5.8). The cost per mile (~\$25,000 per mile) of extending a 33-kV line was taken from GoI's electricity authority guidance document and its maintenance cost was assumed to be 3% of the capital cost. 97,98

The total cost of grid extension is the sum of line extension and line maintenance costs for all ports. Shore power projects usually have a life of 20 years⁹⁹ and we use this as the useful life of the shore power system. The cost of installing a shore power system at the port is assumed to be ~\$4.5M based on estimates from shore power equipment manufacturers. To determine the total number of shore power systems required by the ports, we find the number of vessels

simultaneously docked at each port during each hour of the year. We assume that the maximum of this number represents the number of charging points needed at each port. The total cost of deploying shore power systems is determined by summing the cost of installing shore power systems across all ports. The cost to the vessel operator of retrofitting a ship with shore power infrastructure (including cabling, switchboards, transformer, frequency converters and mechanical modifications) is between \$300K-\$2M.⁴⁶ The total cost of retrofitting is determined by summing the cost of vessel retrofit for all the berthed vessels.

2.4 Results and Discussion

Table 2.1 Summary statistics of ships calling at major ports in India 2017-2018. 5,732 unique ships visited major ports during the year.

Vessel class	Vessel calls	Unique vessels	Total hours (1000s)	Average call duration (hours)	Average auxiliary capacity (kW)	Total energy use (GWh)	Mean age (yrs.)
Auto Carrier	343	181	9	26	730	6.6	13
Bulk	5,833	2,560	430	74	380	170	9
Container	4,933	577	170	35	640	95	13
Crude Oil Tank er	1,210	444	56	46	1,100	60	13
General Cargo	2,292	575	150	64	630	100	14
Passenger	473	40	25	54	2,800	54	20
RoRo	23	12	1.5	63	95	0.16	10
Tanker	6,830	1,343	270	39	610	160	12
All Major Ports	21,937	5,732	1,100	50	630	650	13

Our analysis is based on a dataset, which we believe is comprehensive, of the 21,937 port calls that 5,732 unique vessels made to the 12 major Indian ports in 2017-18 (see Appendix A table 5.9). The average at-berth duration across all ports was ~50 hours per vessel per call. **Table 2.1** shows that the calls were dominated by tanker ships (chemical tankers, oil products tankers, LNG and liquefied petroleum gas (LPG) tankers), bulk carriers and container ships. On average, bulk carriers had the longest stays averaging 3 days per berth call. Auto-carriers had the shortest

stays, averaging just over 1 day per berth call. Averaged across all types of vessels at each port, the shortest average vessel call duration was for Jawaharlal Nehru Port in Mumbai (JNPT; 28 hours). The longest average vessel call duration was at the ports of Kolkata (77 hours) and Haldia (53 hours).

2.4.1 Environmental Consequences

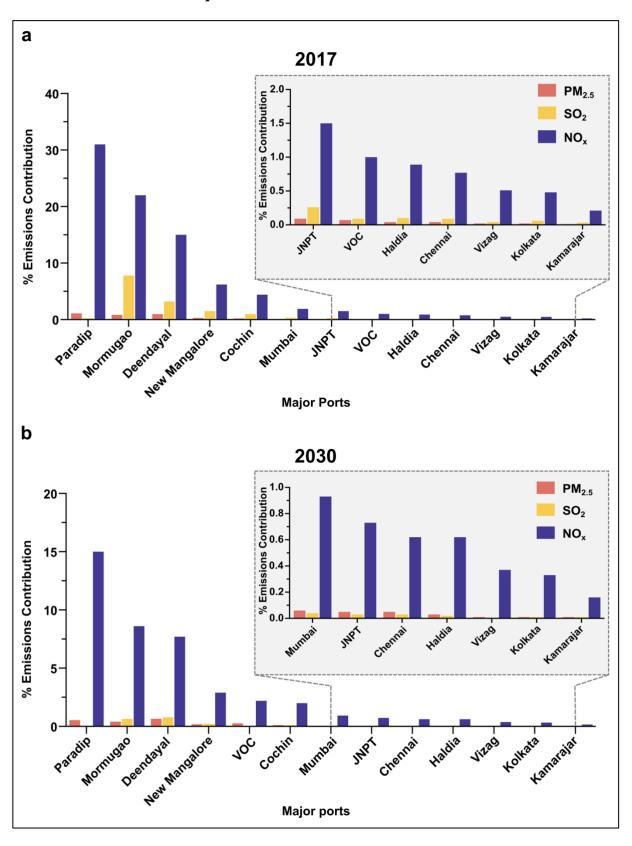


Figure 2.2 Annual emissions contributions for PM2.5, SO2, NOx and CO2 to total city emissions in (a) 2017 and (b) 2030 from berthed ships burning MGO at major ports. The shipping growth rate in (a, b) is assumed to be 3% per year (2007-2017 Indian shipping annual growth rate)^{89,90}.

2.4.1.1 Relative Contribution of Major Port Emissions to Total City Emissions

Ships berthed at major ports are a significant source of local SO₂ and NO_x emissions in Indian port cities. If shipping activity were to grow at 3% per year (2007-2017 Indian shipping growth rate)^{89,90} and ships were to continue burning RO or MGO, then the relative share for emissions from berthed ships for both fuel types decrease in 2030, except for increase in shipping's share of NOx emissions at some ports. The emissions from berthed ships burning MGO as a percentage of total city emissions in 2017 and 2030 are shown in Figure 2.2 (see Appendix A Table 5.26). For the case where berthed ships burn RO, their percentage contribution to total city emissions in 2017 and 2030 is included in Appendix A Table 5.25. If shipping activity were to grow in line with the sensitivity analysis scenario wherein the volume of trade grows at 18% annually^{57,58}, we anticipate the relative proportion of emissions from ships to increase (see Appendix A Tables 5.27 and 5.28). This growth is due to the reduction of the emissions intensity of other sectors as standards such as Bharat Stage VI, which will reduce the sulfur content of road diesel by a factor of 50, come into force. India has also started to require that SO₂, PM_{2.5}, and NO_x emissions from coal fired power plants—which have so far been unabated—be drastically reduced by implementing post-combustion treatment of flue gases. 92,100 In this case, NOx emissions from berthed ships will constitute a major portion of the total city emissions.

2.4.1.2 Annual Emissions from Ships Berthed at Major Ports

The annual PM_{2.5}, SO₂, NO_x and CO₂ from ships burning RO at major Indian ports was 850, 7,700, 9,500 and 470,000 tonnes, respectively (see Appendix A Table 5.29). If ships were to burn MGO, then the annual PM_{2.5}, SO₂, NO_x and CO₂ at Indian major ports are estimated to be

190, 1,400, 9,000 and 450,000 tonnes respectively (see Appendix A Table 5.29). Our analysis has produced a unique annual hourly inventory of PM_{2.5}, SO₂, NO_x and CO₂ emissions from berthed vessels for India's 12 major ports (details in Appendix A 5.9.3).

2.4.1.3 Change in Emissions if Vessels Switch to Shore Power

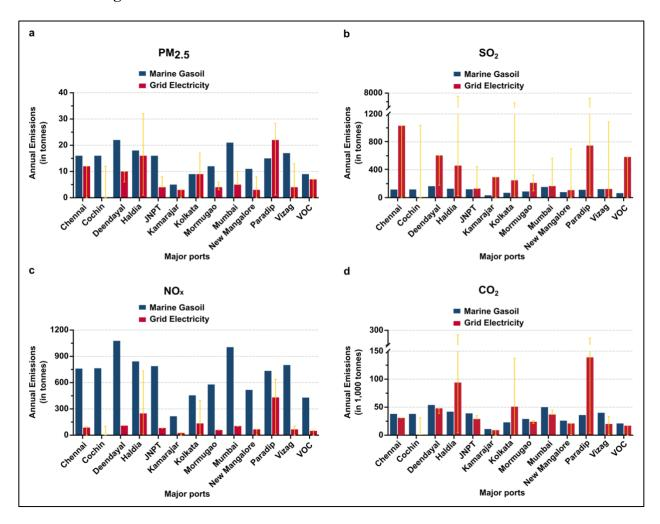


Figure 2.3 Change in total emissions (in tonnes) for (a) PM2.5, (b) SO2, (c) NOx, and (d) CO2 at major ports, if ships were to use shore power instead of burning MGO for meeting their electricity requirement. Baseline emission factors are based on the grids of the state in which the port is located. However, the high and low estimates (indicated by the yellow whiskers) are based on East, West, North, and South regional grids.

Because of the low sulfur content of MGO, and assuming that the high sulfur intensity of India's power system remains unchanged when vessels are required to burn MGO, if vessels switched from burning MGO to shore power, net emissions of PM_{2.5} would decline by 46% (86 tonne

reduction); NO_x emissions would fall by 84% (7,500 tonne reduction), but SO₂ and CO₂ emissions would increase by 240% (3,300 tonne increase) and by 17% (75,000 tonne increase), respectively (see Appendix A Tables 5.31 and 5.32). The case for the switch from RO to shore power is discussed in Appendix A 5.9.4. The annual PM_{2.5}, SO₂, NO_x, and CO₂ emissions from grid electricity in 2017 was 100, 4,700, 1,500, and 520,000 tonnes respectively (Appendix A Table 5.30).

Figure 2.3 explains the change in emissions for different pollutant categories when ships switch from burning MGO to shore power for the 12 ports we studied. For MGO, switching to shore power increases SO₂ emissions across 11 out of 12 ports except for Cochin. This is due to the lower amount of sulfur emitted by the combustion of fuel in comparison to burning coal for electricity generation. The source of electricity generation in Cochin is hydropower and thus SO₂ emissions from the grid don't increase from the switch. He also estimate the change in emissions when ships switch from burning RO to shore power across major ports (see Appendix A Figure 5.9, Tables 5.31 and 5.32). For RO, switching to shore power increases SO₂ emissions at Chennai, V.O. Chidambaranar (VOC), Kamarajar and Paradip ports. Chennai, VOC and Kamarajar are located in the state of Tamil Nadu, where lignite is burned for power generation. Paradip port is located in the state of Odisha (eastern India), where low grade coal from Mahanadi Coalfields is used for power generation (see Appendix A Figure 5.10). How the low quality of coal use, the emissions factors for generating units in Tamil Nadu and Odisha are an order of magnitude higher than other states (see Appendix A Table 5.17).

2.4.2 Annual Fuel Cost Savings due to Switching from Fuel Oil to Shore Power

The median savings per vessel call for switching from RO and MGO to shore power is \$210 and \$1,500, respectively (see Appendix A Table 5.34). The median annual fuel cost savings per

vessel for switching from RO to shore power is \$610 and the median annual fuel cost savings per vessel for switching from MGO to shore power is \$3,700 (see Appendix A Figure 5.11(a)). The savings are greatest for bulk carriers, tanker and general cargo ships.

Over the expected life of all vessels, using a discount rate of 7%, switching from RO and MGO to shore power yields a net private benefit of \$73M and \$370M, respectively (see Appendix A Table 5.33). While the median lifetime savings per vessel for switching from RO to shore power is \$5,300, the median lifetime savings per vessel for switching from MGO to shore power is \$33,000 (see Appendix A Figure 5.11(b)). The typical cost of retrofitting a vessel is \$300K-\$2M. For RO, only 0.2% of the vessels (9 vessels) had annual savings above \$300K and for MGO, 2.4% of the vessels (138 vessels) had savings above \$300K. Thus, very few ship operators would reduce their fuel costs enough to pay for the cost of retrofitting their ships for shore power.

2.4.3 Health Consequences

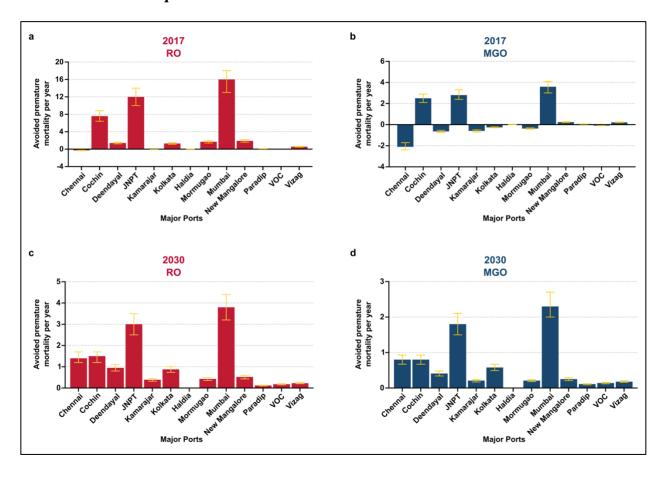


Figure 2.4 Estimates of premature deaths avoided across major ports by switching from RO (a, c) and MGO (b, d) to shore power in 2017 and 2030 by treating each city as a homogeneous well mixed region. The growth in shipping is assumed to be 3% each year^{89,90} and the error bars represent 95% confidence interval (CI).

It is difficult to quantify the effect of a shift to shore power on premature mortality without running integrated air quality assessment models. However, a zeroth-order analysis, performed by treating each city as a homogeneous well mixed region suggests that switching from RO to shore power in the absence of emissions regulation for power generation and transportation sector might avoid of the order of 40 premature deaths each year (see Appendix A Table 5.35). Switching from MGO to shore power might avoid roughly five premature deaths each year (see Appendix A Table 5.36).

If shipping grows at 3% per year, 89,90 as it has in the decade from 2007 to 2017, while power generation and road transportation become cleaner, switching from RO and MGO to shore power in 2030 would avoid roughly ten premature deaths each year (see Appendix A Tables 5.37 and 5.38). Figure 2.4, respectively, show the health benefits of switching from RO and MGO to shore power in 2017 and 2030, although these numbers are highly uncertain and should merely be treated as an indication that the effect of shore power on premature mortality is likely to be small. For RO, the analysis suggests that, in Tamil Nadu, any shift to shore power would increase premature mortality, since much of the state's electricity is generated by burning lignite. Further, this suggests that the decision of the VOC port in Tamil Nadu to start deploying shore $power^{60}$ at VOC-III and VOC-III berths 105 may actually be detrimental to air quality and human health. Until the GoI enforces its proposed regulations for cleaning the power generation sector, switching from MGO to shore power would increase premature mortality in the states of Gujarat, Tamil Nadu and West Bengal. On the other hand, if shipping grows at 18% per year^{57,58} as India's Ministry of Shipping projects, while power generation and road transportation become cleaner, switch from RO and MGO to shore power in 2030 would avoid roughly 100 and 40 premature deaths annually (see Appendix A Table 5.12, Tables 5.39 and 5.40). In the absence of chemical transport models, it is possible to qualitatively assess the effect of a switch to shore power on the concentration of pollutants. A switch from fuel oil to shore power moves pollution emissions from high population density areas (near the port) to a lower density area (near power plants). For example, an analysis of the wind rose for the city of Cochin (refer to Appendix A Figure 5.14) shows that pollution from the port is likely to be blown toward densely-populated areas of Cochin for 9 months of the 12 months of the year. The nearest coalfired power plant (Mettur Thermal Power Station; capacity: 1,440 MW) is situated ~260 km

away and has a population density of ~730 people per km² in nearby region. As such, our initial hypothesis would be that any reduction in pollution at the port would improve the air quality over Cochin and be beneficial for the health of its residents. The effect is similar across other major ports including the ones where electricity generation is coal based (see Appendix A 5.9.6.2).

2.4.4 Cost Effectiveness of Shore Power in India

The total cost, for all 12 ports of constructing and maintaining overhead power lines from the nearest substation to the port is \$1.5M (i.e., an annual amortized cost over 20 years, discounted at 12% of ~\$200K). Our analysis showed that, to obtain the benefits described above, 249 berths would need to be equipped for shore power across the country. The total cost of installation of shore side infrastructure for all the ports is ~\$1.1B. This translates roughly to an annual amortized cost of ~\$140M-\$150M. Given that we estimate that a shift to shore power from RO is likely to avoid of the order of 40 premature deaths each year, this suggests a cost effectiveness of ~\$4 million per premature death avoided. If ships use low-sulfur fuel (e.g., MGO), little public health benefit is likely to accrue. As discussed previously, for vessel operators, the benefits of shore power, as measured by lower fuel costs, are unlikely to exceed the costs of retrofit. We also conducted a sensitivity analysis to the local price of electricity for RO and MGO. This has been discussed in Appendix A 5.10.2.

2.4.5 Effect of Renewable Electricity Generation

We estimate the cost of supplying electricity to berthed ships via installing grid connected solar photovoltaic (PV) systems in the ports. The net cost of installing solar PV systems to the port including system capital cost, maintenance cost, feed-in revenue to the port and electricity procurement cost across the major ports is ~\$0.4B (see Appendix A 5.10.3). This translates to

annual amortized cost of \$52M-\$55M to the ports, net of the avoided cost of purchasing electricity. Since it is reasonable to assume that the marginal source of electricity at all locations in India is currently always unabated coal, a switch to a solar PV system sized to supply the annual demand for electricity for berthed ships would produce zero net emissions and completely eliminate the emissions generated by burning oil (RO/MGO). For ships burning RO, a switch to solar PV would avoid roughly 50 premature deaths each year (see Appendix A Table 5.45) resulting in a cost effectiveness of ~\$1M per premature death avoided. In the case of ships burning MGO, this will avoid roughly 20 premature deaths (see Appendix A Table 5.46) with a cost effectiveness of ~\$3M per premature death avoided.

2.5 Conclusions

Our results indicate that for most vessels, the cost to install the technology and enable the vessel to connect to shore power exceeds the net private benefit to vessel operators. The switch to shore power is unlikely to produce a net public benefit now or in the near future until the grid has become cleaner. On the basis of net private benefit, operators would choose to retrofit only about 0.2% of the vessels in our dataset to receive shore power. Thus, on its own, installation of the shore power infrastructure would not likely incentivize significant uptake of shore power use for vessels. In many cases, a shift to shore power would move pollution away from densely populated cities to the less densely populated areas where power plants are typically situated. Since it is impossible to quantify the effect of this shift without using chemical transport models, our analysis tacitly assumes that the ports and power plants are part of a single well-mixed cell. With this assumption, and given the current Indian electricity generation mix, we observe relatively modest public health benefits from a switch to shore power. Based on these results and without more detailed analysis—which our hourly emissions inventory could facilitate—the

government would be ill-advised to incentivize vessel retrofits or to construct the costly infrastructure needed to provide shore power. We identify several sources of uncertainty and Appendix A 5.10 discusses how we address them.

India's trade with China is growing at ~19% per year. ¹⁰⁶ China has declared DECAs across its coastline and is promoting shore power use. ¹⁰⁷ Here we have only accounted for vessel calls at major Indian ports. For vessels calling at both Chinese and Indian ports, and which have been retrofitted to receive shore power in response to Chinese regulations, it would be cheaper to use shore power at Indian ports than burning low sulfur fuel.

Our analysis provides some evidence that emissions at Indian ports could be cut by making ports more efficient. For example, our raw data suggest that at the port of New Mangalore, the loading and unloading rate in 2017 was ~10 containers per hour, compared to ~50 containers per hour at POLA in 2013.¹⁰⁸

In summary, until the bulk power supply in India is cleaned up, or ports develop their own cleaner sources of power, our study finds that switching berthed vessels to shore power at major ports in India is unlikely to yield a public benefit large enough to justify an investment that private sector actors are unlikely to make themselves. For this reason, national policy by GoI should focus on cleaning up the power sector in India.

2.6 Acknowledgements

This work was supported by the center for Climate and Energy Decision Making (SES-0949710), through a cooperative agreement between the National Science Foundation and Carnegie Mellon University. We thank officials from Government of India's Ministry of Shipping (Minister of Shipping; Secretary of Shipping; Joint Secretary-Ports), the Indian Ports Association (Managing Director and Executive Director), Port Trusts (Chairpersons and Traffic

Departments), Indian Coast Guard (Additional Director General and Staff Officers), and the Indian Army (Additional Director General of Artillery), who assisted us in obtaining the vessel call data used in this study. We also thank Deputy Conservators, and Research Divisions of all major ports in India. We thank Ankush Das for his inputs on developing the python web scraper. We acknowledge the advice of Dr. James J. Corbett; Dr. Anthony F. Molland; Dr. Louis Browning; Dr. Brett Goldsworthy; Guiselle Aldrete, and Abhijit Aul. We thank Bill Jackson and Laurent Cremillieux of Schneider Electric for shore power industry background information. We thank Dr. Jai Asundi and Parixit Chauhan for substation location data. We thank Christopher Oberschelp and Deependra Marwar for their inputs on coal fired electricity generation in India.

3 Chapter 3. Pollution from Freight Trucks in the Contiguous
United States: Public Health Damages and Implications for
Environmental Justice

Abstract

PM_{2.5} produced by freight trucking gives rise to significant adverse impacts on human health. Here we explore the spatial distribution of freight trucking emissions and demonstrate that the public health impacts disproportionately affect certain racial and ethnic groups. Based on the US federal government data, we quantify heterogeneity of trucking emissions and find that ~10% of NO_x and ~12% of CO_2 emissions from all sources in the US come from freight trucks annually. The environmental and climate social cost due to NO_x, PM_{2.5}, SO₂, and CO₂ from freight trucking in the US are estimated respectively to be \$11B, \$5.5B, \$100M, and \$25B (assuming a social cost of carbon of \$40 per ton). If a quarter of the freight currently carried on trucks could be moved to rail that would reduce PM_{2.5} emissions by 1.3%, NO_x emissions by 9%, and CO₂ emissions by 22%. Texas, Pennsylvania, Indiana, New Jersey, and New York export ~49% of total annual US trucking pollution damage, while at the same time Texas, New York, Pennsylvania, New Jersey, and Illinois import ~44% of total annual trucking pollution damage. We demonstrate that more freight pollution occurs in both counties and census tracts with a higher proportion of Black and Hispanic residents. A higher proportion of Black and Hispanic residents are also more likely to experience importers of pollution from other counties. Local agencies should consider these effects while evaluating the equity of prospective emissions reduction strategies.

This chapter is intended for submission to the Proceedings of the National Academies of Sciences (PNAS) as: "Lathwal P., Vaishnav P., Morgan M. G., Pollution from Freight Trucks in the Contiguous United States: Public Health Damages and Implications for Environmental Justice."

3.1 Introduction

Medium and heavy-duty vehicles (MHDVs) account for ~21% of transport sector's energy use¹⁰⁹ and ~24% of total transportation greenhouse gas (GHG) emissions.¹¹⁰ Transportation is the largest source of greenhouse gas emissions in the United States, accounting 29% of total emissions in 2019. They are also a major source of pollutants such as fine particulate matter (PM2.5), oxides of nitrogen (NOx), and GHGs, especially carbon dioxide (CO2).^{111,112} While reducing emissions from freight trucking is desirable, and mitigation costs are lower for road transport than for other modes⁴, the tight coupling between economic growth and road freight makes it difficult to achieve reductions.¹⁴ In 2017, the most recent year for which Commodity Flow Survey (CFS) data are available, freight trucks carried ~72% (\$10.4 trillion) of total domestic freight by value.¹¹³ Absent major policy interventions, as other transportation modes become cleaner, and the volume of freight truck VMT¹¹⁴ grows, the proportion of emissions from freight trucking will likely increase in the coming decades.

Air pollutant emissions have steadily declined in the US over the decades due to federal emissions control regulation such as the Clean Air Act (CAA)¹¹⁵, and the switch to ultralow sulfur fuel diesel (ULSD). ¹¹⁶ Yet, it is estimated that exposure to PM_{2.5} continues to cause between ~85,000 and 200,000^{117–119} premature deaths each year in the US. While current policies prioritize emissions reduction, they provide little guidance on addressing environmental justice when implementing air pollution reductions or on how to address distributional impacts. ¹²⁰ Even though absolute PM_{2.5} concentrations have declined by ~70% since early 1980s, ¹²¹ racial-ethnic and socio-economic disparities ^{122–126} continue to exist. ^{119,121} A recent paper by Tessum et al. ¹¹⁹

found higher than average PM_{2.5} exposures across minority groups in comparison to white population from different sources. Although the authors report overall disparity in exposure through population-weighted ambient concentrations, no study has explored the impacts of air pollution on racial and ethnic minorities from the freight trucking sector using a bottom-up inventory. Our analysis fills this gap.

The design of effective abatement policies to curtail air pollution from freight trucking requires granular and high-quality information on emissions from trucks. The most comprehensive publicly available emissions inventory in the US is produced by the Environmental Protection Agency (EPA) and is called the National Emissions Inventory (NEI). 127 This is a national compilation of emissions by the US EPA from different local agencies and is released approximately every 3 years (the most recent version is for 2017). For on-road mobile sources such as trucks, the EPA uses emissions reported by local agencies. ¹²⁸ As such, estimates can vary at the local level depending on the method used to aggregate emissions in different counties. Many counties do not report their information: just over 50% of the counties submitted information to EPA for compilation in NEI 2017.¹²⁸ For counties that do not submit data, EPA estimates county emissions based on historical information the EPA has for the county. As a result, there are methodological differences and potential inconsistencies in how the NEI estimates emissions for each county. Developing our own emissions inventory allows us to follow a methodologically consistent approach. The advantages of developing an emissions inventory from the "bottom-up" are well documented in the literature. 112,129,130 For instance, the US EPA distributes emissions based on road lengths and population and not on actual road activity. Consequently, this leads to the under-estimation of emissions on rural interstate

highways that are sparsely populated but are heavily traversed by freight trucks. Building a bottom-up emissions inventory allows us to avoid that.

In this study, we explore the environmental and public health impacts from freight trucking sector and make *three* contributions to the literature. First, we conduct a bottom-up assessment, which is spatially resolved and based on the most recently available national freight data, the Freight Analysis Framework Version 4 (FAF4),¹³¹ of freight trucking emissions for the contiguous US. We report environmental, climate, and public health air pollution monetized damages due to freight trucking at the county level for the contiguous states.

Second, we quantify the extent of air pollution health damages that are being exported from or imported to individual counties due to freight trucking activity. Since emission sources at distances as great as 800 km can cause air pollution related health damages ¹³², the burden of freight trucking on human health impacts that arise from emissions within and outside a county's boundary may be considerably different. We develop our estimates using publicly available data from the US federal government (FAF4 data) which we combine with the reduced complexity model (RCM) Estimating Air Pollution Social Impact Using Regression (EASIUR)^{133,134} and the source-receptor Air Pollution Social Cost Accounting (APSCA) model. ¹³² In doing so, we explore the spatial heterogeneity in air pollution damages at the county level based on source-receptor relationships. We focus on air pollution damages attributable to outdoor PM_{2.5} exposure because it is responsible for ~90% of all air pollution related health damages. ¹³⁵

Third, we perform the analysis at the resolution of individual counties and census tracts to estimate air pollution related health damages and distributional effects. We observe distributional impacts of air pollution across racial and ethnic groups both at the county and at the census tract resolution.

3.2 Materials and Methods

3.2.1 Study Area and Scope

Our study includes freight shipments in the 48 contiguous US states (excluding Alaska, Hawaii, Puerto Rico, and other US territories). **Figure 3.1** describes the method we use to compute trucking emissions, air pollution, and climate change damages. We consider the county as the basic unit of spatial resolution for calculating monetized damages and the census tract for the environmental justice results in our work. The reference year used in the study is 2017, as the latest year for which the national emissions inventory (NEI) is available. This allows us to compare our emissions results with the NEI. The approach we use to extract freight trucking emissions from the NEI is discussed in Appendix B 6.1.

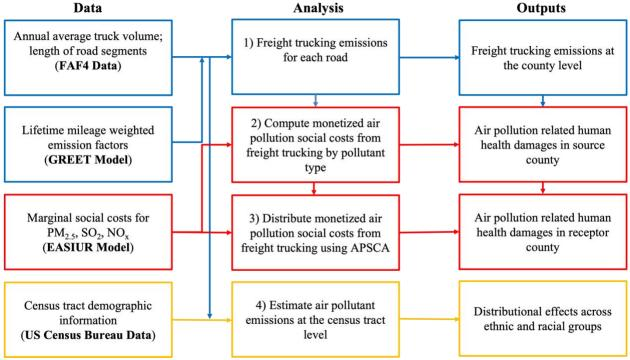


Figure 3.1 Step process detailing our modeling approach.

3.2.2 Data

We use the Federal Highway Administration's (FHWA's) FAF4 data¹³¹ to estimate freight flowing through 132 domestic zones in the US. It builds on the CFS data, ¹¹³ which is a publicly available dataset and provides information on national freight flows in the US. As a result, the FAF4 information is more comprehensive in coverage than the CFS data because it includes industries and shipments that are not included in CFS while providing shipment information at the county level. ¹³⁶ Although a more recent version of the Freight Analysis Framework Version 5 (FAF5) is available, it has yet to be updated with information on county level freight shipments. Thus, we use the FAF4 data throughout the analysis except for our analysis of modal shift to class-1 railroads where we use the CFS data. Additionally, FAF4 data includes a shape file of FAF4 zones providing detailed information on the road network (~446,000 miles; see

Figure 3.2(A)) and relevant freight attributes such as the annual average daily traffic volumes on road segments, road lengths and route type. The distribution of trucking VMT by road type is included in Appendix B 6.2. To explore the environmental justice implications of air pollution related damages, we use census data from the US Census Bureau. ¹³⁷

3.2.3 Estimating freight trucking VMT

Road length: The FAF4 road network data consist of road links (RLs) and average daily long distance and local truck traffic counts for different freight vehicles in 2012. We estimate the route road length (in miles) for each road link by taking the difference between the starting and ending mile posts reported in the data for each road link. We dropped 94 out of 670,045 road links for where the result is a negative road length, which we assume to be an error in recording the observations. Links with negative lengths account for ~0.01% of the total so that dropping them should have a negligible effect on the results.

Annual average truck counts: For determining vehicle categories for freight truck counts, we assume that all long-haul highway trips are conducted by heavy duty tractor-trailer diesel trucks (class 8b or above) whereas all non-long haul (local) highway freight trips are conducted by single unit trucks (class 6 trucks). Since freight trucking is mostly diesel powered, we assume based on Bickford et al. 130 that 98% of all trucks in our freight data are diesel trucks.

Furthermore, the reported average daily truck counts include non-cargo freight vehicles such as commuter and transit buses. In 2012, there were 765,000 bus registrations out of ~58 million truck registrations (excluding sport utility vehicles, vans, and other light vehicles). 138,139 Thus, to exclusively reflect diesel cargo freight trucks in our truck counts and remove the effect of buses and other non-cargo vehicles, we adjust the daily average truck count on each road link by subtracting 1% of total vehicle counts on each link. Mathematically, we express annual MHDV daily truck traffic on each road link as:

Equation 3.1

$$MHDV_{i,daily} = FAFAADTT_{i,daily} * DF * TF$$

Where,

 $MHDV_{i,daily}$ is the daily average MHDV count on a road link i (expressed as volume per day per section of the road)

 $FAFAADTT_{daily}$ is the FAF4 annual average daily truck traffic for long-distance and non-long distance freight trucks on road link i (expressed as volume per day per section of the road)

DF is the diesel fraction to adjust vehicle counts to include only diesel freight trucks and its value is assumed to be 0.98 from literature¹³⁰

TF is the truck fraction to remove the effect of commuter and transit buses from the annual average daily truck traffic counts. Its value is assumed to be ~0.99 based on the vehicle registration data

Annual Freight Trucking Vehicle Miles Traveled: We estimate the daily medium and heavy-duty vehicle miles traveled (MHDVMT) for each road link by multiplying MHDV_{i,daily} by the length of the road segment. We annualize the VMT on each road link by multiplying by 365. However, the MHDVMT obtained is for the year 2012, and the base year of our analysis is 2017. Using annual VMT data¹⁴⁰ provided by the US Department of Transportation (DOT), we estimate compounded annual growth rate (CAGR) increase in MHDVMT between 2012 and 2017. The MHDVMT in 2017 for each road link is then estimated as:

Equation 3.2

$$MHDVMT_{i} = MHDV_{i,daily} * RL_{i} * Year_{days} * GF_{VMT}$$

Where,

 \textit{MHDVMT}_i is the annualized VMT for medium and heavy-duty vehicles in 2017 for each road link i

 $MHDV_{i,daily}$ is the daily average medium and heavy-duty vehicle count on a road link i (expressed as volume per day per section of the road)

RL is length of the road segment (in miles) for each road link i

 $Year_{days}$ is 365, the number of days in a year

 $GF_{VMT} = (1 + CAGR_{VMT})^{2017-2012}$ is the growth in MHDVMT between 2012 and 2017. $CAGR_{VMT}$ is estimated to be 2% each year based on authors' calculations from freight trucks' VMT data¹⁴⁰ provided by the US DOT.

3.2.4 Estimating spatially resolved emissions arising from freight trucking

We estimate spatially resolved emissions at the county level for PM_{2.5}, SO₂, NO_x, and CO₂ in each county by multiplying MHDVMT by the lifetime VMT weighted emission factors (in g/mile) from the Greenhouse Gases, Regulated Emissions, and Energy Use in Transportation (GREET) model¹⁴¹ (see Appendix B 6.3) for all the road segments contained in the county. For PM_{2.5} emissions, we include tire and break wear emissions in addition to primary PM_{2.5} emissions. Absent better data, we use a constant emission factor irrespective of whether the road is in an urban or rural area, even though emission factors may likely be higher in urban areas. To examine the implications of doing this, we perform a sensitivity analysis with a different set of emission factors for heavy duty trucking. The results are included in Appendix B 6.3. We sum the air pollutant and GHG emission estimates from road links within a county to estimate county level total for 2017. The emissions at the county level are estimated as:

Equation 3.3

$$E_{k,p} = \sum_{i \in K} MHDVMT_i * EF_p$$

Where,

 $E_{k,p}$ is the total MHDV emissions (in tons) for pollutant p (PM_{2.5}, SO₂, NO_x, CO₂) in each county, k

 $MHDVMT_i$ is the VMT on road segment i for MHDVs

 \mathbf{EF}_{p} is the emission factor (in g/mile) for pollutant \mathbf{p} for the freight truck category under consideration

K is the set of all road segments i contained within county k. The sum is performed over all the road segments i that are contained within the county k

3.2.5 Estimating public health and climate damages due to freight trucking

Using state-of-the-art chemical transport models (CTMs) to estimate the concentration of air pollutants that results from emissions is very computationally intensive. In order to reduce the computational burden for policy analysis, air quality researchers have developed integrated RCMs to estimate monetized air pollution damages. RCMs divide the entire US into a grid of cells and include a set of look up tables of marginal social costs (MSC; in US \$ per ton of pollutant emitted) for emissions associated with each grid cell. For our analysis, we assume that trucking emissions are marginal so that the public health damages due to CAPs are a simple product of total emissions and MSC for a given pollutant species, location, and height. While the MSC for CAPs is sensitive to location and height, the MSC for CO₂ does not depend on these factors, and we estimate damages from CO₂ emissions by multiplying emissions by a social cost of carbon (which we assume to be \$40 per ton CO₂). 142

We use an RCM called EASIUR^{133,134} to estimate marginal damages due to primary PM_{2.5}, SO₂, and NO_x. for 148*112 cells with each grid cell 36 km*36 km in size. Since we are interested in on-road freight transport emissions, we use the annual MSC associated with all area sources with a zero-stack height. We ignore seasonal variation. Next, we conduct an overlay analysis and find how much of each county's area lies within the bounds of each grid cell. We repeat this exercise for each grid cell in the contiguous US and distribute the marginal social costs through a weighting factor based on the area of county contained in each grid cell. Finally, we calculate the marginal damages as a product of the MSC in each county multiplied by the emissions of a particular pollutant species at a given location. EASIUR assumes a value of statistical life (VSL) of \$8.6M (2010 US \$) and a social cost of carbon of \$40 per ton of CO₂. ¹⁴³ The marginal damages are then converted to 2017 dollars using the Consumer Price Index (CPI). ¹⁴⁴

Mathematically, this can be expressed as:

Equation 3.4

$$MD_p = \sum_{k} MSC_{k,p} * E_{k,p} * f_{CPI}$$

Where,

 MD_p is the marginal damage in 2017 dollars for the US for pollutant \mathbf{p} (PM_{2.5}, SO₂, and NO_x)

 $MSC_{k,p}$ is the marginal social cost in county k for pollutant p (expressed in US p per ton of pollutant emitted)

 $\boldsymbol{E}_{\boldsymbol{k},\boldsymbol{p}}$ is the emissions for county \boldsymbol{k} for pollutant \boldsymbol{p} (expressed in tons)

 f_{CPI} is the consumer price index adjustment for 2017 (constant value)

EASIUR provides an estimate of all the damages that occur everywhere from the emissions that *originate* within county, regardless of where those damages occur. To understand *where* damages occur, we employ source-receptor relationships from the APSCA model to spatially disaggregate social cost of pollutants. As a boundary check, we also calculate air pollution damage estimates from freight trucking at the source counties using another RCM called the Air Pollution Emission Experiments and Policy Version 3 (AP3). In both cases, we find reasonable consistency. The results of the comparison of the public health damages from freight trucking are included in Appendix B 6.4.

3.2.6 Emissions reduction due to modal shift to rail

According to the Association of American Railroads (AAR), US railroads move a ton of freight roughly 472 miles with a gallon of diesel fuel. ¹⁴⁶ Thus, shifting freight tonnage from diesel freight trucks to class-1 railroads holds significant potential for GHG mitigation. We assume that all trips greater than 300 miles might be shifted to rail and use data from CFS 2017. CFS

provides information on 5,978,523 shipments and each shipment record has shipment value along with a weighting factor. Multiplying the shipment value with the assigned weighting factor allows us to estimate total ton-miles shipped each year for trips.¹⁴⁷ This can be expressed as:

Equation 3.5

$$Ton-miles_l = \sum_{s=1}^{n} Weighting \ Factor_l * \left(rac{Shipment \ Weight_l}{2000}
ight) * Shipment \ Distance \ Routed_l$$

Where,

 $Ton-miles_l$ are ton-miles of shipment l

Weighting Factor $_{l}$ is the weighting factor of shipment l

Shipment Weight_l is the weight of the shipment l. We divide this by 2000 since the shipment weight is in pounds

Shipment Distance Routed $_l$ is the routed distance between the origin and destination of the shipment l

We assume that all freight trucking beyond 300 miles is conducted by long-haul heavy-duty tractor-trailer diesel trucks and assume that each truck carries on average 20 tons of freight. The approach used to estimate emissions factors (in g/ton-mile) both for heavy duty diesel truck and Class 1 railroad is provided in Appendix B 6.5. Next, we estimate total emissions for PM_{2.5}, SO₂, NO_x, and CO₂ for freight trucks and rail. Finally, we estimate the percentage change that results from a switching 5% to 50% of ton-miles from freight trucks to rail.

3.2.7 Impact of freight trucking pollution across demographic groups

While the monetized environmental and climate change impacts are felt across different geographical sub-units, here, we focus on the distributional effects of freight trucking emissions on different ethnic and racial subgroups. This is important because the literature shows that, historically, adverse air pollution-related health impacts have been inequitable. 122–126 To evaluate

46

differences in the impacts of pollution from freight trucking on different racial groups, we use county level population data from US Census Bureau's 2010 decennial census. ¹³⁷ Based on county as the unit of spatial aggregation, we focus on seven self-identified racial and ethnic subgroups, selected so that they are mutually exclusive: (1) Black or African American alone (variable code P003003), (2) Hispanic or Latino origin by race (variable code P005010), (3) American Indian and Alaskan Native alone (variable code P003004), (4) Asian alone (variable code P003005), (5) Native Hawaiian and Other Pacific Islander alone (variable code P003006), (6) some other race alone (variable code P003007), and (7) two or more races (variable code P003008). We model emissions for pollutant p (PM2.5, SO2, and NOx) in county c as a function of the demographic and other attributes of the census tract where the emissions occur and an unobserved error term ($\epsilon_{p,c}$). β is the modeled coefficient for each corresponding independent variable X for county c. The model specification is:

Equation 3.6

$$\begin{split} Y_{p,c}(X) &= \beta_0 + \beta_{area} log(X_c^{area}) + \beta_{black} X_c^{black} + \beta_{amerind} X_c^{amerind} + \beta_{haw} X_c^{haw} \\ &+ \beta_{asian} X_c^{asian} + \beta_{hisp} X_c^{hisp} + \beta_{twomore} X_c^{twomore} + \beta_{totpop} log(X_c^{totpop}) \\ &+ \beta_{medinc} log(X_c^{medinc}) + \epsilon_{p,c} \end{split}$$

Where,

 $Y_{p,c}$ is the log of freight trucking emissions for pollutant p (PM_{2.5}, SO₂, and NO_x) in county c X_c^{area} is the area of the county c

 X_c^{black} is the proportion of the total population in county c that is black

 $X_c^{amerind}$ is the proportion of the total population in county c that is American Indian and Alaska native

 X_c^{haw} is the proportion of the total population in county c that is Hawaiian and other Pacific Islanders

 X_c^{asian} is the proportion of the total population that is Asian in county c

 X_c^{hisp} is the proportion of the total population in county c identifying as Hispanic or Latino $X_c^{twomore}$ is the proportion of the total population identifying in county c as having two or more races

 X_c^{totpop} is the total population in county c

 X_c^{medinc} is the median income of the house hold in county c

We then perform the same analysis at the census tract level. To calculate the emissions that occur within each census tract, we download census tract shapefiles from the U.S. Census Bureau. ¹⁴⁸ Using the shapefile of the FAF4 road network, we estimate the centroid of each road segment. We then use the "rgeos" package in the R programming environment to identify which census tract each road segment centroid is located in. We repeat the calculations described in **Equation 3.3** of section **3.2.4** but sum the emissions that occur along each road segment over all the road segments that fall within a census tract (instead of summing over all the road segments that fall within a county).

Finally, the effect of trucking emissions on minority populations in the census tract is evaluated using linear regression. We model emissions for pollutant p (PM_{2.5}, SO₂, and NO_x) in census tract t as a function of the demographic and other attributes of the census tract where the emissions occur and an unobserved error term $(\epsilon_{p,t})$. β is the modeled coefficient for each corresponding independent variable X for census tract t. The model specification is:

Equation 3.7

$$\begin{split} Y_{p,t}(X) &= \beta_0 + \beta_{area}log(X_t^{area}) + \beta_{black}X_t^{black} + \beta_{amerind}X_t^{amerind} + \beta_{haw}X_t^{haw} \\ &+ \beta_{asian}X_t^{asian} + \beta_{hisp}X_t^{hisp} + \beta_{twomore}X_t^{twomore} + \beta_{totpop}log(X_t^{totpop}) \\ &+ \beta_{medinc}log(X_t^{medinc}) + \beta_{GDP}log(X_t^{GDP}) + \epsilon_{p,t} \end{split}$$

Where,

 $Y_{p,t}$ is the log of freight trucking emissions for pollutant p (PM_{2.5}, SO₂, and NO_x) in census tract t

 X_t^{area} is the area of the census tract t

 X_t^{black} is the proportion of the total population in the census tract t that is black

 $X_t^{amerind}$ is the proportion of the total population in the census tract t that is American Indian and Alaska native

 X_t^{haw} is the proportion of the total population in the census tract t that is Hawaiian and other Pacific Islanders

 X_t^{asian} is the proportion of the total population that is Asian in census tract t

 X_t^{hisp} is the proportion of the total population in census tract t identifying as Hispanic or Latino

 $X_t^{twomore}$ is the proportion of the total population identifying in census tract t as having two or more races

 X_t^{totpop} is the total population in census tract t

 X_t^{medinc} is the median income of the house hold in census tract t

 X_t^{GDP} is the GDP of the county where the census tract t is located

To assess what factors affect whether the county where the census tract is located is a net importer or exporter, we run a logit model specification which is expressed as:

Equation 3.8

$$\begin{split} logit\left(p_{p,t}(x)\right) &= log\left(\frac{p(x)}{1-p(x)}\right) = \eta_{p,t}(x) \\ \eta_{p,t}(x) &= \beta_0 + \beta_{area}log(X_t^{area}) + \beta_{black}X_t^{black} + \beta_{amerind}X_t^{amerind} + \beta_{haw}X_t^{haw} \\ &+ \beta_{asian}X_t^{asian} + \beta_{hisp}X_t^{hisp} + \beta_{twomore}X_t^{twomore} + \beta_{totpop}log\left(X_t^{totpop}\right) \\ &+ \beta_{medinc}log\left(X_t^{medinc}\right) + \beta_{GDP}log\left(X_t^{GDP}\right) + \epsilon_{p,t} \end{split}$$

Where,

p(x) is the probability of the county where the census tract t is located of being a net importer or exporter for pollutant p (PM_{2.5}, SO₂, and NO_x)

 X_t^{area} is the area of the census tract t

 X_t^{black} is the proportion of the total population in the census tract t that is black

 $X_t^{amerind}$ is the proportion of the total population in the census tract t that is American Indian and Alaska native

 X_t^{haw} is the proportion of the total population in the census tract t that is Hawaiian and other Pacific Islanders

 X_t^{asian} is the proportion of the total population that is Asian in census tract t

 X_t^{hisp} is the proportion of the total population in census tract t identifying as Hispanic or Latino

 $X_t^{twomore}$ is the proportion of the total population identifying in census tract t as having two or more races

 X_t^{totpop} is the total population in census tract t

 X_t^{medinc} is the median income of the house hold in census tract t

 $\boldsymbol{X_t^{GDP}}$ is the GDP of the county where the census tract t is located

3.3 Results

3.3.1 Freight Trucking Emissions in the US

Table 3.1 shows freight trucking emissions for the year 2017. We also compare these estimates with available values from the US EPA's economy wide NEI 2017. While the methods and scales used in compiling NEI 2017 are different than those for the FAF4 data, the comparison serves as a check that results are comparable. We observe that NO_x and CO₂ emissions from diesel freight trucks are a non-trivial share of total US emissions. The estimated emissions diverge from values estimated by 2017 NEI between 11% and 47% for different pollutants and the directionality of the difference is not preserved across pollutant/ GHG type. The largest differences arise for PM_{2.5} (FAF4 less by 46%) and CO₂ (FAF4 larger by 47%). There are several possible reasons for this. First, we observe that VMT estimated from FAF4 data is ~30% larger than the VMT reported for 2017 by US Department of Transportation (DOT). 140 This VMT difference is propagated in the analysis when we estimate emissions for different pollutants and GHGs in our work. Second, FAF4 models truck-counts and distributes them into long distance and non-long-distance freight routes whereas the NEI estimates are based on the Highway Performance Monitoring System (HPMS) data that are supplied to MOtor Vehicle Emission Simulator (MOVES) model to estimate VMT across counties. ¹⁴⁹ Accordingly, there is an underlying difference in how VMT estimates are measured in the two datasets. Third, FAF4 provides an average daily vehicle count on each road segment but provides no information on the type of vehicle category traveling on the roads. Hence, it is challenging to determine the type of truck and to use specific vehicle emission factors for other vehicle categories such as refuse trucks. Finally, FAF4 excludes idling emissions and intra-FAF zone trips less than 50 are not included in the FAF4 data.

Table 3.1 Freight trucking emissions comparison between FAF4 and NEI for 2017. NO_x and CO_2 constitute a non-trivial share of US emissions. The difference in estimates column provides the percentage difference of FAF4, 2017 diesel truck emission estimates from NEI, 2017 diesel truck emission values. The estimates in the last two columns provide percentage contribution of freight trucking emissions to total US emissions from FAF4 and NEI data. These are obtained by dividing the FAF4 and NEI freight trucking emissions by emissions from all sources in NEI, 2017.

Pollutan t	FAF4 freight trucking emissions (in tons)	NEI freight trucking emissions (in tons)	% Diff	Total NEI emissions (tons)	% US emissions from MHDVs in FAF4 data	% US emissions from MHDVs in NEI data
PM _{2.5}	28K	51K	-46%	5.2M	0.53%	1.0%
SO ₂	4.6K	3.7K	24%	2.5M	0.18%	0.10%
NO _x	1.1M	1.3M	-11%	11M	10%	12%
CO ₂	640M	430M	47%	5.3B	12%	8.2%

3.3.2 Environmental Impacts of Freight Trucking

Figure 3.2(B-D) shows county level spatial distribution of PM_{2.5}, NO_x, and SO₂ emissions from MHDV trucking. Based on where the freight trucking activity occurs, we observe that NO_x trucking emissions are high in counties in the northeast, southern, and western parts of the US. The emissions burden is highest in the counties that include the road network in the FAF4 network (see **Figure 3.2(A)**).

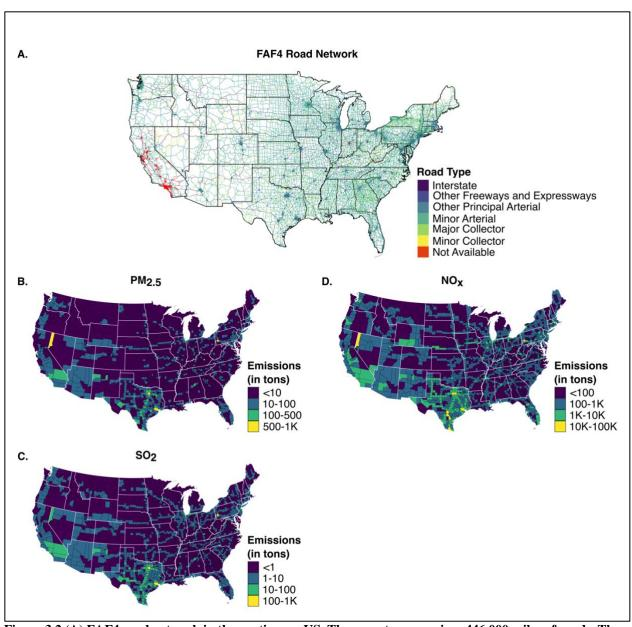


Figure 3.2 (A) FAF4 road network in the contiguous US. These routes comprise ~446,000 miles of roads. The dataset includes interstate highways, national highway system (NHS) roads, rural and urban principal arterials along with intermodal connectors. (b, c, d) $PM_{2.5}$, SO_2 , and NO_x emissions (in tons) from freight trucks at the county level in the US in 2017. (B-D) County level spatial distribution of $PM_{2.5}$, $PM_{2.5}$,

3.3.3 Spatially Resolved Public Health Impacts of Freight Trucking

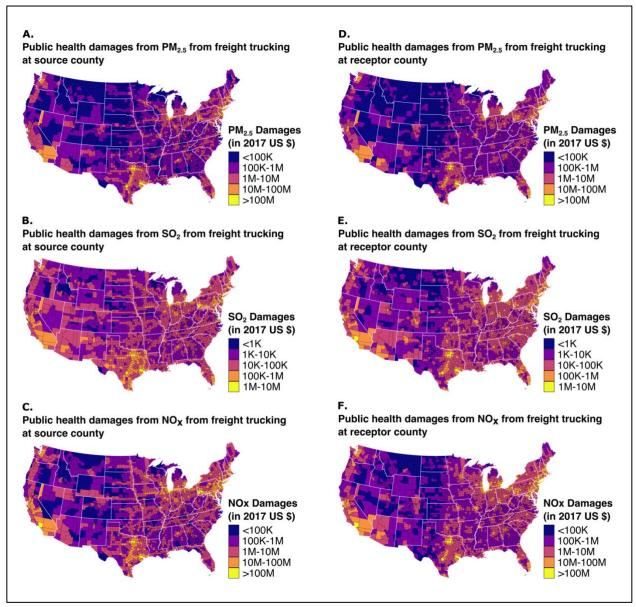


Figure 3.3 (A-C) Public health damages from $PM_{2.5}$, SO_2 , and NO_x due to freight trucking aggregated at the source counties. The source county damage shows total air pollution damage that occurs across all other counties due to the freight trucking activity originating from the source county. It includes the air pollution damage that occurs from the county within itself. (D-F) Public health damages from $PM_{2.5}$, SO_2 , and NO_x due to freight trucking aggregated at the receptor counties. The receptor damage at a county includes total air pollution damage due to freight trucking activity occurring in other counties. It includes the damage that occurs within the receptor county due to freight trucking activity within the receptor county.

We estimate the total annual public health damage resulting from diesel trucks for PM_{2.5}, SO₂, and NO_x, to be \$5.5B, \$100M, \$11B, respectively, and the societal damage from CO₂ emissions

to \$25B, assuming a social cost of carbon of \$40 per ton. 143 While the numbers for PM_{2.5}, SO₂, and NO_x, are estimates of the human health damage that occurs everywhere from emissions that originate in each county, here we also estimate the damages that occur within each county from the emissions within that county and from other counties. This allows us to estimate the total damage that occurs within each county and whether the county is a net importer or exporter of air pollution damages. We do so by disaggregating these damages using APSCA. APSCA provides receptor resolved air pollution damages at the county level. Figure 3.3(A-C) show public health PM_{2.5}, SO₂, and NO_x damages resolved at the source counties due to freight trucking in the US for 2017. This is the total damage from emissions that originate in a particular county and includes the damage caused by source county emissions activity within the county itself. If we exclude the air pollution damage that the source county causes within itself, we observe that the counties located in the states of Texas (\$3.4B), Pennsylvania (\$1.5B), Indiana (\$1.1B), New Jersey (\$1B), and New York (\$800M) contribute ~49% of all exported air pollution related damages occurring in the US. A map of net exporter and net importer counties is included in Appendix B Figure 6.2.

Figure 3.3(D-F) show public health PM_{2.5}, SO₂, and NOx damages resolved at the receptor counties due to freight trucking in the US for 2017. This is the total damage a county receives from emissions occurring in other counties, including from the emissions that occur within the county. Cumulatively, the counties located in the states of Texas (\$2.7B), New York (\$1.4B), Pennsylvania (\$1.1B), New Jersey (\$930M), and Illinois (\$850M) receive ~44% of all imported annual air pollution damage due to freight trucking in the contiguous US.

3.3.4 Modal shift from freight trucks to Class-1 railroads

The relationship between the ton-miles shifted to rail and emissions reduction is linear. If we move 5% and 50% of the total ton-miles in the CFS that are hauled by freight trucks to Class-1 rail, we observe a reduction of SO₂ emissions (4% to 43% reduction) and CO₂ emissions (4% to 43% reduction). However, the shift in ton-miles does not reduce PM_{2.5} appreciably (see Appendix B Figure 6.4). We also do not calculate how the distribution of emissions would change if freight were shifted to rail, but it is possible that such a shift might also have adverse distributional outcomes.

3.3.5 Environmental Justice Implications

While it is difficult to accurately determine air pollutant exposure concentrations without running a CTM, the results included below provide a first order estimate of air pollution emissions in counties and census tracts where minority population groups reside. We observe that freight trucking emissions of PM_{2.5}, SO₂, and NO_x are significantly higher in counties with higher Black and Hispanic populations (**Table 3.2**). This effect is also preserved at the census tract level (**Table 3.3**). If the Black population in the county increases by 1 percentage point, the emissions in that county are 1.8 (1.1-2.9) percentage points higher. Similarly, if the Hispanic population in the county increases by 1 percentage point, then the emissions in that county are 20 (14-28) percentage points higher. The effect of emissions also decreases in census tracts that have higher average household median income in the census tract (0.1% decrease in emissions for a percentage point increase in average median household income). A detailed description of the distribution of the dependent and independent variables including additional diagnostic testing is enclosed in Appendix B 6.6.

Table 3.2 Effect of freight trucking PM_{2.5}, SO₂, and NO_x emissions on racial and ethnic subgroups at the county level. The dependent variable is the log of PM_{2.5}, SO₂, and NO_x emissions emitted by freight trucks in counties. For predictor variables that are log values, the relationship can be estimated as $\%\Delta Y_p = \%\beta \times \Delta X_c$.

For predictors that are not log values, the relationship is estimated as $\%\Delta Y_p = 100 \times (e^{\beta}-1)$. These numbers are statistically significant and the numbers in the parenthesis show 99% confidence intervals.

Duedistans	$Y_p(X) = \log(\text{PM}_{2.5})$	$Y_p(X) = \log(NO_x)$	$Y_p(X) = \log(SO_2)$
Predictors	β Estimates	β Estimates	β Estimates
(Intercept)	-21.06 (-23.44, -18.68)	-19.42 (-22.22, -16.62)	-23.16 (-25.60, -20.72)
$log(X_c^{area})$	0.33 (0.28, 0.38)	0.35 (0.29, 0.41)	0.33 (0.28, 0.39)
X_c^{black}	1.06 (0.75, 1.36)	1.08 (0.72, 1.44)	1.06 (0.74, 1.37)
$X_c^{amerind}$	-0.19 (-0.86, 0.47)	-0.26 (-1.04, 0.52)	-0.21 (-0.89, 0.47)
Xhaw	-31.36 (-69.62, 6.91)	-29.58 (-74.67, 15.51)	-31.07 (-70.30, 8.15)
Xasian	-5.16 (-7.70, -2.62)	-6.13 (-9.12, -3.13)	-5.32 (-7.92, -2.72)
X ^{twomore}	-4.06 (-8.46, 0.33)	-3.62 (-8.80, 1.56)	-4 (-8.50, 0.51)
X_c^{hisp}	3.05 (2.72, 3.38)	3.13 (2.74, 3.52)	3.07 (2.73, 3.41)
$\log(X_c^{medinc})$	0.76 (0.56, 0.97)	0.87 (0.63, 1.11)	0.78 (0.57, 0.99)
$\log(X_c^{totpop})$	0.64 (0.61, 0.68)	0.66 (0.62, 0.70)	0.64 (0.61, 0.68)
Observations	3106	3106	3106
R ² /R ² adjusted	0.499 / 0.498	0.437 / 0.435	0.489 / 0.488

Table 3.3 Effect of freight trucking PM_{2.5}, SO₂, and NO_x emissions on racial and ethnic subgroups at the census tract level. The dependent variable is the log of PM_{2.5}, SO₂, and NO_x emissions emitted by freight trucks in census tracts. For predictor variables that are log values, the relationship can be estimated as $\%\Delta Y_p = \%\beta\times\Delta X_t$. For predictors that are not log values, the relationship is estimated as $\%\Delta Y_p = 100\times(e^\beta-1)$. These numbers are statistically significant and the numbers in the parenthesis show 99% confidence intervals.

Duodiatana	$Y_p(X) = \log(\text{PM}_{2.5})$	$Y_p(X) = \log(NO_x)$	$Y_p(X) = \log(SO_2)$
Predictors	β Estimates	β Estimates	β Estimates
(Intercept)	-12.50 (-13.02, 11.97)	-9.59 (-10.16, -9.02)	-14.42 (-14.95, -13.89)
$log(X_t^{area})$	0.50 (0.48, 0.51)	0.54 (0.52, 0.55)	0.50 (0.49, 0.51)
X_t^{black}	0.75 (0.66, 0.84)	0.79 (0.69, 0.89)	0.75 (0.66, 0.84)
$X_t^{amerind}$	-0.68 (-1.02, -0.33)	-0.79 (-1.17, -0.41)	-0.69 (-1.04, -0.34)
X_t^{haw}	-2.79 (-7.54, 1.95)	-3.70 (-8.86, -1.46)	-2.92 (-7.71, 1.87)
X_t^{asian}	-0.80 (-1.04, -0.55)	-0.61 (-0.88, -0.34)	-0.77 (-1.02, -0.52)
$X_t^{twomore}$	-9.05 (-10.24, -7.86)	-9.01 (10.30, -7.71)	-9.04 (-10.24, -7.83)
X_t^{hisp}	0.64 (0.54, 0.74)	0.73 (0.63, 0.84)	0.66 (0.56, 0.75)
$\log(X_t^{totpop})$	0.24 (0.21, 0.27)	0.24 (0.20, 0.28)	0.24 (0.20, 0.28)
$\log(X_t^{medinc})$	-0.10 (-0.14, -0.05)	-0.12 (-0.17, -0.07)	-0.10 (-0.14, -0.05)
$\log(X_t^{GDP})$	0.05 (0.04, 0.06)	0.05 (0.03, 0.06)	0.05 (0.04, 0.06)
Observations	57766	57766	57766
R ² /R ² adjusted	0.23/0.23	0.224/0.224	0.230/0.229

We also run a model specification (**Table 3.4**) to gauge whether a county is likely to be an exporter or importer based on the total air pollution damage that the county imports or exports. We observe that census tracts with Black, American Indian, and two or more non-white populations have higher odds of being an importer of air pollution damage due to freight trucks.

Table 3.4 Odds ratios of a county being an importer. These numbers are statistically significant and the numbers in the parenthesis show 99% confidence intervals.

Predictors	Odds ratio of being an importer
(Intercent)	0.02 (0.01, 0.03)
(Intercept)	· · · · · · · · · · · · · · · · · · ·
$log(X_t^{area})$	0.94 (0.92, 0.95)
X ^{black}	2.48 (2.19, 2.80)
$X_t^{amerind}$	2.02 (1.38, 3.00)
X_t^{haw}	0 (0.00, 1.75)
X_t^{asian}	0.94 (0.66, 1.34)
$X_t^{twomore}$	49.18 (11.26, 215.72)
X_t^{hisp}	0.32 (0.28, 0.35)
$\log (X_t^{totpop})$	0.95 (0.91, 0.99)
$\log (X_t^{medinc})$	1.21 (1.14, 1.28)
$\log (X_t^{GDP})$	1.32 (1.30, 1.34)

3.4 Conclusions and Policy Implications

Our results suggest that freight trucking contributes significantly to NO_x and CO₂ emissions in the contiguous US. A potential medium-term solution is to shift a fraction of the freight from trucks to railroads to reduce GHG emissions.

We also find that more freight trucking emissions occur in census tracts containing larger proportions of Black and Hispanic populations. While such disproportionate air pollution impacts have been noted in general terms in the research literature, our work documents this effect arising specifically from trucking sector in our work. This disproportionate effect is the result of years of racially and other socially insensitive infrastructure citing policy. ^{150,151} Our

findings indicate that areas with higher proportions of minority populations have higher likelihood of being an importer of air pollution damages. Therefore, local governments should consider conducting more research in areas with high trucking activity emissions to examine whether there are ways to reduce some of the air pollution effects felt by vulnerable population groups. This work also has implications for local governments trying to formulate future emissions reduction policies, especially when air pollution arises from geographical areas that are not within their administrative control.

3.5 Acknowledgements

This work was supported by the center for Climate and Energy Decision Making (SES-0949710), through a cooperative agreement between the National Science Foundation and Carnegie Mellon University. We thank Mr. Chester Ford and Mr. Birat Pandey at the Federal Highway Administration for their help with understanding the FAF4 dataset and the underlying assumptions. We also thank Peter Tschofen, Jinhyok Heo, Erin Mayfield, Brian Gentry, Nicholas Z. Muller, and Peter J. Adams for their suggestions on using reduced complexity models.

4 Chapter 4: Conclusions and Policy Implications

In this brief final chapter, I summarize the key findings of my work and outline how I believe it is relevant for policymakers involved in public decision-making.

In Chapter 2,²⁹ I find that given the current generation mix in India, switching to shore-power will be ineffective in improving local air quality in India. The reduction in premature mortality is likely small. These results ought to prompt a reevaluation of the Government of India's (GoI's) preferred strategies for reducing urban air pollution, as they have already started deploying shore power infrastructure at ports in India. More generally, the findings of our work are likely to be applicable to developing countries with a dominant fossil-fuel-based electricity generation mix where the location of population, ports, and generators are not widely separated. Governments in such situations should consider prioritizing investments to reduce the emissions intensity of the power generation sector before or at least in parallel with efforts to electrify other sectors. In Chapter 3, I develop an approach to estimate the annual monetized impact of air pollution damages due to freight trucking. The monetized environmental and climate air pollution damages due to freight trucking roughly amount to \$40B each year. This is approximately a third of total transportation related air pollution damages in the US (~\$120B). These social costs can be expected to increase each year with burgeoning consumer demand and uptake in ecommerce. We also find that NO_x and CO₂ emissions and related public health damages arising from freight trucking contribute an important share of total US emissions and will likely increase as a proportion of economy-wide emissions in the coming decades. As the Biden Administration puts in place policies to decarbonize the electricity system by 2035, ¹⁵³ devising a feasible strategy to reduce the emissions intensity of medium and long-haul trucking should play a crucial role in meeting those goals successfully. Our results also show that air pollution due to freight

trucking disproportionately impacts people of color: more freight pollution occurs in census tracts with a higher proportion of Black residents. Counties with a higher proportion of Black and Hispanic residents are more likely to be importers of pollution from other counties. This finding is timely because the Biden administration is working on an infrastructure deal¹⁵⁴ that provides ~\$580B over a decade for repairing and rebuilding the nation's highways, bridges, railroads, and other essential services. Therefore, it is an opportune moment to undo the harm caused by decades of socially unjust and racially insensitive infrastructure policies.

There has been a rush amongst truck manufacturers towards making electric and autonomous trucks. However, this has been subject to much hype over the years. ¹⁵⁵ Future work that I plan, that is described in **Appendix C**, will allow me to assess the consequences of shifting to electric autonomous freight trucking. In that work, I will seek to evaluate where long-haul electric trucking technology stands today and assess automated trucks in terms of their potential social benefits and costs.

5 Appendix A: Supplementary Information for Chapter 2

5.1 IMO MARPOL history and population densities of major port cities

5.1.1 IMO International Convention for the Prevention of Pollution from Ships (MARPOL)

Annex VI "Regulation for the Prevention of Air Pollution from Ships" of MARPOL regulates the international standards for NO_x, SO_x, and PM emissions from ships. As of October 22, 2019, the convention has been ratified by 158 contracting states and covers ~99% of the gross tonnage of world's merchant fleet. The Annex VI standards were developed in 1997 and came into effect starting 2005 which were then revised and adopted in October 2008. Finally, the revised regulation came into effect in July 2010. Among the key developments were the introduction of emission control areas (ECAs) to reduce air pollution in ecologically sensitive sea areas as well as the introduction of a global sulfur cap in marine fuel use. The global sulfur limit was reduced from 3.50% to 0.50% from 1 January 2020 onwards.

Table 5.1 gives a list of ECAs across the world. Also, there are three regional domestic emission control areas (DECAs)¹⁵⁹ in China covering Yangtze River Delta, the Bohai Rim, and the Pearl River Delta that aren't under the regulatory oversight of IMO MARPOL Annex VI.

Table 5.1 List of ECAs adoption, their entry into force, and the effective date of implementation. The table has been adapted from IMO website. 160

Special Areas	Adopted	Date of Entry into Force	In Effect From
Baltic Sea (SO _x) Baltic Sea (NO _x)	26 Sept 1997 7 July 2017	19 May 2005 1 Jan 2019	19 May 2006 1 Jan 2021
North Sea (SO _x) North Sea (NO _x)	22 Jul 2005 7 July 2017	22 Nov 2006 1 Jan 2019	22 Nov 2007 1 Jan 2021
North American ECA (SO _x and PM); (NO _x)	26 Mar 2010	1 Aug 2011	1 Aug 2012 1 Jan 2016
United States Caribbean Sea ECA (SO _x and PM); (NOx)	26 Jul 2011	1 Jan 2013	1 Jan 2014 1 Jan 2016

5.1.2 Population densities of cities near major ports in India

Table 5.2 gives population densities for cities that are adjacent to the major ports in India. The population density was maximum for the city of Mumbai (31,000 persons per km²) and minimum for Tuticorin (~400 persons per km²).

Table 5.2 Population density of cities located near major ports in India.

Port City	Population density (people per km²)
Chennai	26,553 ¹⁶¹
Kochi	7,139 ¹⁶²
Mumbai	30,716 ¹⁶³
Kolkata	24,679 ¹⁶⁴
Haldia	1400 ¹⁶⁵
Mangalore	$3,220^{166}$
Mormugao	$3,450^{167}$
Tuticorin	378 ¹⁶⁸
Visakhapatnam	3,800 ¹⁶⁹
Gandhidham	8,384 ¹⁷⁰
Paradip	2,931 ¹⁷¹

5.2 Materials and Methods

5.2.1 Study Area and Scope

Table 5.3 shares geographic details of the major ports.

Table 5.3 Indian Major Ports with their latitude, longitude and state information.

Port	State	Port Latitude	Port Longitude	Remarks
Chennai	Tamil Nadu	13.0815° N	80.2921° E	
Kochi	Kerala	9.9546° N	76.2678° E	also known as Cochin Port
Deendayal	Gujarat	23.01666° N	70.2166° E	formerly known as Kandla Port
Jawaharlal Nehru (JNPT)	Maharashtra	18.9499° N	72.9512° E	also known as JNPT, Nhava Sheva
Kamarajar	Tamil Nadu	13.2593° N	80.3374° E	formerly known as Ennore Port
Kolkata	West Bengal	22.5461° N	88.3149° E	
Haldia	West Bengal	22.0447°N	88.0888°E	
Mormugao	Goa	15.4088N	73.8011E	

Mumbai	Maharashtra	18.9000° N	72.8166° E	
New Mangalore	Karnataka	12.9281° N	74.8222° E	
Paradip	Odisha	20.2654°N	86.6762°E	
V.O. Chidambaranar (VOC)	Tamil Nadu	8.7563° N	78.1791° E	formerly known as Tuticorin Port
Visakhapatnam	Andhra Pradesh	17.6868° N	83.2903° E	also known as Vizag Port

Emissions contribution of cargo vessels at small ports: There are 205 non-major ports in the country out of which only a few are developed for cargo operations. In 2017-2018, major ports accounted for 58% of total freight cargo by volume across the county (see page 11). Roughly ~33% non-major ports (i.e., 68) handled cargo and constituted 42% of the total cargo traffic handled by the end of 2018 (see page 8 and page 11). Table 5.4 below provides overview of non-major ports' cargo statistics in India. In December 2018, India had a registered fleet of 1,400 vessels out of which 944 vessels were involved in coastal trade and the remainder 456 vessels were involved in overseas trade. The coastal vessel fleet in India constituted ~0.7% of the gross register tonnage (GRT) compared to major ports in 2018 (see Table 3.6). Nearly 98% of all coastal ships registered in India were less than 10,000 tonnes in size. In our data on major ports, we observe that ~87% of all ocean-going cargo vessels were greater than 10,000 tonnes in size (median GRT: 32,297 tonnes; mean GRT: 36,268 tonnes; min GRT: 396 tonnes, and max GRT: 167,572 tonnes).

Table 5.4 Summary statistics of non-major ports in India. This data is collated from Government of India (GoI's) annual report on ports' statistics (page XIV) for the year 2017-2018.¹⁷³

State	Region	# Non-Major Ports	Cargo Traffic (Million Tonnes)	% Cargo Share
Gujarat	West Coast	46	370.77	70.1
Andhra Pradesh	East Coast	12	86.29	16.3
Maharashtra	West Coast	48	37.91	7.2
Odisha	East Coast	13	22.6	4.3
Tamil Nadu	East Coast	16	1.1	0.2
Karnataka	West Coast	9	0.68	0.1
Goa	West Coast	5	0.07	0

Daman & Diu	West Coast	2	9.67	1.8
Kerala	West Coast	17		
Lakshadweep	West Coast	10		
Puducherry	East Coast	3		
West Bengal	East Coast	1		
Andaman & Nicobar Islands	East Coast	23		
Total		205	529.09	100

Emissions contributions from boats and fishing vessels: According to a 2010 emissions assessment on the city of Mumbai, we observe that cargo vessel emissions (containers, bulk carriers, and general cargo) dominate fishing vessel emissions. We reproduce the results of the report and also estimate the percentage share of fishing activity emissions around Mumbai relative to all other vessel categories (see **Table 5.5**). Thus, the relative share of fishing activity at major ports is small compared to other vessel categories.

Table 5.5 Emissions burden (in tons) for marine vessels in the city of Mumbai for the year 2010.¹⁷⁴

Vessel Category	PM (tons)	SO ₂ (tons)	NO _x (tons)
Bulk	1.2	13	12
Container	0.1	0.7	0.7
General Cargo	0.5	5.4	4.9
Fishing Vessels	0	0.4	0.3
Total Annual Emissions	1.8	20	18
% share of fishing activity	2%	2%	2%
emissions			

5.2.2 Vessel Call Information

We obtained vessel call information from the Port Trusts, with the approval of the Secretary of Shipping, Ministry of Shipping (MoS), Joint Secretary (Ports), MoS, and Chairperson of major port trusts. In our data collection efforts, we were supported by the Managing Director (MD), Indian Ports Association (IPA), Executive Director (ED), IPA, Former Additional Director General (ADG) of Artillery, Indian Army, and ADG, Indian Coast Guard (ICG). This

information is collected by the Port Trust's traffic or research department. The raw vessel activity information shared by the ports included the vessel call number (VCN), a unique registration number which was used to identify a particular vessel call at the port level, the ship's name, time of vessel arrival at the berth, time of vessel departure from the berth, type of cargo, as well as deadweight tonnage (DWT) and GRT for the vessels.

Table 5.6 shares the date-time window of the vessel activity information shared by major ports. The datasets received from the ports were approximately one-year duration from March 2017 to March 2018 except for the ports of Chennai (1.5 years) and Kamarajar (1.6 years). So, for the vessel activity datasets of Chennai and Kamarajar, we used the March 2017-March 2018 data for these ports. Haldia Dock Complex (HDC), shared data from April 2018-March 2019 so we use April 2018- March 2019 time period data for HDC.

Table 5.6 Date and time windows for vessel activity data shared by major ports of India. Chennai and Kamarajar ports shared vessel activity data which spanned >1 year. HDC shared data from April 2018 to March 2019.

Port	State	Min Date	Max Date	Years
Chennai	Tamil Nadu	3/25/17	9/26/18	1.5
Cochin	Kerala	4/1/17	3/31/18	1.0
Deendayal	Gujarat	3/28/17	3/31/18	1.0
Jawaharlal Nehru Port (JNPT)	Maharashtra	3/30/17	3/31/18	1.0
Kamarajar	Tamil Nadu	3/30/17	10/30/18	1.6
Kolkata	West Bengal	3/27/17	3/29/18	1.0
Haldia	West Bengal	4/13/18	3/30/19	1.0
Mormugao	Goa	3/14/17	3/29/18	1.0
Mumbai	Maharashtra	3/25/17	3/30/18	1.0
New Mangalore	Karnataka	3/28/17	3/31/18	1.0
Paradip	Odisha	9/1/17	8/29/18	1.0
VOC	Tamil Nadu	3/29/17	3/30/18	1.0
Vizag	Andhra Pradesh	3/31/17	3/31/18	1.0

5.2.2.1 Scraping the vessel call information

The raw vessel activity data from Port Authorities was missing in key attributes, for instance, ship's IMO registration number or MMSI number. In many cases, vessel type of the ships wasn't shared in the raw dataset. These parameters were required to determine the vessel type and size of the auxiliary engine (in kW) of the ship's onboard diesel generator, vis-à-vis for the type of vessel under consideration. In order to find the missing attributes, we built a web scraper in python which utilized the website MarineTraffic ¹⁷⁵ to complete missing information. The scraper obtained data from the website MarineTraffic¹⁷⁵, which is a partially open database that provides a number of vessel characteristics along- with real time positions and position history of ships. The website has over 600,000 registrations 176 and 20 million visits 177 on their platform every month. It uses 2,000 Automatic Identification System (AIS) stations to collate data across 165 countries. ¹⁷⁸ Also, Marine Traffic has a memorandum of understanding (MoU) with the United Nations Conference on Trade and Development (UNCTAD)^{179,180} and collaborates with IMO on their projects. This gave us assurance about the reliability and trustworthiness of the database. Wherever available, the scraper used the available vessel information such as the vessel name, DWT, GRT and the vessel flag to ping an automated query via the Google's Custom Search JSON API¹⁸¹ which opened the MarineTraffic website link from the Google search results and scraped the webpage for the relevant information. Since it was possible that the search results weren't accurate for the web scraper, we established boundary checks, for example, (1) GRT and DWT comparison for given and scraped vessel records before accepting a scraped search result to our dataset, (2) logical flags which gave a true or false value reflecting whether a vessel's information was scraped successfully or not depending on the available vessel

information from the ports. For the cases where logical flags were false, we searched for the information manually.

5.2.2.2 Cleaning the vessel call information

Out of the 41 vessel categories, 25 were relevant for our study and 16 other categories were rejected. Categories of ships included in the analysis were (1) Passenger/Cargo Ship, (2) Oil Products Tanker, (3) Container Ship, (4) Crude Oil Tanker, (5) Passenger Ship, (6) General Cargo, (7) Oil/Chemical Tanker, (8) Ro-Ro Cargo, (9) Cement Carrier, (10) Vehicle Carrier, (11) LNG Tanker, (12) Deck Cargo Ship, (13) Cargo/ Containership, (14) Chemical Tanker, (15) Bulk Carrier, (16) Ro-Ro/ Container Carrier, (17) LPG Tanker, (18) Heavy Load Carrier, (19) Wood Chips Carrier, (20) Asphalt/Bitumen Tanker, (21) Tanker, (22) OBO Carrier, (23) Self Discharging Bulk Carrier, (24) Reefer, and (25) Shuttle Tanker. Categories of ships which were discarded in this analysis were (1) Offshore Supply Ship, (2) Suction Dredger Pontoon, (3) Tug, (4) Barge, (5) Hopper Dredger, (6) Research/Survey Vessel, (7) Yacht, (8) Fishery Research Vessel, (9) Anchor Handling Vessel, (10) Navy, (11) Fishing Vessel, (12) Inland Cargo, (13) Crew Boat, (14) Fire Fighting Vessel, (15) Replenishment Vessel, and (16) Unknown category of vessels. We grouped the above categories according to the classification shown in **Table 5.7**.

Table 5.7 Classification used for grouping different vessel types.

S No.	Vessel Type	Vessel group class
1	BULK CARRIER	Bulk
2	SELF DISCHARGING BULK CARRIER	
3	CARGO/CONTAINERSHIP	Container
4	CONTAINER SHIP	
5	CEMENT CARRIER	
6	DECK CARGO SHIP	
7	GENERAL CARGO	Ganaral Cargo
8	HEAVY LOAD CARRIER	General Cargo
9	REEFER	
10	WOOD CHIPS CARRIER	

11	CRUDE OIL TANKER	Crude Oil Tanker
12	SHUTTLE TANKER	
13	ASPHALT/BITUMEN TANKER	
14	CHEMICAL TANKER	
15	LNG TANKER	
16	LPG TANKER	Tanker
17	OBO CARRIER	Tunter
18	OIL PRODUCTS TANKER	
19	OIL/CHEMICAL TANKER	
20	TANKER	
21	PASSENGER SHIP	Passenger
22	PASSENGER/CARGO SHIP	
23	RO-RO CARGO	Ro-Ro
24	RO-RO/CONTAINER CARRIER	
25	VEHICLES CARRIER	Auto Carrier

In the analysis, we ignore shift cases within the port (i.e., ships being moved within the port depending on berth availability). Also, we reject any vessel call less than or equal to 5 hours in berthing duration (~0.2% out of 23,755 vessel calls). It takes roughly between 20 minutes and 2 hours 182 to connect a ship to shore power system and similar time frame to disconnect the ship from shore power connection. This is because vessels with port call duration of less than or equal to 5 hours won't have enough time to connect to shore power. **Table 5.8** shows quantiles of port call duration for different vessel categories. There are port calls which have really high values for time spent at ports. Hence, these values can bias the analysis. In order to control for these effects, we consider only those vessel calls which are less than or equal to ~228 hours (98th percentile of port call duration across different vessel categories). Port call durations which were greater than 228 hours were dropped from our analysis.

Table 5.8 Quantile distributions of port call duration (in hours) in ports' vessel data. We also observe that there is a long tail of port call duration for some vessel categories in the raw dataset which can induce bias in our results, if we assume that vessels connect to shore power in the remaining time spent at port. So, we delete all vessel calls which have port call duration $> 98^{th}$ percentile of call duration (~ 228 hours) in the dataset.

Vessel type	Total hours	Call duration (in hours)
-------------	-------------	--------------------------

	Unique vessels	Vessel Calls		1%	10 %	50%	98%	100%
Asphalt/Bitumen Tanker	18	140	6.4K	16	21	29	220	414
Bulk Carrier	2,699	6,500	570K	16	30	65	330	2.4K
Cargo/Containersh ip	10	120	10K	7	12	47	170	4.4K
Cement Carrier	7	150	8.4K	18	26	52	120	190
Chemical Tanker	58	270	10K	8	15	31	120	180
Container Ship	579	5,100	190K	6	12	27	120	7.3K
Crude Oil Tanker	453	1,300	77K	14	26	42	150	8.8K
Deck Cargo Ship	4	9	940	35	61	85	230	240
General Cargo	585	2,300	190K	5	15	50	240	15K
Heavy Load Carrier	15	25	1.7K	8	13	41	280	340
LNG Tanker	9	13	410	20	22	24	75	76
LPG Tanker	184	1,100	51K	11	19	34	180	1.7K
OBO Carrier	1	1	46	46	46	46	46	46
Oil Products Tanker	205	1,900	92K	10	21	35	130	3.2K
Oil/Chemical Tanker	900	3,800	150K	9	15	33	120	1.5K
Passenger ship	30	130	16K	6	9	12	2.2K	3.4K
Passenger/Cargo ship	13	390	56K	7	29	54	1.3K	7.3K
Reefer	1	1	180	180	180	180	180	180
Ro-Ro Cargo	10	19	1.3K	9	26	75	120	140
Ro-Ro/Container Carrier	2	5	150	6	8	35	48	49
Self-Discharging Bulk Carrier	2	6	920	31	37	110	440	500
Shuttle Tanker	1	1	37	37	37	37	37	37
Tanker	3	3	99	24	26	35	40	40
Vehicles Carrier	222	460	12K	5	8	16	120	270
Wood Chips Carrier	3	18	2.3K	26	85	130	190	200

Table 5.9 shows the number of vessel calls dropped at each step of the data cleaning process. In the end, our vessel call data consisted of 21,937 unique vessel calls made by 5,732 unique ships. The distribution of port call duration in the annual vessel activity data is shown in **Figure 5.1**.

Table 5.9 Snapshot of vessel calls at each point of the cleaning process. Indian major ports received 24,202 vessel calls in 2017-2018 out of which 21,937 were relevant for our study.

Vessel type	Unique	Relevant	Rejecting	Cleaned
	vessel calls	cargo vessel	outlier port	annual
		categories	call	vessel
			durations	activity
			(98 th %ile cutoff)	
Anchor Handling Vessel	10	0	0	0
Asphalt/Bitumen Tanker	138	138	135	124
Barge	23	0	0	0
Bulk Carrier	6,462	6,462	6,139	5,828
Cargo/Containership	122	122	120	120
Cement Carrier	154	153	153	153
Chemical Tanker	269	269	267	262
Container Ship	5,132	5,121	5,089	4,813
Crew Boat	1	0	0	0
Crude Oil Tanker	1,262	1,259	1,249	1,209
Deck Cargo Ship	9	9	8	7
Firefighting Vessel	31	0	0	0
Fishery Research Vessel	1	0	0	0
Fishing Vessel	1	0	0	0
General Cargo	2,338	2,335	2,258	2,089
Heavy Load Carrier	25	25	24	24
Hopper Dredger	8	0	0	0
Inland Cargo	134	0	0	0
LNG Tanker	13	13	13	13
LPG Tanker	1,094	1,094	1,078	1,033
Navy	3	0	0	0
OBO Carrier	1	1	1	1
Offshore Supply Ship	139	0	0	0
Oil Products Tanker	1,937	1,936	1,917	1,775
Oil/ Chemical Tanker	3,785	3,784	3,773	3,619
Passenger Ship	128	127	119	118
Passenger/Cargo Ship	390	390	369	355

Reefer	1	1	1	1
Replenishment Vessel	2	0	0	0
Research/Survey Vessel	17	0	0	0
Ro-Ro Cargo	19	19	19	18
Ro-Ro/Container Carrier	5	5	5	5
Self-Discharging Bulk Carrier	6	6	5	5
Shuttle Tanker	1	1	1	1
Suction Dredger Pontoon	30	0	0	0
Tanker	3	3	3	3
Tug	20	0	0	0
Unknown	1	0	0	0
Vehicles Carrier	464	464	461	343
Wood Chips Carrier	18	18	18	18
Yacht	5	0	0	0
All Major Ports	24,202	23,755	23,225	21,937

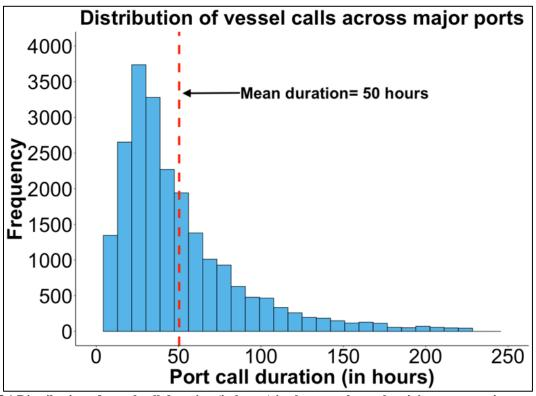


Figure 5.1 Distribution of vessel call duration (in hours) in the annual vessel activity across major ports in India. There were 21,937 vessel calls in 2017- 2018 with a median vessel call duration of \sim 39 hours and mean vessel call duration of \sim 50 hours.

Table 5.10 and Table 5.11 provide summary statistics of vessel call data at the port level.

Table 5.10 Port call distribution of different vessel types across major ports in India. Deendayal port had the highest energy consumption of ~77 GWh at berth. Additionally, JNPT had the shortest port call duration (~28 hours) compared to Kolkata where the port call duration was the longest (~77 hours).

~28 nours) compare Port	Vessel class	t call duration wa Total energy required (MWh)	Average port call duration (hours)	Average auxiliary power (kW)
Chennai	Auto Carrier	1.7K	48	780
	Bulk	4.6K	86	320
	Container	14K	32	770
	Crude Oil Tanker	5K	63	1K
	General Cargo	11K	52	540
	Passenger	6K	80	2.2K
	RoRo	8	32	84
	Tanker	13K	53	570
	Total	55K	50	670
Cochin	Auto Carrier	4	8	525
	Bulk	520	94	250
	Container	5.7K	17	630
	Crude Oil Tanker	5.8K	47	1.1K
	General Cargo	4.3K	53	620
	Passenger	32K	57	1.9K
	RoRo	5	30	38
	Tanker	6.9K	42	650
	Total	55K	38	940
Deendayal	Auto Carrier	31	59	520
	Bulk	19K	76	360
	Container	1.6K	24	620
	Crude Oil Tanker	17K	47	1.2K
	General Cargo	11K	54	620
	RoRo	8	57	71
	Tanker	29K	36	640
	Total	77K	49	620
Haldia	Auto Carrier	240	54	550
	Bulk	26K	71	410
	Container	3.5K	33	380
	Crude Oil Tanker	1.8K	47	800
	General Cargo	3.3K	71	830
	Tanker	25K	45	570
	Total	61K	55	490
JNPT	Bulk	62	16	490

	Container	41K	27	860
	Crude Oil Tanker	930	38	760
	General Cargo	4.5K	57	850
	Tanker	10K	29	630
	Total	57K	28	80
Kamarajar	Auto Carrier	1.6K	14	740
	Bulk	7.7K	49	410
	Container	42	17	600
	Crude Oil Tanker	470	34	720
	General Cargo	370	44	800
	RoRo	1	7	95
	Tanker	5.4K	33	660
	Total	16K	37	560
Kolkata	Auto Carrier	43	13	270
	Bulk	1.5K	108	340
	Container	13K	83	220
	General Cargo	8.6K	86	470
	Passenger	5.2K	145	1.9K
	Tanker	4.8K	45	410
	Total	33K	77	340
Mormugao	Bulk	11K	66	420
	Container	2.1K	31	570
	Crude Oil Tanker	420	28	710
	General Cargo	21K	102	870
	Passenger	3.9K	11	7.2K
	Tanker	3K	27	650
	Total	42K	59	930
Mumbai	Auto Carrier	2.8K	31	780
	Bulk	17K	115	320
	Container	50	63	630
	Crude Oil Tanker	7.3K	42	1K
	General Cargo	16K	59	520
	Passenger	5.9K	27	5.5K
	RoRo	130	91	130
	Tanker	23K	39	620
	Total	72K	59	670
New Mangalore	Auto Carrier	5	9	525
			9	323

	Container	2.9K	39	530
	Crude Oil Tanker	7.7K	45	970
	General Cargo	3.3K	42	720
	Tanker	16K	40	650
	Total	37K	46	630
Paradip	Bulk	34K	61	400
	Container	460	42	430
	Crude Oil Tanker	8.5K	43	1.2K
	General Cargo	1.8K	42	690
	Tanker	7.9K	37	680
	Total	53K	55	530
Vizag	Auto Carrier	100	93	550
	Bulk	24K	81	400
	Container	5.2K	26	660
	Crude Oil Tanker	5K	50	1K
	General Cargo	8K	66	850
	Passenger	1.4K	35	2.1K
	RoRo	5	45	100
	Tanker	14K	37	580
	Total	58K	56	570
VOC	Auto Carrier	20	37	550
	Bulk	13K	85	350
	Container	5.9K	27	480
	Crude Oil Tanker	250	87	970
	General Cargo	7.1K	65	540
	RoRo	3	75	38
	Tanker	4.7K	48	490
	Total	31K	56	450

Table 5.11 Port call distribution and unique vessels across individual major ports. Port of Deendayal received highest number of vessel calls (2,654

calls) compared to Kamarajar port which received the least number of vessel calls (794 calls). **Port** Total # Vessel calls by port Avg. call Vessel duration calls (hours) Bulk **Crude Oil** General **Passenger** RoRo **Tanker** Auto **Container** Carrier **Tanker** Cargo Chennai 1,589 Cochin 1,421 1,276 Deendayal 2,654 Haldia 2,250 **JNPT** 2,469 1,767 Kamarajar Kolkata 1,238 Mormugao Mumbai 2.124 New 1,323 Mangalore **Paradip** 1,892 1,344 VOC 1,308 Vizag 1,915

5.2.2.3 Data Validation

Table 5.12.

Here, we validate our datasets with publicly available information from the GoI. For all the ports, we removed non-cargo vessels, navy ships and any ships with port call duration > 228 hours (~9.5 days; 98th percentile of the port call duration in our data set). The ports report vessel calls and not unique vessels in their Annual Administration Reports. This was confirmed with the traffic managers at respective ports.

Chennai Port: According to Chennai Port Trust's Annual Administration Report for 2017-2018¹⁸³, the port handled 1,852 merchant vessels and 549 government vessels in the entire year (Pg. 21). Amongst these, there were 1,567 cargo vessel calls (see Table No. 7A, Pg. 80) ¹⁸³ excluding the 33 passenger vessel calls. The data shared by port to us had 2,401 (1852+549) vessel calls. The cleaned dataset consists of 1,589 vessel calls that includes 1,556 cargo vessel calls and 33 passenger vessel calls. Also, the average berthing time both in the annual report and our data is 2.1 days (Pg. 82). Additionally, the report shares the activity details of select ships. We compare and validate our data with the sample of ships mentioned in the annual report in

Table 5.12 Comparison of ships mentioned in the Chennai Annual Administration Report 2017-2018¹⁸³ with vessel details in authors' cleaned dataset.

Serial	Annual Report Data	Our Data
Number		
1	MV MAERSK KURE with deadweight tonnage	MAERSK KURE (IMO: 9085522) with DWT
	(DWT) 90,456 tonnes arrived on 02/24/2018.	84,900 tonnes arrived on 02/24/2018 and
		departed on 02/26/2018
2	MT FOUR SMILE with DWT 160,572 tonnes	FOUR SMILE (IMO: 9189146) with DWT
	arrived on 03/16/2018.	160,573 tonnes arrived on 03/16/2018 and
		departed on 03/18/2018
3	MT ANKLESHWAR with DWT 147,563.7	ANKLESHWAR (IMO: 9074860) with DWT
	tonnes arrived on 09/23/2017	147,563 tonnes arrived on 09/23/2017 and
		departed on 09/26/2017
4	Passenger ship MV MAGELLAN arrived on	Passenger ship MAGELLAN (IMO: 8217881)
	04/08/2017	with DWT 7,186 tonnes on 04/08/2017 and
		departed on 04/08/2017

<u>Deendayal Port:</u> The port handled 2,747 cargo vessel calls in 2017-2018 (Pg. 22).¹⁸⁴ In comparison, we have 2,654 cargo vessel calls in our data. The average berthing duration both in the annual report and our data is 2.0 days (Pg. 41).¹⁸⁴ Additionally, the port received 1,585 tanker vessel calls (Pg. 35) compared to 1,575 tanker vessel calls in our dataset.

Kamarajar Port: The port handled 794 cargo vessel calls¹⁸⁵ in 2017-2018. Our dataset consisted of 794 cargo vessel calls.

Kolkata and Haldia Port: In 2017-2018, Kolkata Port handled 1,196 cargo vessel calls (excluding passenger ships) at Kolkata Dock System (KDS) (Table VIII, Pg. 96) and 2,316 cargo vessel calls at the Haldia Dock Complex (HDC) (Table VIII, Pg. 97). After cleaning the raw vessel data from ports, there were 1,219 cargo vessel calls at KDS and 2,250 cargo vessel calls at HDC. Also, KDS handled ~640,000 TEUs (Twenty-foot equivalent units) of container traffic (see Table 2.5 on Pg. 19). This included ~330,000 imported TEUs and ~310,000 exported TEUs. In our dataset, the total number of containers handled at KDS were ~640,000 TEUs and consisted of ~330,000 imported TEUs and ~310,000 exported TEUs. Our raw data didn't include details for HDC, so we weren't able to compare the TEUs for HDC.

Mumbai Port: In 2017-2018, the port handled 2,210 cargo vessel calls and 40 passenger vessel calls (Table VII, Pg. 42). ¹⁸⁷ Our data consists of 2,124 vessel calls that includes 2,084 cargo vessel calls and 40 passenger vessel calls. The average berthing duration at the port for cargo ships was 2.2 days (Table VIII). ¹⁸⁷ In comparison, the average berthing duration in our data for cargo ships was 2.4 days.

<u>New Mangalore Port:</u> The port handled 1,360 cargo vessel calls (Table C-II). After cleaning the data, we were left with 1,323 cargo vessel calls. The average berthing duration at the port

was 1.9 days (Table P-I AR). ¹⁸⁸ In comparison, the average berthing duration at the port in the cleaned dataset is 1.9 days.

<u>Paradip Port:</u> The port handled 1,840 vessel calls (Pg. 11) in 2017-2018 that included 1,831 cargo vessel calls (see Table O-I on Pg. 58). The raw data shared by the port had 1,905 cargo vessels. After cleaning the data, we have 1,892 cargo vessel calls. **Table 5.13** shows a comparison of cargo vessels for different ship categories between values reported in the annual report and our dataset.

Table 5.13 Comparison of vessel categories between cleaned data with those mentioned in Paradip Annual Administration Report 2017-2018. 189

Vessel Category	Annual Report Vessel Calls	Cleaned Data Vessel Calls
Container	22	25
Bulk Carrier (break, dry, liquid)	1,345	1,344
General Cargo	0	56
Tankers (liquid bulk)	464	467
Total	1,831	1,892

VOC Port: The port received 1,482 vessel calls (see Table 7, Pg. 87) in 2017-2018 and the average berthing duration of 2.2 days (see Table 8, Pg. 88). ¹⁹⁰ After cleaning the data, we have 1,308 vessel calls in the dataset. The average berthing duration in our dataset was 2.3 days. *Visakhapatnam Port:* The port handled 2,015 vessel calls in 2017-2018 (Pg. 1). ¹⁹¹ This included 1,977 cargo vessel calls with an average berthing duration of 2.4 days (see Annexure-21, Pg. 90). From the 1,973 vessel calls shared by the port, we removed non-cargo ships, navy ships and ships with outlier port call duration. Finally, we have 1,915 vessel calls in our dataset that consists of 1,895 cargo vessel calls and 20 passenger vessel calls. The average berthing duration in our dataset was 2.3 days.

5.3 Determining Auxiliary Engine Loads

We spoke to people working in marine emissions assessment to seek guidance for calculating auxiliary engine loads of vessels calling at Indian ports. We communicated with (1) Prof. James J Corbett (Associate Director for Marine Policy Program, School of Marine Science and Policy, University of Delaware)¹⁹², (2) Prof. Anthony F. Molland (author of 'The Maritime Engineering Reference Book: A Guide to Ship Design, Construction and Operation'; Emeritus Professor, University of Southampton, UK)¹⁹³, (3) Dr. Louis Browning (Technical Director, ICF)¹⁹⁴, (4) Ms. Guiselle Aldrete (author of 'Port of Long Beach's 2018 Inventory'; Consultant, Starcrest Consulting Group)¹⁹⁵, (5) Mr. Abhijit Aul (Regulatory Affairs Lead, Lloyd's Register)¹⁹⁶, (6) Brett Goldsworthy¹⁹⁷ (Researcher, University of Tasmania, Australia) and (7) Laurie Goldsworthy¹⁹⁸ (Research Fellow, Australian Maritime College, University of Tasmania, Australia). Goldsworthy et al. 75 conducted a study to estimate auxiliary engine power defaults at berth and validated it against local survey of ships. They compiled auxiliary engine operating loads in Table 1 of the paper 75 from sources such as the Third IMO Greenhouse Gas Study 2014⁴¹, Starcrest's Port of Los Angeles (POLA)⁷⁶ and Port of Long Beach (POLB)⁷⁷ emissions inventory. For vessel categories which weren't available in the Goldsworthy paper, we used auxiliary engine load values from POLB, 2017. 199 The auxiliary engine emission factors (in g/kWh) for ships were taken from Table 2-16 in US EPA's report⁷⁴ on preparing mobile source emission inventories and are reproduced in **Table 5.14** below.

Table 5.14 Ships' auxiliary engine emission factors (in g/kWh) for different pollutant types. These are taken from US EPA's report.⁷⁴

Fuel Type	Sulfur	NO _x (g/kWh)	PM _{2.5} (g/kWh)	SO _x (g/kWh)	CO ₂ (g/kWh)
RO (2.7% S)	2.70%	14.7	1.32	11.98	722.54
MGO (0.5% S)	0.50%	13.9	0.29	2.12	690.71

We were recommended to calculate auxiliary engine loads for each ship instead of using a default bin value for a given size of vessel due to differences in auxiliary engine usage and ship mix at ports. **Table 5.15** provides vessel categories and their auxiliary engine power defaults (in kW) used in this study. We adjusted auxiliary engine loads for different vessel categories depending on the vessel size. The underlying assumption was that the auxiliary engine load of a ship varies linearly with the ship's DWT. However, for passenger ships, we were advised to use the passenger capacity of ship (PAX) instead of DWT to determine auxiliary engine loads of the ships. Therefore, we estimate auxiliary engine loads for all vessel categories using their DWT except for passenger ships, where we use their PAX to estimate hoteling loads.

Table 5.15 AE power defaults (in kW) by vessel category at berth. For passenger ships, we use PAX instead of DWT to linearly interpolate their hoteling loads. The values in Min. DWT and Max. DWT column for passenger ships denote the capacity of the passenger ships denote the capacity of the passenger ship in the table below. For categories which didn't have a range of auxiliary power information available, we used a constant linear function.

Vessel class	Min. AE capacity	Max. AE capacity	Min. DWT (tonnes)	Max. DWT	Capacity units
	(kW)	(kW)	(tollies)	(tonnes)	units
Auto Carrier	0	1,284	0	31,143	
Bulk	0	280	0	9,999	
Bulk	280	280	10,000	34,999	
Bulk	280	370	35,000	59,999	
Bulk	370	600	60,000	99,999	
Bulk	600	600	100,000	199,999	
Bulk	600	600	200,000	299,999	
Container < 1000	0	340	3,816	15,704	
Container-1000	340	600	15,716	27,604	DWT
Container-2000	600	700	27,616	39,504	(expressed in tonnes)
Container-3000	700	940	39,516	63,304	in tomics)
Container-5000	940	970	63,316	99,004	
Container-8000	970	1,000	99,016	146,604	
Container-12000	1,000	1,200	146,616	176,366	
Container-14500	1,320	1,320	176,366	182,304	
General Cargo	0	120	0	4,999	
General Cargo	120	330	5,000	9,999	
General Cargo	970	970	10,000	70,000	

RoRo	0	229	0	43,878	
Crude Oil	0	250	0	4,999	
Tanker					
Crude Oil	250	375	5,000	9,999	
Tanker					
Crude Oil	375	625	10,000	19,999	
Tanker					
Crude Oil	625	750	20,000	59,999	
Tanker					
Crude Oil	750	750	60,000	79,999	
Tanker	7.50	1.000	00.000	110.000	
Crude Oil	750	1,000	80,000	119,999	
Tanker	1.000	1.250	120,000	100.000	
Crude Oil	1,000	1,250	120,000	199,999	
Tanker Crude Oil	1,500	1,500	200,000	399,999	
Tanker	1,300	1,300	200,000	399,999	
Tanker	0	250	0	4,999	
				·	
Tanker	250	375	5,000	9,999	
Tanker	375	625	10,000	19,999	
Tanker	625	750	20,000	59,999	
Tanker	750	750	60,000	79,999	
Tanker	750	1,000	80,000	119,999	
Tanker	1,000	1,250	120,000	199,999	
Tanker	1,500	1,500	200,000	299,999	
RoRo	0	229	0	43,878	
Passenger	0	3,000	0	1,500	
Passenger	3,000	6,500	1,500	2,000	Number of
Passenger	6,500	9,500	2,000	2,500	Passengers
Passenger	9,500	10,000	2,500	3,000	

Table 5.16 provides vessel information about passenger ships in our dataset that we collected manually.

Table 5.16 Auxiliary capacity information of passenger ships in our dataset. We collated passenger capacities of respective ships from online sources such as the manufacturers of these ships and government records.

Vessel name	IMO number	DWT (tonnes)	Auxiliary capacity (kW)	Passenger capacity (persons)	
LAKSHADWEEP SEA	9448102	779	731	2:	50
ISLAND SKY	8802894	695	652	1	16

82

KAVARATTI	9238260	2387	2241	700
ARABIAN SEA	9448097	725	681	250
LAGOONS	9651010	1179	1107	400
ARTANIA	8201480	4661	4375	1188
AZAMARA JOURNEY	9200940	2700	2534	694
SEVEN SEAS	9247144	5400	5069	706
VOYAGER				
INSIGNIA	9156462	2700	2534	824
CORALS	9651008	1179	1107	400
MINICOY	9224075	183	172	150
VALIYAPANI	9372951	43	40	150
EUROPA 2	9616230	5285	4961	516
PARALI	9372937	43	40	150
AMINDIVI	9217101	183	172	150
SKIP JACK	9382657	68	64	50
KALIGHAT	8713926	719	675	400
WORLD ODYSSEY	9141807	3460	3248	520
SEABOURN ENCORE	9731171	7000	6571	604
NAUTICA	9200938	2948	2767	824
STAR LEGEND	9008598	5170	4853	208
SILVER SPIRIT	9437866	3882	3644	608
SILVER DISCOVER	8800195	938	880	128
NIPPON MARU	8817631	4840	4543	532
PACIFIC PRINCESS	9187887	3376	3169	826
BLACK WATCH	7108930	5656	5309	330
MAGELLAN	8217881	7186	6745	1452
NANCOWRY	8606434	5014	4706	1200
HS MARCO POLO	6417097	5180	4862	1250
SWARAJ DWEEP	9101168	4701	4413	1200
CAMPBELL BAY	9309124	1128	1059	500
NICOBAR	8606161	4963	4659	1200
HARSHA VARDHANA	7219026	5269	4946	748
VIKING SUN	9725433	4797	4503	930
MEIN SCHIFF 1	9106297	6500	6101	2894
COSTA LUMINOSA	9398905	7600	7134	2826
SILVER WHISPER	9192179	2980	2797	382
CELEBRITY	9192399	11763	11042	2038
CONSTELLATION	, -, - , -,	-1.00		_000
COSTA	8716502	7781	7304	1680
NEOCLASSICA				

MEIN SCHIFF 5	9753193	7900	7415	2790
AIDABELLA	9362542	8765	8227	2500
LUCKY SEVEN	8943703	4000	3755	892
ARCADIA	9226906	10939	10268	2388

We also see that the reported container vessel sizes range from 1,000 to 14,500 Twenty-Foot Equivalents (TEUs). However, our dataset had DWT as a measure of the tonnage. Thus, it became necessary to establish a relationship between TEU and DWT using linear regression. The linear relationship between DWT and TEU was found to be the following for container ships in the dataset:

$$DWT = 3815.7 + 11.9 \times TEU$$

The linear relationship was statistically significant (**Figure 5.2**) and was used to estimate the auxiliary load for all the vessel calls that were made by container ships. This allowed us to compute DWT for respective container ships which were later used to bound container of different sizes. Despite this, there were 64 vessel calls (63 containers and 1 general cargo) out of 23,755 calls for which auxiliary loads weren't in the capacity bins. These comprised ~0.2% of our vessel call data and their hoteling loads were determined using the "Container <1000" TEUs vessel category.

84

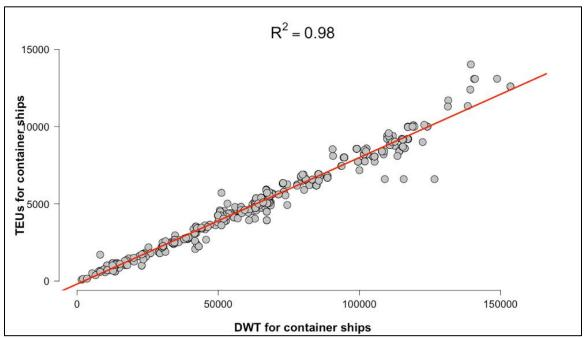


Figure 5.2 Scatterplot of linear regression relationship between TEU and DWT for 577 container ships. The red line shows the least squares fit (R^2 =0.9747 and p-value~0).

Below, we describe several examples of how data were obtained from www.marinetraffic.com and how we used this information to calculate auxiliary loads for vessels in our dataset.

Example 1:

Known fields:

Port-Visakhapatnam; Vessel Name-APOLLO; IMO Number-9114608, DWT-148,435; GRT-79,832

Unknown fields:

Vessel Type, Aux. Load

Our python scraper does an automated Google search by stringing together all the known information about a vessel to generate a Google search string in the following format: $query = name + "vessel" + "gross tonnage" + str(original_grt) + "marinetraffic"$ For the above example, this Google search query translates to

APOLLO vessel gross tonnage 79,832 marinetraffic

Our scraper parses through the HTML page and finds the ship's *Vessel Type*. The vessel type of the ship was found to be *Crude Oil Tanker*. Before accepting the search result, the scraper does a check based on the observed *GRT* from the raw data and found *GRT* on marinetraffic.

$$if\ found_{grt}\ and\ (abs(ext{min}imum_{grt}-orginial_{grt}) < 400):$$

$$match = TRUE$$

In this case, the GRT noted both in the port records given to us and in <u>www.marinetraffic.com's</u> records was 79,832. As such, the $abs(minimum_{grt} - original_{grt})$ is 0 and the search result is recorded in a .csv file with the details from marinetraffic.

From **Table 1** of Goldsworthy et al., we assign it to the following capacity bin:

Now, applying linear interpolation to the above, we get

$$AuxLoad = DWT * \left(\frac{Max_{aux} - Min_{aux}}{Max_{DWT} - Min_{DWT}}\right) + \left(\frac{Min_{aux} * Max_{DWT} - Min_{DWT} * Max_{aux}}{Max_{DWT} - Min_{DWT}}\right)$$

$$AuxLoad = 148,435 * \left(\frac{1250 - 1,000}{199,999 - 120000}\right) + \left(\frac{1,000 * 199,999 - 120,000 * 1,250}{199,999 - 120,000}\right)$$

$$Aux Load \approx 1,089 kW$$

Example 2:

Known fields:

Port-Chennai, Vessel Name-MESSINI, GRT-25,499

Unknown fields:

IMO Number, Vessel Type, Aux. Load, DWT

Our python scraper does an automated Google search by stringing together all the known information about a vessel to generate a Google search string in the following format:

query = name + "vessel" + "gross tonnage" + str(original_grt) + "marinetraffic"
For the above example, this Google search query translates to

MESSINI vessel gross tonnage 25,499 marinetraffic

Our scraper parses through the HTML page and finds the ship's *IMO Number*, *DWT*, and *Vessel Type*. The IMO Number of the ship is 9142942, its DWT is 34,167 tonnes and the vessel type was found to be *Container Ship*. Before accepting the search result, the scraper does a check based on the observed *GRT* from the raw data and found *GRT* on marinetraffic.

$$if\ found_{grt}\ and\ (abs(minimum_{grt}-orginial_{grt})<400):$$

$$match=TRUE$$

Again, *abs(minimum_{grt} – original_{grt})* is 0 and the search result is recorded in a .csv file with the details from www.marinetraffic.com. We had to scrape the DWT since we didn't have it in the raw data, and it was found to be 34,167 tonnes. Since this is a container ship, we need to convert the DWT to TEU for assigning auxiliary load. We found a linear regression relationship between DWT and TEUs in our data set for all the container ships. This relationship was found to be as follows:

$$DWT = 3815.7 + 11.9 \times TEU$$

Using this linear relationship, we found that this ship belongs to container 2000 to container 2999 bin range. From **Table-1** of Goldsworthy et al., we assign it to the following capacity bin:

Min Aux. Load(kW) Max Aux. Load(kW) Min DWT(Tonnes) Max DWT(Tonnes)

600 700 27,616 39,504

Now, applying linear interpolation to the above, we get

$$AuxLoad = DWT * \left(\frac{Max_{aux} - Min_{aux}}{Max_{DWT} - Min_{DWT}}\right) + \left(\frac{Min_{aux} * Max_{DWT} - Min_{DWT} * Max_{aux}}{Max_{DWT} - Min_{DWT}}\right)$$

$$AuxLoad = 34,167 * \left(\frac{700 - 600}{39,504 - 27,616}\right) + \left(\frac{600 * 39,504 - 27,616 * 700}{39,504 - 27,616}\right)$$

$Aux Load \approx 655 kW$

Example 3:

Known fields:

Port-Cochin, Vessel Name-ARABIAN SEA, DWT-725, GRT-3,261

Unknown fields:

IMO Number, Vessel Type, Aux. Load

Our python scraper does an automated Google search by stringing together all the known information about a vessel to generate a Google search string in the following format: $query = name + "vessel" + "gross tonnage" + str(original_grt) + "marinetraffic"$ For the above example, this Google search query translates to

ARABIAN SEA vessel gross tonnage 3,261 marinetraffic

Our scraper parses through the HTML page and finds the ship's *IMO Number and Vessel Type*. The IMO Number of the ship is 9448097 and its vessel type was found to be *Passenger Ship*. Before accepting the search result, the scraper does a check based on the observed *GRT* from the raw data and found *GRT* on marinetraffic.

$$if\ found_{grt}\ and\ (abs(minimum_{grt}-orginial_{grt})<400):$$

$$match=TRUE$$

The GRT in the raw data was 3,261 and that on www.marinetraffic.com was 3,261, so, the $abs(minimum_{grt} - original_{grt})$ is 0 and the search result is recorded in a .csv file with the details from marinetraffic. For passenger ships, we used passenger capacity (PAX) compared to DWT as a measure of loading of the ship. The passenger capacity of the ship is 250 people. From Table-1 of Goldsworthy et al., we assign it to the following capacity bin:

Now, applying linear interpolation to the above, we get

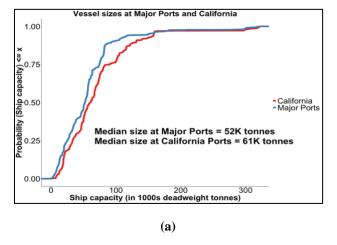
$$AuxLoad = Passengers * \left(\frac{Max_{aux} - Min_{aux}}{Max_{pax} - Min_{pax}}\right) + \left(\frac{Min_{aux} * Max_{pax} - Min_{pax} * Max_{aux}}{Max_{pax} - Min_{pax}}\right)$$

$$AuxLoad = 250 * \left(\frac{3,000 - 0}{1,500 - 0}\right) + \left(\frac{0 * 1,500 - 0 * 3000}{1,500 - 0}\right)$$

$Aux Load \approx 500 kW$

Similarly, auxiliary loads for other vessels were estimated. Hopefully, this should further clarify as to how we estimated auxiliary engine loads for vessels in our dataset.

Comparison of Vessel Ages and Sizes at Indian and Californian Ports: Since some of the auxiliary engine power values came from Californian vessels at POLA and POLB, we compared ages and sizes of ships calling at Indian and Californian ports. Data about vessels visiting Californian ports (POLA and POLB) were obtained from the lead author of an earlier study of shore power at these ports.⁴⁷ In an initial comparison (**Figure 5.3 (a)-(b)**), we observed that the vessels calling at Indian major ports were of roughly the same vintage as those calling at POLA and POLB but were typically somewhat smaller than their counterparts in California.



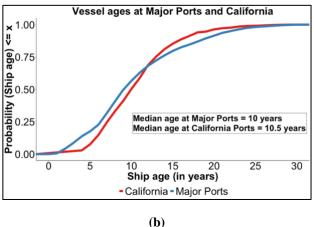


Figure 5.3 (a) distribution of vessel sizes. The vast majority of vessels calling at the Indian ports are smaller than the ones calling at California. (b) Distribution of ages of vessels calling at Californian and Indian major ports. The data suggests that the that the vessels calling at the ports have similar ages.

<u>Comparison of vessel call duration at Indian and Californian Ports:</u> We also compared the time spent at berth by vessels calling at Indian and Californian ports. **Figure 5.4** shows cumulative distribution functions (CDF) for time spent at berth by vessels calling at Indian major ports against those located in California. We observe that the median port call duration for major ports (39 hours) is higher than that for Californian ports (9 hours). But the average port call duration for Californian ports (82 hours) is higher than that of major ports (50 hours).

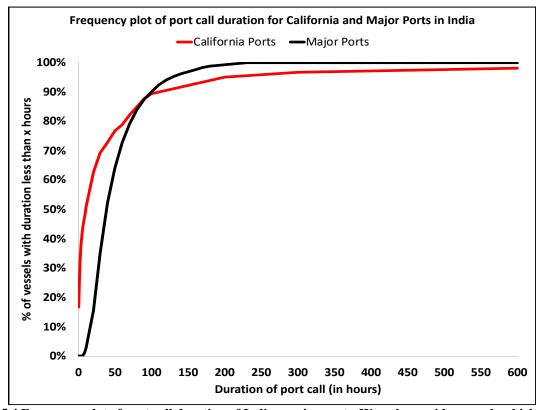


Figure 5.4 Frequency plot of port call duration of Indian major ports. We only consider vessels which stayed in the port greater than or equal to 5 hours and less than or equal to 228 hours.

5.4 India's Grid Electricity Emission Factors

<u>Coal based power generation between 2012 and 2017:</u> While the total thermal power capacity has increased by ~96% between 2010 and 2015 (see Table 1 of Sahu et al.), ²⁰⁰ only 16% of the total installed capacity was based on super-critical technology and the remaining 84% utilized sub-critical technology in 2015.²⁰¹ There were no ultra-super-critical technology based thermal power plants then. Moreover, an ultra-super-critical equipped thermal power plant generates only ~14% less SO₂ in comparison to a sub-critical power plant.²⁰² Thus, emission regulations that mandate post combustion treatments have a much greater effect on emissions than the technology type of the coal power plant.²⁰² In India, mandates for post-combustion treatment have been delayed. Hence, using emission factors based on coal power generation in 2012 doesn't affect our results very much because there aren't any retrofits installed by the power plant operators until 2017 to curtail the thermal power generation emissions. Coal based power generation between 2017 and 2030: In 2015, the Ministry of Power introduced a set of new emission standards for coal-based power plants and pledged that all new coal capacity additions will be supercritical units as part of the 13th plan period (2017) onwards).²⁰³ Thus, most of the new coal capacity after 2017 will be less polluting and the coal power plant operators are required to retrofit their facilities with emissions control technology in this decade. However, all power plants in 2017 were given a 5-year extension to retrofit their thermal units by 2022. Despite the seven years since the initial notification, a report from the Centre for Science and Environment (CSE) finds that ~70% of coal power plants will continue to be non-compliant with the emission standards by 2022.²⁰⁴ Still, in our results, we have accounted for the effect of cleaning up of the coal power generation sector between 2017 and 2030 by

scaling the coal power plant emission factors in the states where the ports are located. We scale

NO_x emission factor by 10, SO₂ emission factor by 20, and PM_{2.5} emission factor by 250 when considering the emissions from coal power generation during 2017 and 2030. These scaling factors were derived from a report published by Center for Study of Science, Technology, and Policy in 2018.⁹²

In our analysis, we assume that a kilowatt-hour of electricity supplied to a ship produces the same emissions as the average kilowatt-hour of electricity generated in the state. Mathematically, the emission factor in a particular state can be expressed as:

$$EF = \frac{Emissions_{coal} + Emissions_{nat.gas} + Emissions_{ren.} + Emissions_{nucl.}}{Total\ Generation}$$

$$EF = \frac{\left(EF_{coal}*Prop_{coal} + EF_{nat.gas}*Prop_{nat.gas} + EF_{ren.}*Prop_{ren.} + EF_{nucl.}*Prop_{nucl.}\right)*Total \, Generation}{Total \, Generation}$$

Here,

 $EF = \text{Emission factor (in g/kWh) for pollutant PM}_{2.5}, SO_2, NO_x \text{ and CO}_2 \text{ in the state}$

Emissions_{coal}= Emissions from coal combustion during electricity generation

Emissions_{nat,qas}= Emissions from natural gas during electricity generation

*Emissions*_{ren} = Emissions from renewables (solar, wind, hydro) during electricity generation

Emissions_{nucl} = Emissions from nuclear during electricity generation

EF_{coal}= Emission factor of coal (in g/kWh)

 $EF_{nat.gas}$ = Emission factor of natural gas (in g/kWh)

 EF_{ren} = Emission factor of renewables (in g/kWh)

 EF_{nucl} = Emission factor of nuclear (in g/kWh)

 $Prop_{coal}$ = Proportion of coal in the electricity generation mix

 $Prop_{nat,aas}$ = Proportion of natural gas in the electricity generation mix

 $Prop_{ren}$ = Proportion of renewables (solar, wind, hydro) in the electricity generation mix

Prop_{nucl.}= Proportion of nuclear in the electricity generation mix

Total Generation= Total electricity generation from all sources in the state

Total generation cancels out throughout the equation. The first term in the numerator stays but the second term is eliminated because the proportion of natural gas is small (~4%); the third and fourth term is eliminated because the emissions index from renewables and nuclear is zero.

Then the equation becomes

$$\textit{EF} = \frac{(\textit{EF}_{coal} * \textit{Prop}_{coal} * \textit{Total Generation})}{\textit{Total Generation}}$$

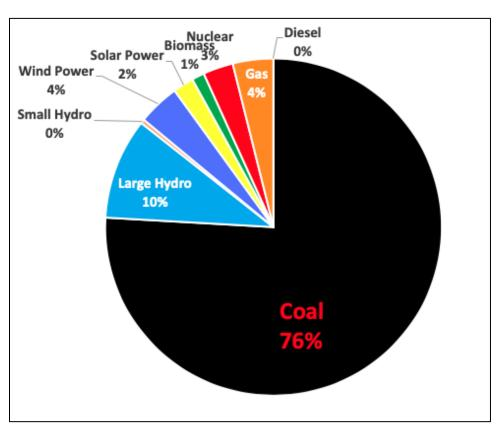


Figure 5.5 India's power generation mix in 2017 by different fuel sources. The total electricity generation as of 03/31/2018 was $\sim 1,300,000$ GWh.²⁰⁵

Figure 5.5 shows India's electricity generation mix with coal being the leading source of fuel for electricity generation. Based on our assumptions, more electricity needs to be generated in power plants to meet the energy demand of the vessels as there is some energy loss in transmission and

distribution (T&D). We address the emissions intensity sensitivity by performing our analysis at the state level while bounding the minimum and maximum values of emissions' intensities of grid electricity in respective states. **Figure 5.6** and **Table 5.17** provides state and regional emission factors for PM2.5, SO2, NO_x and CO2 for states where the major ports are located. Also, the state of Goa doesn't have its own generating units and purchases power from power stations (mostly thermal) from the regional grid.²⁰⁶ So, we use the average emission factors for the western region in the case of Goa.

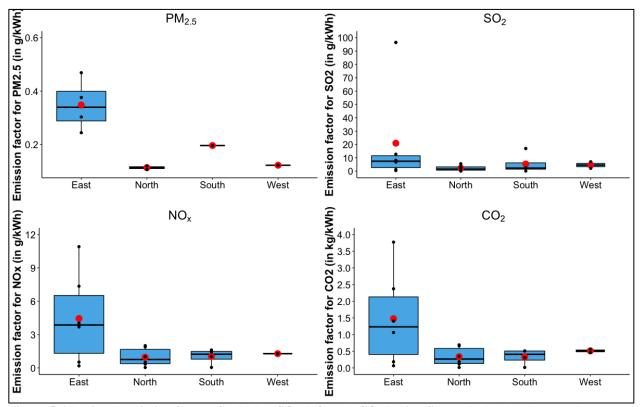


Figure 5.6 Regional emission factors for $PM_{2.5}$, SO_2 , NO_x and CO_2 Indian States. Red color denotes the mean value of emission factor in each region. We use state data on generation from the Central Electricity Authority (CEA)⁸² and combine it with peer reviewed data on annual coal generation at the state level in India in $2012^{81,207}$ to estimate these values.

Table 5.17 State level emission factors from previous figure for $PM_{2.5}$, SO_2 , NO_x and CO_2 . All values are in g/kWh and reported up to two significant digits. Baseline emission factors are for the state's electricity grid. The ranges in parenthesis signify minimum and maximum values of emission factors for the region (east, west, north, and south). SO_2 emission factor for Tamil Nadu and Odisha are an order of magnitude higher than other states.

State PM	$I_{2.5}$ (g/kWh)	SO ₂ (g/kWh)	$NO_x(g/kWh)$	$CO_2(g/kWh)$
----------	-------------------	-------------------------	---------------	---------------

Gujarat	0.12 (0.067-0.12)	7.0 (2.1-7.0)	1.3 (1.3-1.3)	560 (460-560)
Maharashtra	0.067 (0.067-0.12)	2.1 (2.1-7.0)	1.3 (1.3-1.3)	460 (460-560)
Andhra	0.057 (0.002-0.20)	1.9 (0.065-17)	1.0 (0.038-1.6)	310 (13-510)
Pradesh				
Tamil Nadu	0.20 (0.002-0.20)	17 (0.065-17)	1.4 (0.038-1.6)	510 (13-510)
West Bengal	0.24 (0.009-0.47)	6.8 (0.42-97)	3.7 (0.18-11)	1400 (64-3800)
Odisha	0.38 (0.009-0.47)	13 (0.42-97)	7.4 (0.18-11)	2400 (64-3800)
Kerala	0.002 (0.002-0.20)	0.065 (0.065-	0.038 (0.038-	13 (13-510)
		17)	1.6)	
Karnataka	0.083 (0.002-0.20)	2.6 (0.065-17)	1.6 (0.038-1.6)	510 (13-510)
Goa	0.095 (0.067-0.12)	4.5 (2.1-7.0)	1.3 (1.3-1.3)	510 (460-560)

Table 5.18 shows electricity grid emission factors used in the analysis for 2017 and 2030.

Table 5.18 Electricity grid emission factors used for coal fired power plants for the year 2017 and 2030. For 2030, we assume that retrofits to curb PM2.5, SO2, and NOx would be introduced at coal power plants as per GoI's directives and thus we scale the emission factors accordingly. We scale NO_x emission factor by 10, SO_2 emission factor by 20, and $PM_{2.5}$ emission factor by 250 when considering the emissions from coal power generation between 2017 and 2030. 92

Port	State	2017 Grid Emission Factors (g/kWh)			2030 Grid I	Emission I	Factors (g/	kWh)	
		PM _{2.5}	SO_2	NO _x	CO ₂	PM _{2.5}	SO ₂	NO _x	CO ₂
Chennai	Tamil Nadu	0.2	17	1.4	510	0.00078	0.85	0.14	510
Cochin	Kerala	0.002	0.065	0.038	13	0.000008	0.0033	0.0038	13
Deendayal	Gujarat	0.12	7	1.3	560	0.00049	0.35	0.13	560
JNPT	Maharashtra	0.067	2.1	1.3	460	0.00027	0.1	0.13	460
Kamarajar	Tamil Nadu	0.2	17	1.4	510	0.00078	0.85	0.14	510
Kolkata	West Bengal	0.24	6.8	3.7	1400	0.00098	0.34	0.37	1400
Haldia	West Bengal	0.24	6.8	3.7	1400	0.00098	0.34	0.37	1400
Mormugao	Goa	0.095	4.5	1.3	510	0.00038	0.23	0.13	510
Mumbai	Maharashtra	0.067	2.1	1.3	460	0.00027	0.1	0.13	460
New Mangalore	Karnataka	0.083	2.6	1.6	510	0.00033	0.13	0.16	510
Paradip	Odisha	0.38	13	7.4	2400	0.0015	0.64	0.74	2400
VOC	Tamil Nadu	0.2	17	1.4	510	0.00078	0.85	0.14	510
Vizag	Andhra Pradesh	0.057	1.9	1	310	0.00023	0.097	0.1	310
All Ports		0.15	7.5	2.1	730	0.0006	0.38	0.21	730

95

5.5 Energy Cost and Savings

The exchange rate of US dollar (USD) to Indian Rupee (INR) used was Rs. 68.96 (November 30, 2018). 86 **Table 5.19** provides electricity tariffs in states where the major ports are located.

Table 5.19 Electricity tariffs for supplying shore power electricity to major ports.

Port	State	Electricity tariff (Rs/kWh)	Electricity tariff (\$/kWh)
Chennai	Tamil Nadu	6.35 ²⁰⁸	0.09
Cochin	Kerala	5.80 ²⁰⁹	0.08
Deendayal	Gujarat	6.60 ²¹⁰	0.10
JNPT	Maharashtra	6.00 ²¹¹	0.09
Kamarajar	Tamil Nadu	6.35 ²⁰⁸	0.09
Kolkata	West Bengal	7.13 ²¹²	0.10
Haldia	West Bengal	7.13 ²¹²	0.10
Mormugao	Goa	9.20 ²¹³	0.09
Mumbai	Maharashtra	6.00 ²¹¹	0.09
New Mangalore	Karnataka	7.15 ²¹⁴	0.10
Paradip	Odisha	5.30 ²¹⁵	0.08
VOC	Tamil Nadu	6.35 ²⁰⁸	0.09
Visakhapatnam	Andhra	4.75 ²¹⁶	0.07
	Pradesh		

5.6 Global Emissions Inventory Comparison

The Emission Database for Global Atmospheric Research (EDGAR) 2015 emissions inventory⁸⁷ comprises of emissions from various categories. We grouped these sources in broad sectors, namely, (1) Energy, (2) Ships, (3) Air, (4) Industry, (5) Transport, and (6) Residential. **Table 5.20** provides the classification of sectors that we used from EDGAR 2015 emissions inventory to estimate city emissions where the major ports are located.

Table 5.20 Sector classification that we used in estimating EDGAR city emissions from various sources in port cities.

Sector	Sub Sector			
Energy	Power Industry (ENE)			
Ships	Shipping (TNR_Ship)			
Air	Aviation climbing&descent (TNR_Aviation_CDS)			

	Aviation cruise (TNR_Aviation_CRS)			
	Aviation landing&takeoff (TNR_Aviation_LTO)			
Industry	Combustion for manufacturing (IND)			
	Fuel exploitation (PRO)			
	Fossil Fuel Fires (FFF)			
	Chemical processes (CHE)			
	Food and Paper (FOO_PAP)			
	Non-ferrous metals production (NFE)			
	Non-metallic minerals production (NMM)			
	Oil refineries and Transformation industry (REF_TRF)			
	Iron and steel production (IRO)			
	Solvents and products use (PRU_SOL)			
Transport	Railways, pipelines, off-road transport (TNR_Other)			
	Road transportation no resuspension (TRO_noRES)			
	Road transportation resuspension (TRO_RES)			
Residential	Energy for buildings (RCO)			
	Solid waste incineration (SWD_INC)			
	Solid waste landfills (SWD_LDF)			

Table 5.21 provides the latitude and longitudes of the areas where $0.1 \text{ deg.} \times 0.1 \text{ deg.}$ cells were selected to estimate relative contribution of berthed ships to total city emissions.

Table 5.21 Port latitude and longitude considered for EDGAR city level emissions estimation. The latitude and longitude ranges show the city rectangle area which was considered for calculating contributions of major ports' emissions in the city. The area ranges included major sources of pollution in the city such as airports, oil refineries and industrial areas.

Major Port	Port Latitude	Port Longitude	Latitude	Longitude
			Range	Range
Chennai	13.08	80.29	12.80-13.30	80.00-80.40
Cochin	9.95	76.26	9.90-10.20	76.20-76.40
Deendayal	23.01	70.21	22.90-23.20	70.00-70.30
JNPT	18.94	72.95	18.90-19.10	72.70-73.00
Kamarajar	13.25	80.33	12.90-13.30	79.70-80.40
Kolkata	22.54	88.31	22.00-22.70	88.00-88.50
Haldia	22.04	88.08	22.00-22.70	88.00-88.50
Mormugao	15.40	73.80	15.30-15.40	73.70-73.90
Mumbai	18.90	72.81	18.90-19.10	72.70-73.00
New Mangalore	12.92	74.82	12.80-13.00	74.70-74.90
Paradip	20.26	86.67	20.20-20.30	86.40-86.70

97

VOC	8.75	78.17	8.70-8.80	78.00-78.30
Vizag	17.68	83.29	17.70-17.80	83.10-83.30

Power sector growth rate assumptions: We relied on a Center for Study of Science, Technology and Policy (CSTEP) report that uses state level generation emission factors and annual coal consumption at the plant level to model coal-based emissions from 2015-2030. The SO_x, NO_x and PM₁₀ emissions from coal power generation grew from 6,449, 2,996, 605 kilotons (kT) in 2015 to 13,494, 6050, and 790 kT in 2030 respectively. We assume that the increase in emissions in representative of growth in the power generation sector and thereby assume a 5% yearly growth rate from 2017-2030. Additionally, we validated our estimation via other growth projections sources such as the Brookings India's projection for grid electricity requirement, which predicted similar growth rates for the power sector (4.6%-5.6% per year). 93

5.7 Health Effects of Pollution Reduction

To determine annually avoided premature deaths in port cities, we estimate percentage reduction in ports at berth pollution while taking into account the population of port cities. The population of port cities are provided in **Table 5.22**. Table 2 of Lee et al.⁹⁴ provides absolute change in global premature mortality avoided across each of the 21 global burden of disease (GBD) regions for black carbon (BC), SO₂ and NO_x to a 10% reduction in precursor emissions. We use BC estimates instead of PM_{2.5} for estimating health effects due to PM_{2.5} changes. From Table 2, the premature deaths avoided in South Asia were SO₂- 5,600 (4,700-6,500); NO_x- 1,600 (1,300-1,900); and black carbon (BC)- 330 (280-380). The range in parenthesis shows a 95% confidence interval (CI).

Table 5.22 2019 population of cities located near major ports in India.

Port Cities	Population (2019)
Chennai (located near Chennai and Kamarajar port)	$11M^{161}$
Kochi	$3M^{217}$
Gandhidham (located near Deendayal port)	$370K^{218}$
Kolkata	$15M^{164}$
Haldia	$170K^{219}$
Mormugao	180K ¹⁶⁷
Mumbai (located near Mumbai and JNPT port)	$20M^{220}$
Mangalore (located near New Mangalore port)	620K ¹⁶⁶
Paradip	69K ²²¹
Tuticorin (located near VOC port)	570K ¹⁶⁸
Vizag	$4.3M^{169}$

5.8 Cost of Grid Extension, Shore Infrastructure and Vessel Retrofitting

We estimate the maximum hourly load demand at berth and establish that a 33-kV line is sufficient to meet the hourly peak loads of auxiliary engines at all ports as shown in **Table 5.23**.

Table 5.23 Port-wise hourly peak berthing load, hourly excess solar generation, transformer ratings, number of circuit breakers and cables needed.

Port	Hourly Max Berth Load (MW)	Hourly Max Solar Gen. (MW)
Chennai	13	24
Cochin	34	24
Deendayal	16	31
Haldia	13	25
JNPT	10	22
Kamarajar	4	6
Kolkata	11	15
Mormugao	46	19
Mumbai	29	30
New Mangalore	9	16
Paradip	11	23
VOC	7	13
Vizag	14	25

Table 5.24 shows the distance between the port and the nearest available substation.

Table 5.24 Distance from the port to the nearest distribution substation.

Port	Port Lat.	Port	Sub	Sub Station	Distance
		Long.	Station	Long.	(in miles)
			Lat.		
Chennai	13.0815	80.2921	13.0963912	80.3066884	1
Cochin	9.9546	76.2678	9.87524876	76.3016032	6
Deendayal	23.01666	70.2166	23.1543316	70.1062696	12
JNPT	18.9499	72.9512	18.9060914	72.9821779	4
Kamarajar	13.2593	80.3374	13.2018393	80.3176312	4
Kolkata	22.5461	88.3149	22.5646042	88.3149442	1
Haldia	22.0447	88.0888	22.0262806	88.1401794	4
Mormugao	15.4088	73.8011	15.4570222	73.8318855	4
Mumbai	18.9	72.8166	18.9308377	72.8617593	4
New Mangalore	12.9281	74.8222	12.8144974	74.8967631	9
Paradip	20.2654	86.6762	20.2817459	86.6341554	3
VOC	8.7563	78.1791	8.75320468	78.1258279	4
Vizag	17.6868	83.2903	17.6719108	83.3005694	1

5.9 Extended Results and Discussion

5.9.1 Major ports' emissions as a proportion of total city emissions

Table 5.25 and **Table 5.26** share pollutant burden which ports contribute to local air quality in the nearby cities for RO and MGO fuel type. The compounded annual growth rate (CAGR) is assumed to be ~3% each year which was the decadal growth rate in Indian shipping from 2007-2017.^{89,90}

Table 5.25 Major ports' contribution to city emissions in 2017 and 2030 when berthed ships burn RO. Growth rate in shipping is assumed to be 3% annually from 2017-2030.89,90

Port	At berth emissions as % of total city emissions 2017			At berth entotal city en		
	%PM _{2.5} %SO ₂ %NO _x %PM _{2.5} %SO ₂				%SO ₂	%NO _x
Chennai	0.19	0.49	0.81	0.21	0.16	0.65
Cochin	1.0	5.3	4.6	0.56	0.63	2.1
Deendayal	4.3	16	16	2.9	4.3	8.1
JNPT	0.43	1.4	1.6	0.21	0.15	0.77
Kamarajar	0.05	0.14	0.22	0.06	0.05	0.17
Kolkata	0.09	0.31	0.51	0.06	0.06	0.35

Haldia	0.16	0.57	0.94	0.11	0.10	0.65
Mormugao	3.7	32	23	1.8	3.5	9.1
Mumbai	0.54	1.8	2.0	0.27	0.20	0.98
New Mangalore	1.4	8.0	6.6	0.80	1.2	3.1
Paradip	4.7	1.5	33	2.4	0.11	15
VOC	0.30	0.48	1.1	1.2	0.13	2.3
Vizag	0.09	0.23	0.54	0.06	0.02	0.40

Table 5.26 Major ports' contribution to city emissions in 2017 and 2030 when berthed ships burn MGO. Growth rate in shipping is assumed to be 3% annually from 2017-2030.89,90

Port		emissions as emissions 2		At berth emissions as % of total city emissions 2030				
	%PM2.5	%SO ₂	%NO _x	%PM2.5	%SO ₂	%NO _x		
Chennai	0.04	0.09	0.77	0.05	0.03	0.62		
Cochin	0.22	0.98	4.4	0.12	0.11	2.0		
Deendayal	0.97	3.2	15	0.65	0.78	7.7		
JNPT	0.09	0.26	1.5	0.05	0.03	0.73		
Kamarajar	0.01	0.03	0.21	0.01	0.01	0.16		
Kolkata	0.02	0.06	0.48	0.01	0.01	0.33		
Haldia	0.04	0.1	0.89	0.03	0.02	0.62		
Mormugao	0.83	7.8	22	0.41	0.64	8.6		
Mumbai	0.12	0.33	1.9	0.06	0.04	0.93		
New Mangalore	0.31	1.5	6.2	0.18	0.22	2.9		
Paradip	1.1	0.26	31	0.54	0.02	15		
VOC	0.07	0.09	1.0	0.26	0.02	2.2		
Vizag	0.02	0.04	0.51	0.01	0.0	0.37		

Table 5.27 and **Table 5.28** share pollutant burden of shipping in port cities for RO and MGO when the CAGR is assumed to be 18%.^{57,58} This is the projected growth rate for Indian shipping by the GoI for the period 2017-2025.

Table 5.27 Major ports' contribution to city emissions in 2017 and 2030 when berthed ships burn RO. Growth rate in shipping is assumed to be 18% annually from 2017-2030. 57,58

Port	At berth e total city e			At berth emissions as % of total city emissions 2030			
	%PM _{2.5}	%SO ₂	%NO _x	%PM _{2.5}	%SO ₂	%NO _x	
Chennai	0.19	0.5	0.8	1.7	1.3	5.4	

Cochin	1.0	5.3	4.6	4.3	4.7	16
Deendayal	4.3	16	16	20	26	44
JNPT	0.43	1.4	1.6	1.7	1.2	6.2
Kamarajar	0.05	0.1	0.2	0.44	0.36	1.4
Kolkata	0.09	0.3	0.5	0.48	0.43	2.9
Haldia	0.16	0.6	0.9	0.89	0.79	5.2
Mormugao	3.7	32	23	13	22	47
Mumbai	0.54	1.8	2.0	2.1	1.5	7.8
New Mangalore	1.4	8.0	6.6	6.1	8.9	21
Paradip	4.7	1.5	33	16	0.86	61
VOC	0.30	0.5	1.1	8.7	1.0	16
Vizag	0.09	0.2	0.5	0.48	0.19	3.0

Table 5.28 Major ports' contribution to city emissions in 2017 and 2030 when berthed ships burn MGO. Growth rate in shipping is assumed to be 18% annually from 2017-2030. 57,58

Port Port	At berth e			At berth em	issions as ^c	% of
	total city of	emissions 2	2017	total city em	issions 203	80
	%PM2.5	%SO ₂	%NO _x	%PM _{2.5}	%SO ₂	%NO _x
Chennai	0.04	0.09	0.77	0.27	0.17	3.5
Cochin	0.22	0.98	4.4	0.72	0.65	11
Deendayal	0.97	3.2	15	3.7	4.4	33
JNPT	0.09	0.26	1.5	0.27	0.16	4.1
Kamarajar	0.01	0.03	0.21	0.07	0.05	0.93
Kolkata	0.02	0.06	0.48	0.08	0.06	1.9
Haldia	0.04	0.10	0.89	0.15	0.11	3.5
Mormugao	0.83	7.8	22	2.4	3.6	36
Mumbai	0.12	0.33	1.9	0.35	0.20	5.2
New Mangalore	0.31	1.5	6.2	1.0	1.3	15
Paradip	1.1	0.26	31	3.1	0.11	50
VOC	0.07	0.09	1.0	1.5	0.14	11
Vizag	0.02	0.04	0.51	0.08	0.03	2.1

5.9.2 At Berth Emissions from burning RO and MGO

Table 5.29 provides PM_{2.5}, SO₂, NO_x and CO₂ emissions by burning RO and MGO. Additionally, the table provides load demand, energy available for meeting the requirement, annual electricity

cost, annual fuel cost and net savings at the port level by switching from RO and MGO to shore based electricity.

Table 5.29 Annual emissions from berthed ships for PM2.5, SO2, NOx, CO2, port's electricity load, fuel cost and savings.

Port	Price	Demand	Supply	Elec	Residu	al Oil (RO;	2.7% S)				Marine	Gas Oil (M	GO; 0.5%	6 S)		
				Cost	Fuel cost	Savings	PM _{2.5}	SO ₂	NO _x	CO ₂	Fuel cost	Savings	PM _{2.5}	SO ₂	NO _x	CO ₂
	\$/kWh	GWh	GWh	M \$	M \$	M \$	MT	MT	MT	1000 MT	M \$	M \$	MT	MT	MT	1000 MT
Chennai	0.09	55	61	4.9	5.6	0.7	72	650	800	39	8.7	3.8	16	120	760	38
Cochin	0.08	55	61	4.4	5.7	1.3	73	660	810	40	8.8	4.4	16	120	760	38
Deendayal	0.10	77	86	7.7	8.0	0.3	100	930	1.1K	56	12.0	4.6	22	160	1.1K	54
JNPT	0.09	57	63	5.1	5.9	0.8	75	680	830	41	9.1	4.0	16	120	790	39
Kamarajar	0.09	16	17	1.4	1.6	0.2	21	190	230	11	2.5	1.1	5	33	220	11
Kolkata	0.10	33	36	3.3	3.4	0.1	43	390	480	24	5.2	2.0	10	69	450	23
Haldia	0.10	61	67	6.1	6.3	0.2	80	730	890	44	9.7	3.6	18	130	840	42
Mormugao	0.09	42	46	3.8	4.3	0.6	55	500	610	30	6.7	2.9	12	88	580	29
Mumbai	0.09	72	80	6.5	7.5	1.0	95	870	1.1K	52	12	5.1	21	150	1K	50
New Mangalore	0.10	37	41	3.7	3.8	0.1	49	450	550	27	5.9	2.2	11	79	520	26
Paradip	0.08	53	59	4.2	5.5	1.2	70	630	780	38	8.4	4.2	15	110	730	36
VOC	0.09	31	34	2.8	3.2	0.4	41	370	450	22	4.9	2.2	9	65	430	21
Vizag	0.07	58	64	4.0	6.0	1.9	76	690	850	42	9.2	5.2	17	120	800	40
All Major Ports	0.09	650	720	58	67	8.7	850	7.7K	9.5K	470	100	45	190	1.4K	9K	450

Table 5.30 provides PM_{2.5}, SO₂, NO_x and CO₂ emissions from shore power to meet berthed vessels' load requirement.

Table 5.30 Annual emissions from shore power to meet berthing load requirement at ports. The 2030 scenario assumes that air pollution control technologies for $PM_{2.5}$, SO_2 , and NO_x have been installed on coal power

plants.

Port	2017				2030 (wł	nen the gr	id is clean	er)
	PM2.5 (MT)	SO ₂ (MT)	NO _x (MT)	CO ₂ (MT)	PM _{2.5} (MT)	SO ₂ (MT)	NO _x (MT)	CO ₂ (MT)
Chennai	12	1K	87	31K	0	52	9	31K
Cochin	0	4	2	780	0	0	0	780
Deendayal	10	600	110	48K	0	30	11	48K
JNPT	4	130	82	29K	0	7	8	29K
Kamarajar	3	290	25	8.8K	0	15	3	8.8K
Kolkata	9	250	130	51K	0	12	13	51K
Haldia	16	460	250	94K	0	23	25	94K
Mormugao	4	210	59	24K	0	11	6	24K
Mumbai	5	170	100	37K	0	8	10	37K
New Mangalore	3	110	67	21K	0	5	7	21K
Paradip	22	750	430	140K	0	37	43	140K
VOC	7	580	49	17K	0	29	5	17K
Vizag	4	120	66	20K	0	6	7	20K
All Major Ports	100	4.7K	1.5K	520K	0	240	150	520K

5.9.3 Hourly Load Profile and Hourly Emissions Inventory

Figure 5.7 shows hourly emissions for SO₂ for each hour of the year across the port of Chennai and Cochin. The hourly emissions inventory for other ports were similar. There were some ports such as Chennai and Kamarajar, which shared vessel activity data for more than one year. For calculating hourly emissions inventory for ports where more than one-year of data are available, we took the mean value of emissions in 2017 and 2018 to be representative of the hourly emissions. Further, the hourly bins had vessels coming in and going out at edge points. For instance, a vessel calling in at 12:55 pm is considered in the 12:00-13:00 hours hourly bin.

However, it only spent 5 minutes in that window. In order to account for edge effects and avoid inflation in emission estimates, we balanced this by counting the vessel in the window on only one side (either arrival or departure) instead of counting it in both hourly windows of arrival and departure.

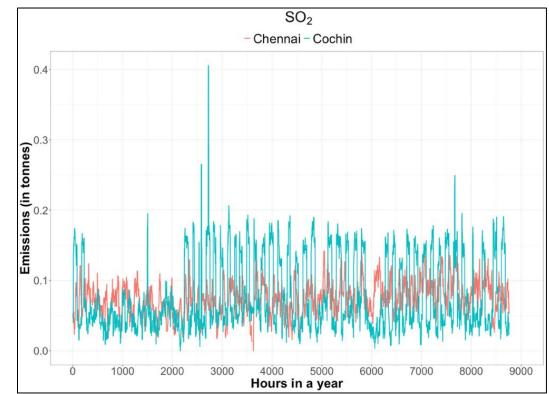
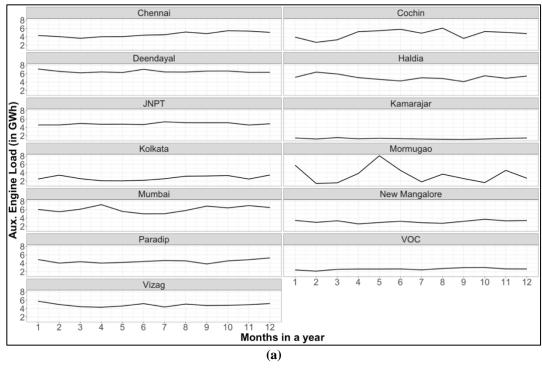


Figure 5.7 Hourly SO_2 emissions from berthed ships at Chennai and Kochi from 01/01/2017 00:00 hours to 01/01/2018 00:00 hours. The emissions of $PM_{2.5}$ and NO_x approximately follow identical hourly profiles for other major ports.

Figure 5.8(a) provides monthly energy requirement of berthed ships (in GWh). While the need for electricity remains more or less roughly constant in ports with some minor fluctuations, we observe some seasonality in electricity requirement in summer (April-May) and winter (October-December) months for Mormugao, Cochin and Mumbai. The daily energy consumption pattern of berthed ships is shown in **Figure 5.8(b)**.



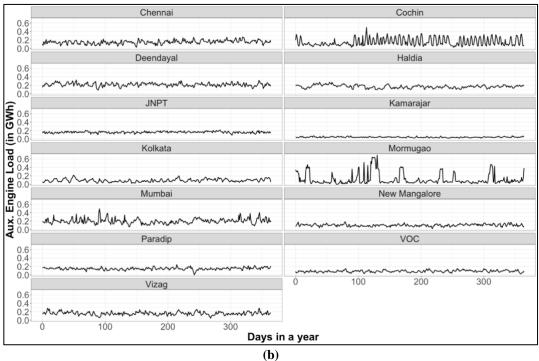


Figure 5.8 (a) Monthly AE load requirement (in GWh) for all berthed ships at major ports from 01/01/2017 00:00 hours to 01/01/2018 00:00 hours. (b) Daily AE load requirement (in GWh) for all berthed ships at major ports.

5.9.4 Change in emissions if vessels were to switch to shore power

The case for switching from RO to shore power is shown in Figure 5.9.

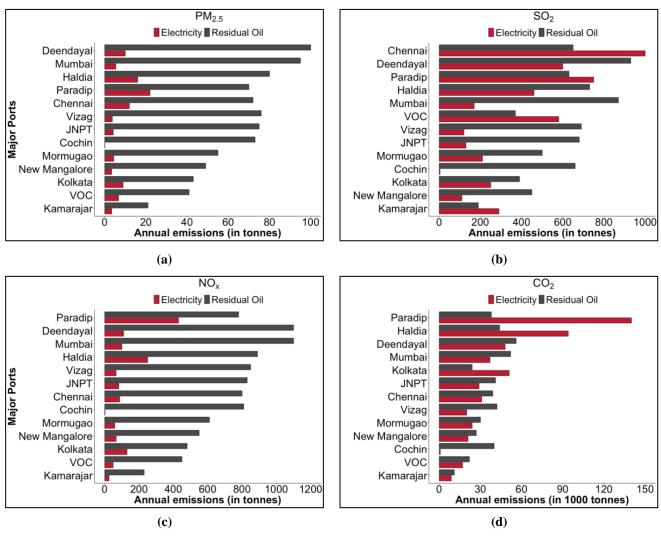


Figure 5.9 Change in total emissions (in tonnes) at major ports, if ships were to use shore power instead of burning RO for meeting their electricity requirement.

If ships were to switch from RO to shore power, emissions from berthed ships would decline for PM_{2.5} by 88% (750 tonne reduction), for SO₂ by 39% (3,000 tonne reduction), for NO_x by 85% (8,000 tonne reduction), but increase for CO₂ by 12% (55,000 tonne increase). **Table 5.31** and **Table 5.32** provide the percentage and absolute change in emissions if the vessels were to switch from burning RO and MGO to shore power at major ports.

Table 5.31 % change in emissions by switching from RO and MGO to shore power at major ports in 2017-2018.

Pollutant or	RO (2.7%	S)		MGO (0.5	MGO (0.5% S)			
GHG	Min change	Change	Max change	Min change	Change	Max change		
PM _{2.5}	-93%	-88%	-81%	-69%	-46%	-12%		
SO ₂	-78%	-39%	190%	24%	240%	1,500%		
NO _x	-90%	-85%	-73%	-89%	-84%	-71%		
CO ₂	-35%	12%	95%	-32%	17%	100%		

Table 5.32 Total emissions change (in tonnes) by switching from RO and MGO to shore power at major ports in 2017- 2018.

Pollutant or	RO (2.7%	S)		MGO (0.5	MGO (0.5% S)			
GHG	Min change	0		Min change	Change	Max change		
PM _{2.5}	-790	-750	-690	-130	-86	-23		
SO ₂	-6K	-3K	15K	330	3.3K	21K		
NOx	-8.5K	-8K	-6.9K	-8K	-7.5K	-6.4K		
CO ₂	-160K	55K	440K	-140K	75K	460K		

Figure 5.10 shows ports for which SO_2 emission factors were an order of magnitude higher compared to other major ports.

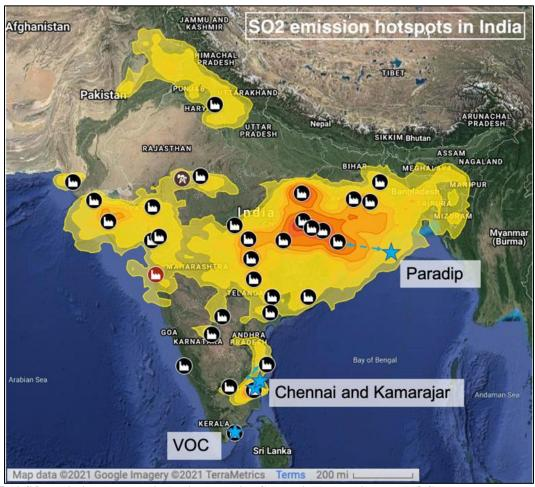


Figure $5.10~SO_2$ emission hotspots in India. Paradip, Chennai, Kamarajar and VOC are located near thermal power plants which use low grade coal for power generation. Hence, their emission factors are higher compared to other major ports. The base map has been adapted from the global SO_2 hotspots tracker and is publicly available. 222

5.9.5 Annual Fuel Cost Savings and Lifetime Savings

Table 5.33 and **Table 5.34** provide the annual fuel cost savings by vessel category and port on an annual, per call and per vessel basis. **Figure 5.11** shows distribution of annual and lifetime savings for the switch from RO and MGO to shore power.

Table 5.33 Fuel cost savings and lifetime savings (in US \$) by switching from RO and MGO to shore power at major ports. For both fuel types, the savings are highest for bulk carriers, tanker and general cargo ships. The useful life of the vessel is assumed to be 27 years which is the 96th percentile of vessel age in our dataset.

Vessel Category		RO (2	.7% S)		MGO (0.5% S)			
	Annual Savings	Savings Per Call	Savings Per Vessel	Lifetime Savings	Annual Savings	Savings Per Call	Savings Per Vessel	Lifetime Savings

				(i	in US \$)			
Auto Carrier	86K	250	480	780K	460K	1.3K	2.5K	4.1M
Bulk	2.5M	430	980	24M	12M	2.0K	4.6K	110M
Container	1.2M	250	2.1K	10M	6.6M	1.3K	11K	53M
Crude Oil Tanker	780K	640	1.8K	5.7M	4.2M	3.4K	9.4K	31M
General Cargo	1.3M	570	2.3K	11M	7.0M	3.1K	12K	59M
Passenger	1M	2.1K	25K	8M	4.1M	8.6K	100K	29M
RoRo	2.2K	95	180	23K	11K	490	940	120K
Tanker	1.8M	270	1.4K	13M	11M	1.6K	8.2K	84M
Total	8.7M			73M	45M			370M

Table 5.34 Port-wise annual savings, average savings per call and median savings per call.

Port name	RO (2.5% S)		MGO (0.5% S)							
	Annual Savings	Savings per Call	Median Savings	Annual Savings	Savings per Call	Median Savings					
	(in US \$)										
Chennai	730K	460	320	3.8M	2,400	1,700					
Cochin	1.3M	900	370	4.4M	3,100	1,300					
Deendayal	260K	97	79	4.6M	1,700	1,400					
Haldia	200K	89	80	3.6M	1,600	1,500					
JNPT	750K	310	270	4.0M	1,600	1,400					
Kamarajar	210K	260	250	1.1M	1,400	1,300					
Kolkata	110K	87	56	2.0M	1,600	1,000					
Mormugao	550K	580	330	2.9M	3,000	1,800					
Mumbai	960K	450	330	5.1M	2,400	1,700					
New Mangalore	120K	93	76	2.2M	1,700	1,400					
Paradip	1.2M	650	500	4.2M	2,200	1,700					
VOC	410K	310	240	2.2M	1,700	1,200					
Vizag	1.9M	1,000	790	5.2M	2,700	2,100					
All Major Ports	8.7M	400	210	45M	2,100	1,500					

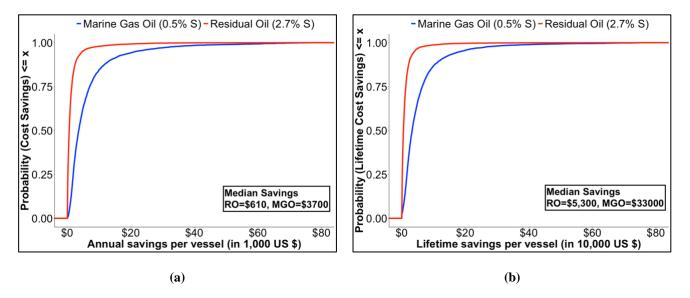


Figure 5.11 (a) Distribution of annual fuel cost savings for switching from RO and MGO to shore power across major ports. (b) Distribution of lifetime fuel cost savings for switching from RO and MGO to shore power across major ports. Median savings were higher for MGO compared to RO in both cases.

5.9.6 Health Effects of Switching from RO and MGO to Shore Power

We consider two scenarios. In the first case, we assume shipping growth rate to be 3% per year (2007-2017 Indian shipping growth)^{89,90} and in the second case, we assume shipping growth rate to be 18% per year (GoI projection).^{57,58}

5.9.6.1 Health Consequences Across Port Cities

Table 5.35 and **Table 5.36** provide estimates of avoided premature deaths by switching from RO and MGO to shore power in 2017. The growth in shipping in each of these scenarios is assumed to be 3% per year (2007-2017 Indian shipping growth). ^{89,90} **Table 5.37** and **Table 5.38** show total annually avoided premature mortality per port in 2030 by switching from RO and MGO to shore power when the power generation and transportation sector become cleaner.

To illustrate our method, let's take the example of the change of PM_{2.5} pollution on premature mortality in Chennai due to switch from RO to shore power when growth in shipping is assumed to be ~3% each year. ^{89,90} In 2017, PM_{2.5} from shipping contributed 0.19% to total city emissions

(compared to total EDGAR emissions) in Chennai and the switch from RO to shore power reduced PM_{2.5} emissions in the port by 84%. The total PM_{2.5} emissions by switching from RO to shore power in Chennai was reduced by 0.16% (0.19% multiplied by 84%). We used BC estimates for estimating health effects of PM_{2.5} changes. A 10% change in BC emissions in South Asia helped avoid 330 (280-380; 95% CI) premature deaths and the population of South Asia was assumed to be 1,447,648,000.⁹⁰ After adjusting these numbers for the population of Chennai (~11M), this translates to 0.04 (0.034 to 0.046) avoided deaths due to PM_{2.5} reduction in the city (see Chennai Port PM_{2.5} results in **Table 5.35**). This approach was used to estimate health effects for different pollutant types across other major ports.

Table 5.35 Avoided premature mortality by switching from RO to shore power in 2017-2018. The growth in shipping is assumed to be 3% each year. 89,90 Also, we assume that no emissions control has been enforced on power generation and road transportation. All values are reported up to 2 significant digits and the parentheses show 95% confidence interval (CI).

Port	PM _{2.5}	SO ₂	NO _x	Avoided Premature Mortality
Chennai	0.04 (0.034 to 0.046)	-1.2 (-0.99 to -1.4)	0.85 (0.72 to 0.99)	-0.28 (-0.23 to -0.33)
Cochin	0.068 (0.058 to 0.078)	6 (5.1 to 7)	1.5 (1.3 to 1.8)	7.6 (6.4 to 8.8)
Deendayal	0.033 (0.028 to 0.037)	0.78 (0.65 to 0.91)	0.6 (0.51 to 0.7)	1.4 (1.2 to 1.6)
JNPT	0.18 (0.16 to 0.21)	9.1 (7.6 to 11)	3.1 (2.6 to 3.6)	12 (10 to 14)
Kamarajar	0.011 (0.0092 to 0.012)	-0.33 (-0.28 to -0.39)	0.24 (0.2 to 0.27)	-0.088 (-0.073 to -0.1)
Kolkata	0.023 (0.02 to 0.026)	0.65 (0.55 to 0.76)	0.6 (0.5 to 0.69)	1.3 (1.1 to 1.5)
Haldia	0.00049 (0.00042 to 0.00056)	0.014 (0.012 to 0.016)	0.013 (0.011 to 0.015)	0.027 (0.023 to 0.031)
Mormugao	0.014 (0.012 to 0.016)	1.3 (1.1 to 1.5)	0.41 (0.34 to 0.47)	1.7 (1.4 to 2)
Mumbai	0.24 (0.2 to 0.27)	12 (9.7 to 13)	4 (3.4 to 4.6)	16 (13 to 18)
New Mangalore	0.019 (0.016 to 0.021)	1.5 (1.2 to 1.7)	0.4 (0.33 to 0.46)	1.9 (1.6 to 2.2)
Paradip	0.005 (0.0042 to 0.0057)	-0.007 (-0.0059 to -0.0082)	0.11 (0.093 to 0.13)	0.11 (0.091 to 0.13)
VOC	0.0032 (0.0027 to 0.0037)	-0.06 (-0.051 to -0.07)	0.062 (0.052 to 0.071)	0.0046 (0.004 to 0.0052)
Vizag	0.0086 (0.0073 to 0.0098)	0.31 (0.26 to 0.36)	0.24 (0.2 to 0.28)	0.56 (0.47 to 0.64)
All Ports	0.64 (0.55 to 0.74)	30 (25 to 34)	12 (10 to 14)	42 (36 to 49)

Table 5.36 Avoided premature mortality by switching from MGO to shore power in 2017-2018. The growth in shipping is assumed to be 3% each year. 89,90 Also, we assume that no emissions control has been enforced on power generation and road transportation. All values are reported up to 2

significant digits and the parentheses show 95% confidence interval (CI).

Port	PM _{2.5}	SO ₂	NO _x	Avoided Premature Mortality
Chennai	0.0026 (0.0022 to 0.003)	-2.9 (-2.4 to -3.3)	0.8 (0.67 to 0.93)	-2.1 (-1.7 to -2.4)
Cochin	0.015 (0.013 to 0.017)	1.1 (0.91 to 1.3)	1.4 (1.2 to 1.7)	2.5 (2.1 to 2.9)
Deendayal	0.0044 (0.0037 to 0.005)	-1.2 (-1 to -1.4)	0.57 (0.48 to 0.66)	-0.64 (-0.54 to -0.75)
JNPT	0.032 (0.027 to 0.037)	-0.17 (-0.14 to -0.2)	3 (2.5 to 3.4)	2.8 (2.4 to 3.3)
Kamarajar	0.00071 (0.0006 to 0.00081)	-0.81 (-0.68 to -0.95)	0.22 (0.19 to 0.26)	-0.59 (-0.5 to -0.69)
Kolkata	0.00041 (0.00035 to 0.00047)	-0.81 (-0.68 to -0.94)	0.55 (0.46 to 0.64)	-0.26 (-0.21 to -0.3)
Haldia	0.0000089 (0.0000075 to 0.00001)	-0.017 (-0.015 to -0.02)	0.012 (0.0099 to 0.014)	-0.0055 (-0.0046 to - 0.0065)
Mormugao	0.0022 (0.0018 to 0.0025)	-0.76 (-0.63 to -0.88)	0.39 (0.32 to 0.45)	-0.37 (-0.31 to -0.43)
Mumbai	0.041 (0.035 to 0.047)	-0.22 (-0.18 to -0.25)	3.7 (3.2 to 4.3)	3.6 (3 to 4.1)
New Mangalore	0.003 (0.0026 to 0.0035)	-0.13 (-0.11 to -0.15)	0.37 (0.31 to 0.43)	0.24 (0.21 to 0.28)
Paradip	-0.00073 (-0.00062 to -0.00084)	-0.04 (-0.033 to -0.046)	0.098 (0.083 to 0.11)	0.058 (0.049 to 0.067)
VOC	0.00021 (0.00018 to 0.00024)	-0.15 (-0.12 to -0.17)	0.058 (0.049 to 0.067)	-0.089 (-0.075 to -0.1)
Vizag	0.0015 (0.0013 to 0.0018)	-0.0012 (-0.001 to -0.0014)	0.22 (0.19 to 0.26)	0.22 (0.19 to 0.26)
All Ports	0.1 (0.087 to 0.12)	-6.1 (-5.1 to -7.1)	11 (9.6 to 13)	5.4 (4.6 to 6.3)

Table 5.37 Avoided premature mortality by switching from RO to shore power in 2030. The growth in shipping is assumed to be 3% each year. 89,90 Also, this is under the assumption that power generation and road transportation have become cleaner. All values are reported up to 2 significant digits and

the parentheses show 95% confidence interval (CI).

Port	PM _{2.5}	SO ₂	NO _x	Avoided Premature Mortality
Chennai	0.052 (0.044 to 0.06)	0.63 (0.53 to 0.73)	0.76 (0.64 to 0.88)	1.4 (1.2 to 1.7)
Cochin	0.038 (0.032 to 0.043)	0.72 (0.6 to 0.83)	0.7 (0.59 to 0.82)	1.5 (1.2 to 1.7)
Deendayal	0.025 (0.021 to 0.028)	0.6 (0.5 to 0.69)	0.33 (0.28 to 0.38)	0.95 (0.8 to 1.1)
JNPT	0.098 (0.083 to 0.11)	1.2 (1 to 1.4)	1.7 (1.4 to 2)	3 (2.5 to 3.5)
Kamarajar	0.013 (0.011 to 0.015)	0.17 (0.15 to 0.2)	0.2 (0.17 to 0.23)	0.39 (0.32 to 0.45)
Kolkata	0.021 (0.018 to 0.024)	0.3 (0.25 to 0.35)	0.56 (0.47 to 0.65)	0.88 (0.74 to 1)
Haldia	0.00044 (0.00038 to 0.00051)	0.0065 (0.0054 to 0.0075)	0.012 (0.01 to 0.014)	0.019 (0.016 to 0.022)
Mormugao	0.0075 (0.0064 to 0.0087)	0.24 (0.2 to 0.28)	0.18 (0.15 to 0.21)	0.43 (0.36 to 0.49)
Mumbai	0.12 (0.11 to 0.14)	1.5 (1.3 to 1.8)	2.2 (1.8 to 2.5)	3.8 (3.2 to 4.4)
New Mangalore	0.011 (0.0097 to 0.013)	0.29 (0.25 to 0.34)	0.21 (0.18 to 0.24)	0.52 (0.43 to 0.6)
Paradip	0.0037 (0.0032 to 0.0043)	0.0027 (0.0023 to 0.0032)	0.11 (0.093 to 0.13)	0.12 (0.098 to 0.14)
VOC	0.015 (0.013 to 0.018)	0.026 (0.022 to 0.031)	0.14 (0.12 to 0.16)	0.18 (0.15 to 0.21)
Vizag	0.006 (0.0051 to 0.0069)	0.04 (0.034 to 0.046)	0.19 (0.16 to 0.22)	0.23 (0.2 to 0.27)
All Ports	0.42 (0.35 to 0.48)	5.7 (4.8 to 6.7)	7.3 (6.1 to 8.4)	13 (11 to 16)

Table 5.38 Avoided premature mortality by switching from MGO to shore power in 2030. The growth in shipping is assumed to be 3% each year. 89,90 Also, this is under the assumption that power generation and road transportation have become cleaner. All values are reported up to 2 significant digits

and the parentheses show 95% confidence interval (CI).

Port	PM _{2.5}	SO ₂	NO _x	Avoided Premature Mortality
Chennai	0.011 (0.0097 to 0.013)	0.067 (0.056 to 0.078)	0.72 (0.61 to 0.83)	0.8 (0.67 to 0.93)
Cochin	0.0084 (0.0071 to 0.0096)	0.13 (0.11 to 0.15)	0.67 (0.56 to 0.77)	0.8 (0.67 to 0.93)
Deendayal	0.0055 (0.0047 to 0.0064)	0.092 (0.077 to 0.11)	0.31 (0.26 to 0.36)	0.41 (0.34 to 0.48)
JNPT	0.021 (0.018 to 0.025)	0.2 (0.17 to 0.23)	1.6 (1.4 to 1.9)	1.8 (1.5 to 2.1)
Kamarajar	0.0029 (0.0025 to 0.0034)	0.019 (0.016 to 0.022)	0.19 (0.16 to 0.22)	0.21 (0.17 to 0.24)
Kolkata	0.0045 (0.0038 to 0.0052)	0.046 (0.038 to 0.053)	0.53 (0.44 to 0.61)	0.58 (0.49 to 0.67)
Haldia	0.000097 (0.000082 to 0.00011)	0.00097 (0.00082 to 0.0011)	0.011 (0.0095 to 0.013)	0.012 (0.01 to 0.014)
Mormugao	0.0017 (0.0014 to 0.0019)	0.039 (0.033 to 0.046)	0.17 (0.14 to 0.2)	0.21 (0.18 to 0.24)
Mumbai	0.027 (0.023 to 0.031)	0.26 (0.22 to 0.3)	2.1 (1.7 to 2.4)	2.3 (2 to 2.7)
New Mangalore	0.0025 (0.0021 to 0.0029)	0.05 (0.042 to 0.058)	0.2 (0.17 to 0.23)	0.25 (0.21 to 0.29)
Paradip	0.00083 (0.00071 to 0.00096)	0.00034 (0.00029 to 0.0004)	0.1 (0.088 to 0.12)	0.11 (0.089 to 0.12)
VOC	0.0034 (0.0029 to 0.0039)	0.0028 (0.0024 to 0.0033)	0.13 (0.11 to 0.16)	0.14 (0.12 to 0.16)
Vizag	0.0013 (0.0011 to 0.0015)	0.0068 (0.0057 to 0.0079)	0.18 (0.15 to 0.2)	0.18 (0.16 to 0.21)
All Ports	0.091 (0.078 to 0.11)	0.91 (0.76 to 1.1)	6.9 (5.8 to 8)	7.9 (6.6 to 9.1)

Table 5.39 and **Table 5.40** provide estimates of avoided premature deaths by switching from RO and MGO to shore power in 2030. The growth in shipping is assumed to be 18% per year (GoI projection).^{57,58}

Table 5.39 Avoided premature mortality by switching from RO to shore power in 2030. The growth in shipping is assumed to be 18% each year. 57,58 Also, this is under the assumption that power generation and road transportation have become cleaner. All values are reported up to 2 significant digits

and the parentheses show 95% confidence interva	al (C	I).
---	-------	-----

Port	PM _{2.5}	SO ₂	NO _x	Avoided Premature Mortality
Chennai	0.41 (0.35 to 0.47)	4.8 (4 to 5.6)	6.3 (5.3 to 7.3)	12 (9.7 to 13)
Cochin	0.29 (0.25 to 0.33)	5.4 (4.5 to 6.3)	5.3 (4.4 to 6.1)	11 (9.2 to 6.1)
Deendayal	0.17 (0.14 to 0.19)	3.6 (3 to 4.2)	1.8 (1.5 to 2.1)	5.6 (4.7 to 2.1)
JNPT	0.77 (0.65 to 0.88)	9.2 (7.7 to 11)	14 (12 to 16)	24 (20 to 16)
Kamarajar	0.11 (0.091 to 0.12)	1.4 (1.1 to 1.6)	1.7 (1.4 to 2)	3.2 (2.7 to 2)
Kolkata	0.16 (0.14 to 0.19)	2.4 (2 to 2.7)	4.6 (3.8 to 5.3)	7.1 (6 to 5.3)
Haldia	0.0035 (0.0029 to 0.004)	0.05 (0.042 to 0.058)	0.096 (0.08 to 0.11)	0.15 (0.13 to 0.11)
Mormugao	0.053 (0.045 to 0.061)	1.5 (1.3 to 1.8)	0.92 (0.78 to 1.1)	2.5 (2.1 to 1.1)
Mumbai	0.97 (0.83 to 1.1)	12 (9.8 to 14)	17 (14 to 20)	30 (25 to 20)
New Mangalore	0.086 (0.073 to 0.099)	2.1 (1.8 to 2.5)	1.5 (1.2 to 1.7)	3.7 (3.1 to 1.7)
Paradip	0.025 (0.022 to 0.029)	0.021 (0.018 to 0.025)	0.44 (0.37 to 0.51)	0.48 (0.41 to 0.51)
VOC	0.11 (0.096 to 0.13)	0.2 (0.17 to 0.24)	1 (0.84 to 1.2)	1.3 (1.1 to 1.2)
Vizag	0.047 (0.04 to 0.054)	0.31 (0.26 to 0.36)	1.4 (1.2 to 1.7)	1.8 (1.5 to 1.7)
All Ports	3.2 (2.7 to 3.7)	43 (36 to 50)	56 (47 to 65)	100 (86 to 120)

Table 5.40 Avoided premature mortality by switching from MGO to shore power in 2030. The growth in shipping is assumed to be 18% each year. Also, this is under the assumption that power generation and road transportation have become cleaner. All values are reported up to 2 significant digits and the parentheses show 95% confidence interval (CI).

Port	PM _{2.5}	SO ₂	NO _x	Avoided Premature Mortality
Chennai	0.067 (0.057 to 0.077)	0.39 (0.33 to 0.45)	4.1 (3.4 to 4.7)	4.6 (3.8 to 5.3)
Cochin	0.049 (0.041 to 0.056)	0.74 (0.62 to 0.86)	3.5 (3 to 4.1)	4.3 (3.6 to 4.1)
Deendayal	0.031 (0.027 to 0.036)	0.52 (0.44 to 0.6)	1.3 (1.1 to 1.5)	1.9 (1.6 to 1.5)
JNPT	0.13 (0.11 to 0.14)	1.2 (0.99 to 1.4)	9.1 (7.7 to 11)	10 (8.8 to 11)
Kamarajar	0.017 (0.015 to 0.02)	0.11 (0.092 to 0.13)	1.1 (0.91 to 1.3)	1.2 (1 to 1.3)
Kolkata	0.026 (0.022 to 0.03)	0.27 (0.22 to 0.31)	3 (2.6 to 3.5)	3.3 (2.8 to 3.5)
Haldia	0.00056 (0.00048 to 0.00065)	0.0057 (0.0048 to 0.0066)	0.064 (0.054 to 0.074)	0.07 (0.059 to 0.074)
Mormugao	0.0096 (0.0082 to 0.011)	0.22 (0.19 to 0.26)	0.7 (0.59 to 0.81)	0.93 (0.79 to 0.81)
Mumbai	0.16 (0.14 to 0.18)	1.5 (1.3 to 1.7)	12 (9.7 to 13)	13 (11 to 13)
New Mangalore	0.015 (0.012 to 0.017)	0.29 (0.24 to 0.33)	1 (0.86 to 1.2)	1.3 (1.1 to 1.2)
Paradip	0.0048 (0.0041 to 0.0055)	0.002 (0.0017 to 0.0023)	0.36 (0.3 to 0.42)	0.37 (0.31 to 0.42)
VOC	0.02 (0.017 to 0.022)	0.017 (0.014 to 0.019)	0.71 (0.6 to 0.82)	0.75 (0.63 to 0.82)
Vizag	0.0077 (0.0066 to 0.0089)	0.04 (0.033 to 0.046)	1 (0.85 to 1.2)	1.1 (0.89 to 1.2)
All Ports	0.53 (0.45 to 0.61)	5.3 (4.4 to 6.1)	38 (32 to 44)	43 (37 to 50)

Figure 5.12 shows total annually avoided premature mortality in 2030 by switching from RO and MGO to shore power when shipping grows at 18% per year ^{57,58} and the power generation and transportation sector become cleaner.

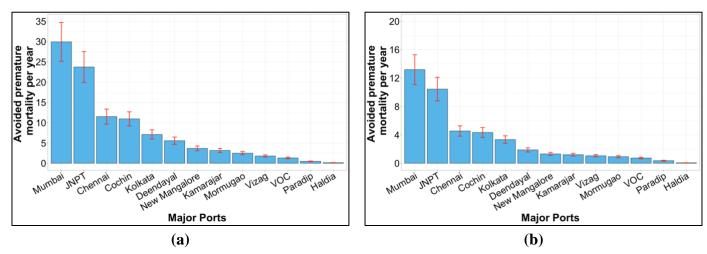


Figure 5.12 (a-b) Avoided premature mortality in 2030 by switching from RO (left) and MGO (right) to shore power. The growth in shipping is assumed to be 18% each year. 57,58 Also, this is under the assumption that power generation and road transportation become cleaner.

Figure 5.13 provides change in premature mortality estimates with percentage change in electricity grid desulphurization.

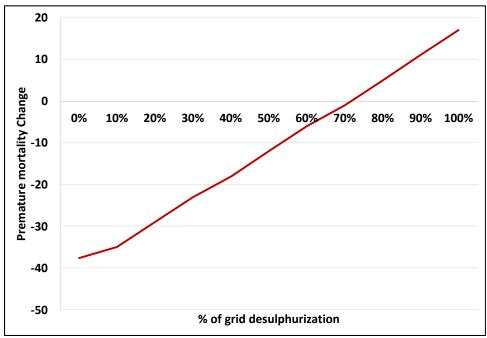


Figure 5.13 Change in premature mortality with % change in grid desulphurization for 2020. Positive values indicate premature mortality avoided and negative values indicate premature mortality across port cities. We assume that ships use MGO in 2020 and the shipping growth is assumed to be 3% each year from 2017-2020. 89,90 We find that the switch over occurs roughly around ~70% of grid desulphurization.

5.9.6.2 Shifting Pollution to Lesser Populated Areas

Cochin Port

Figure 5.14 provides a qualitative understanding of the situation for the port of Kochi, which is in the city center and part of a metropolitan area with a population density of ~4,100 people per km².

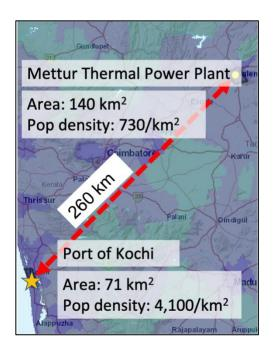


Figure 5.14 Map showing the location of the port and city of Kochi, as well as the population densities of the adjoining areas. The location of the powerplants was obtained from Carbon Brief's coal plant tracker, ²²³ and the population densities were obtained from Socioeconomic Data and Applications Center (SEDAC). ²²⁴ The reader can refer to the wind rose for Kochi here. ²²⁵

Chennai Port and Kamarajar Port

Figure 5.15 shows Chennai city center and part of a metropolitan area with a population density of ~25,000 people per km². We also show the location of Chennai and Kamarajar ports that are located in the state of Tamil Nadu (southern India). The wind blows inland for much of the year in Chennai, meaning that pollution from the port is likely blowing over the densely populated city. The nearest coal-fired power plants are Vallur Thermal Power Plant (capacity: 1,500 MW) and North Chennai Thermal Power Station (capacity: 1,830 MW). They are located ~16 km away (over the crow distance) in a region with a considerably lower population density. The wind blowing over the power plant blows from the north-north east towards the city about a quarter of the time. Thus, we observe an air quality benefit in shifting pollution away from a higher population density area to a lower population density area.

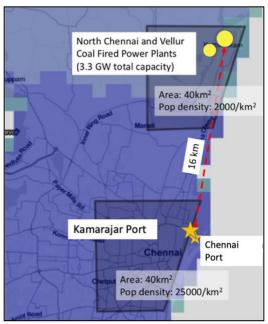


Figure 5.15 Map showing the location of ports and the city of Chennai, as well as the population densities of the adjoining areas. The location of the powerplants was obtained from Carbon Brief's coal plant tracker, and the population densities were obtained from Socioeconomic Data and Applications Center (SEDAC). The reader can refer to the wind rose for Chennai here.

Deendayal Port

Figure 5.16 shows population density of Gandhidham which is ~870 persons per km². The wind blows predominantly from northwest throughout the year. The nearest thermal power station is Mundra Thermal Power Station (capacity: 4,620 MW) and is located ~68 km away (over the crow distance) in a region of low population density (200 persons per km²). Thus, there is some air quality benefit in switching from burning diesel to grid-based electricity at Deendayal Port.

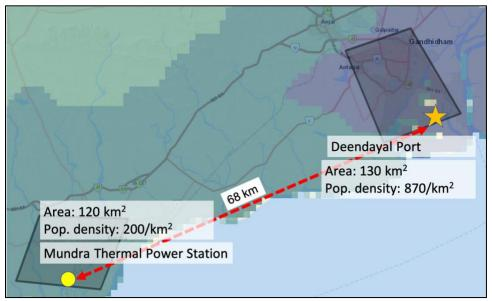


Figure 5.16 Map showing the location of Deendayal Port and the city of Gandhidham, as well as the population densities of the adjoining areas. The location of the powerplant was obtained from Carbon Brief's coal plant tracker, ²²³ and the population densities were obtained from Socioeconomic Data and Applications Center (SEDAC). ²²⁴ The reader can refer to the wind rose for Kandla here. ²²⁷

Mumbai Port and JNPT Port

Figure 5.17 shows the locations of the ports and parts of Mumbai (~33,000 persons per km²) and Navi Mumbai (~2,000 persons per km²). The wind blows inland from the sea ~81% of the time in a year. The nearest thermal power station is Trombay Thermal Plant (capacity: 750 MW) and is located ~8 km away (over the crow distance) from the ports. It has a population density of ~30,000 persons per km² around it. Thus, there is some air quality benefit in switching from burning diesel to grid-based electricity at the ports.

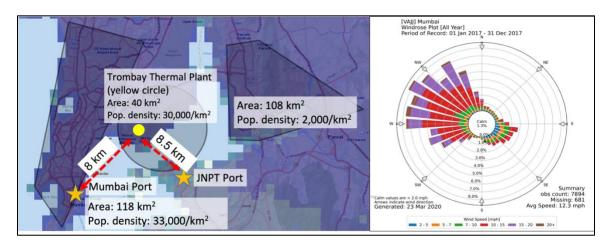


Figure 5.17 Map showing the location of Mumbai and JNPT Port and parts of Mumbai, along with population densities of the adjoining areas. The location of the powerplant was obtained from Carbon Brief's coal plant tracker, ²²³ and the population densities were obtained from Socioeconomic Data and Applications Center (SEDAC). ²²⁴ Wind rose for the city of Mumbai in 2017-2018. ²²⁸

Kolkata Port

Figure 5.18 shows the port and city of Kolkata. The population density of the city is ~29,000 persons per km². The wind rose diagram shows that wind predominantly blows from south-southwest to north- northeast direction for ~40% of the year. This suggests that pollution from the port blows away from the nearby population to the people staying north of the port. The nearest thermal power station is Southern Thermal Power Station (capacity: 136 MW) and is located ~6 km away (over the crow distance) from the port. The area near the power station has a population density of ~23,000 persons per km². This suggests that there is little air quality benefit in switching to shore power at the port of Kolkata.

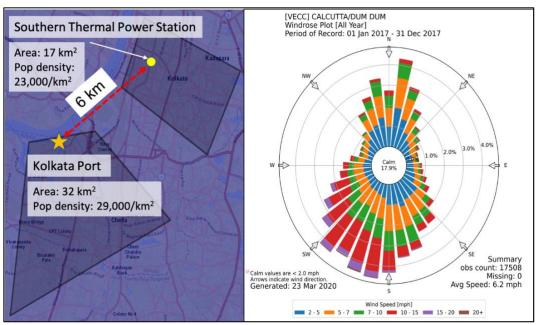


Figure 5.18 Map showing the location of the port and city of Kolkata, along with population densities of the adjoining areas. The location of the powerplant was obtained from Carbon Brief's coal plant tracker, ²²³ and the population densities were obtained from Socioeconomic Data and Applications Center (SEDAC). ²²⁴ Wind rose for the city of Kolkata in 2017-2018. ²²⁸

Haldia Port

Figure 5.19 shows the location of HDC and the city of Haldia that has a population density of ~850 persons per km². The wind rose diagram shows that the wind blows from south to north direction ~ 57% of the time (roughly 5,000 hours) in the year. The nearest power station is Haldia Energy Power Station (Capacity: 1,200 MW) and is located ~11 km away (over the crow distance) in an area that has a population density of ~1,000 persons per km². Thus, there is negative air quality benefit as we are moving pollution from a low population density to a high population density area.

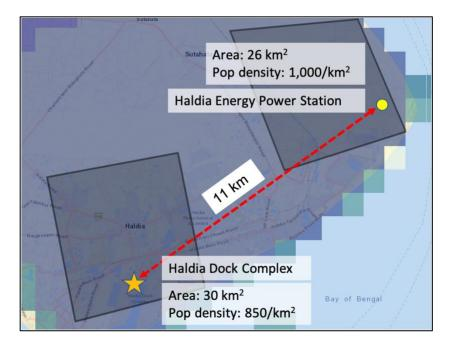


Figure 5.19 Map showing the location of HDC and the city of Haldia, along with population densities of the adjoining areas. The location of the powerplant was obtained from Carbon Brief's coal plant tracker, ²²³ and the population densities were obtained from Socioeconomic Data and Applications Center (SEDAC). ²²⁴ The reader can refer to the wind rose for Haldia here. ²²⁹

New Mangalore Port

Figure 5.20 provides geographic location for the port of New Mangalore and the city of Mangalore which has a population density of ~1,800 persons per km². The nearest thermal power station (Udipi Power Corporation Limited; Capacity- 1,200 MW) is situated ~26 km away (over the crow distance) from the port and the adjoining region has a population density of ~600 persons per km². This improves air quality around the port as we move pollution from a high population density area to a low population density area.

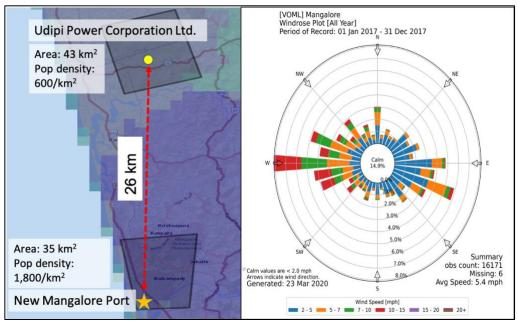


Figure 5.20 Map showing the location of New Mangalore port and city of Mangalore, along with population densities of the adjoining areas. The location of the powerplant was obtained from CarbonBrief's coal plant tracker, ²²³ and the population densities were obtained from Socioeconomic Data and Applications Center (SEDAC). ²²⁴ Windrose for the city of Mangalore in 2017-2018. ²²⁸

Paradip Port

Figure 5.21 show the port and part of the city of Paradip that has a population density of ~1,800 persons per km². Although there are a number of thermal power plants in Paradip, but almost all of them are captive in nature as in they serve manufacturing and oil refineries. So, the state grid is supplied by coal power plants in Talcher. The nearest thermal power plants are Talcher Thermal Power Station (TTPS; capacity- 460 MW) and Talcher Super Thermal Power Station (TSTPS; capacity- 3,000 MW) and are located ~190 km away from the port. The region near the power plant has a population density of ~540 persons per km². So, there is an air quality benefit to the residents of Paradip if we were to use shore power instead of burning diesel.

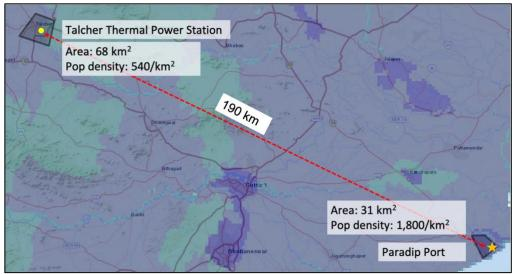


Figure 5.21 Map showing the location of Paradip port and city of Paradip, along with population densities of the adjoining areas. The location of the powerplant was obtained from Carbon Brief's coal plant tracker, ²²³ and the population densities were obtained from Socioeconomic Data and Applications Center (SEDAC). ²²⁴ The reader can refer to the wind rose for Paradip here. ²³⁰

VOC Port (Tuticorin)

Figure 5.22 shows the VOC port and a part of the city of Tuticorin. The population density of the area is ~1,300 persons per km². The nearest thermal power plant is a set of stations- Neyveli Thermal Power Station I (capacity: 1,090 MW) and Neyveli Thermal Power Station II (capacity: 1,970 MW) and located ~0.3 km from the port. The wind rose diagram shows that the wind blows from northwest and west to east ~22% of the year. There seems to be no air quality benefit in terms of air quality if we were to burn coal to supply berthing ships instead of burning diesel.

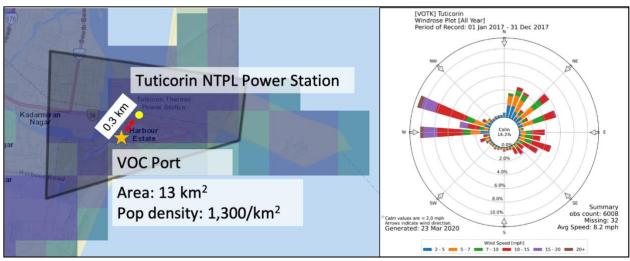


Figure 5.22 Map showing the location of VOC port and the city of Tuticorin and its population density. The location of the powerplant was obtained from Carbon Brief's coal plant tracker, ²²³ and the population densities were obtained from Socioeconomic Data and Applications Center (SEDAC). ²²⁴ Windrose for the city of Tuticorin in 2017-2018. ²²⁸

Vizag Port

Figure 5.23 shows the Vizag Port and the nearby city of Visakhapatnam that has a population density of ~3,000 persons per km². The nearest thermal power plant is Simhadri NTPC Power Plant (capacity: 2,000 MW) and is located ~24 km away. The region near the power plant has a population density of ~1,300 persons per km². The wind blows from west and southwest to east and north east ~33% of the year. So, there seems to be air quality benefit around the port city in switching from burning diesel to shore power.

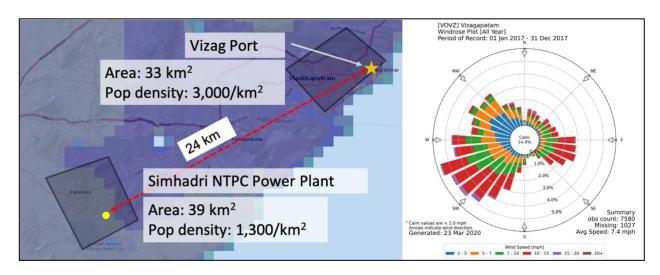


Figure 5.23 Map showing the location of Vizag port and the city of Visakhapatnam and its population density. The location of the powerplant was obtained from Carbon Brief's coal plant tracker, ²²³ and the population densities were obtained from Socioeconomic Data and Applications Center (SEDAC). Windrose for the city of Visakhapatnam in 2017-2018. ²²⁸

5.10 Sensitivity Analysis

5.10.1 Sources of uncertainty

There are a several sources of uncertainty in the emission factors of ships and we have attempted to address them while conducting the analysis. The major sources of uncertainty in our work and the steps taken to address them is shown in **Table 5.41** below.

Table 5.41 Sources of uncertainty and uncertainty analysis conducted by the authors.

S.No.	Uncertainties	How the authors addressed the uncertainty
1.	Do California estimate of	We match for vessel size and compare ages for vessels in
	auxiliary engine loads	both California ports and Indian major ports. This is
	apply to vessels calling at	shown in Figure 5.3 .
	major ports in India?	
2.	Vessel call information	We use primary data from the Ministry of Shipping
	for major ports	(MoS), GoI.
3.	Type of fuel oil used for	We have performed our analysis both for high sulfur fuel
	on-board generation at	(also known as RO; 2.7% S) and Marine Gas Oil (MGO;
	berth	0.5% S). We include the results of MGO in main
		manuscript and keep the results for RO in the SI. This is
		because, starting 01 January 2020, all vessels outside the
		emission control areas (ECAs) are mandated to use
		MGO. ²³¹ We assume that Indian ports are in compliance
		of this directive by the International Maritime
		Organization (IMO).

5.10.2 Price of Electricity

MGO: For an operator to become indifferent between the marginal (i.e., fuel) cost of shore power and burning MGO for on-board generation, the price of electricity would need to rise in Chennai by 78%, in Cochin by 100%, in Deendayal by 60%, in JNPT by 78%, in Kamarajar by 78%, in Kolkata by 60%, in Haldia by 60%, in Mormugao by 78%, in Mumbai by 78%, in New Mangalore by 60%, in Paradip by 100%, in VOC by 78% and in Visakhapatnam (Vizag) by 128% respectively.

<u>RO:</u> To make operators indifferent between the fuel costs associated with shore power, and using on-board generation powered by RO, the price of electricity would need to rise in Chennai by 15%; in Cochin 29%, in Deendayal by 3%, in JNPT by 15%, in Kamarajar by 15%, in Kolkata by 3%, in Haldia by 3%, in Mormugao by 15%, in Mumbai by 15%, in New Mangalore by 3%, in Paradip by 29%, in VOC by 15% and in Visakhapatnam (Vizag) by 48% respectively.

5.10.3 Electricity Generation Source

The capital cost of installing a solar photovoltaic (PV) system was assumed to be ~\$1,000 per kW.²³² As is the current practice in the industry, we assume a maintenance cost of 1% for solar PV system.²³³ We use a loan rate ranging from 11.50%-12.50%²³⁴ for developing the solar PV projects at ports in India. Using NREL's PV Watts calculator²³⁵, we determined annual hourly panel output at respective ports and matched it to the hourly load demand of berthed ships. For times when renewable electricity generation wasn't available (nighttime) or sufficient (cloud cover), the ships were assumed to be powered through grid electricity. During times of excess solar generation, the solar PV system reduces equivalent amount of grid emissions by supplying electricity back to the grid, essentially providing emissions free electricity. Thus, the electricity

generated through solar PV annually completely meets the annual auxiliary engine load demand of berthed ships.

Due to the low penetration of natural gas in the Indian electricity grid, the source of generation of electricity is coal. We assume that the marginal emissions due to grid electricity generation at any given location are roughly identical at all hours. So, the surplus electricity production from the solar PV system can be assumed to offset emissions from grid-based electricity for the load demand of berthed ships.

Table 5.42 provides the technical specifications of the solar panels assumed in the analysis. These were taken from the NREL PV Watts Calculator.²³⁵ The cost of purchasing electricity from the grid across major ports is provided in **Table 5.19**. In the case of excess solar power generation, the system supplies electricity back to the grid. The feed-in tariff for power generated through solar photovoltaic system was assumed to be \$0.035 per kWh.²³⁶ According to the guidance from the Central Electricity Regulatory Commission (CERC), the power factor for renewable generation projects is assumed to be 0.95 (lagging).²³⁷

Table 5.42 Specifications for the PV panels used in the solar PV system. These were used to estimate hourly annual solar generation at the respective ports.

Parameter	Value
Elevation (m):	0
DC System Size (kW):	4
Module Type:	Standard
Array Type:	Fixed (open rack)
Array Tilt (deg):	7
Array Azimuth (deg):	180
System Losses:	14.08
Invert Efficiency:	96
DC to AC Size Ratio:	1.2
Capacity Factor (%)	17.6

Table 5.43 provides the annual electricity required for berthed ships across the year and the size of solar PV system needed to meet that electricity demand.

Table 5.43 Annual port energy requirement and solar PV system capacity.

Port	Annual Port Energy Requirement (GWh)	Solar PV System Capacity (kW)
Chennai	55	35,960
Cochin	56	36,327
Deendayal	78	49,554
JNPT	58	38,493
Kamarajar	16	10,430
Kolkata	33	23,605
Haldia	61	43,899
Mormugao	42	27,765
Mumbai	73	46,654
New Mangalore	38	24,507
Paradip	54	37,093
VOC	31	19,935
Vizag	58	38,716

Table 5.44 shows the annual electricity purchase cost, solar feed-in revenue, solar PV system capital cost and the maintenance cost of the solar PV system.

Table 5.44 Port-wise cost of electricity purchase, solar PV system and maintenance cost, solar feed-in revenue.

Ports	Annual Electricity Expense (M \$)	Solar Feed- in Revenue (M \$)	Solar PV Cost (M \$)	Solar PV Maintenance Cost (100k \$)
Chennai	4.9	1.1	36	3.6
Cochin	4.4	1.1	36	3.6
Deendayal	7.7	1.6	50	5.0
JNPT	5.1	1.2	38	3.8
Kamarajar	1.4	0.3	10	1.0
Kolkata	3.3	0.7	24	2.4
Haldia	6.1	1.3	44	4.4
Mormugao	3.8	1.0	28	2.8
Mumbai	6.5	1.5	47	4.7
New Mangalore	3.7	0.8	25	2.5

Paradip	4.2	1.1	37	3.7
VOC	2.8	0.6	20	2.0
Vizag	4.0	1.2	39	3.9
Total Costs	58	14	430	43

Table 5.45 and **Table 5.46** show the health impacts of supplying electricity to berthed ships via grid connected solar PV system.

Table 5.45 Avoided premature mortality by switching from RO to shore power. We assume that electricity in this case is supplied through solar panels and is emissions free. The growth in shipping is assumed to be 3% each year. 89,90

Port	PM _{2.5}	SO ₂	NO _x	Avoided Premature Mortality
Chennai	0.047 (0.04 to 0.055)	2 (1.7 to 2.4)	0.96 (0.8 to 1.1)	3.1 (2.6 to 3.5)
Cochin	0.068 (0.058 to 0.078)	6.1 (5.1 to 7.1)	1.5 (1.3 to 1.8)	7.7 (6.4 to 8.9)
Deendayal	0.036 (0.031 to 0.042)	2.2 (1.9 to 2.6)	0.67 (0.56 to 0.77)	2.9 (2.5 to 3.4)
JNPT	0.2 (0.17 to 0.22)	11 (9.4 to 13)	3.5 (2.9 to 4)	15 (13 to 17)
Kamarajar	0.013 (0.011 to 0.015)	0.58 (0.49 to 0.68)	0.26 (0.22 to 0.31)	0.86 (0.72 to 1)
Kolkata	0.029 (0.025 to 0.033)	1.8 (1.5 to 2.1)	0.83 (0.7 to 0.96)	2.6 (2.2 to 3.1)
Haldia	0.00062 (0.00053 to 0.00071)	0.038 (0.032 to 0.044)	0.018 (0.015 to 0.02)	0.056 (0.047 to 0.065)
Mormugao	0.015 (0.013 to 0.017)	2.3 (1.9 to 2.6)	0.45 (0.38 to 0.52)	2.7 (2.3 to 3.2)
Mumbai	0.25 (0.21 to 0.29)	14 (12 to 17)	4.4 (3.7 to 5.1)	19 (16 to 22)
New Mangalore	0.02 (0.017 to 0.023)	1.9 (1.6 to 2.2)	0.45 (0.38 to 0.52)	2.4 (2 to 2.8)
Paradip	0.0073 (0.0062 to 0.0084)	0.039 (0.033 to 0.045)	0.25 (0.21 to 0.29)	0.29 (0.25 to 0.34)
VOC	0.0039 (0.0033 to 0.0044)	0.1 (0.088 to 0.12)	0.069 (0.058 to 0.08)	0.18 (0.15 to 0.21)
Vizag	0.009 (0.0076 to 0.01)	0.38 (0.32 to 0.44)	0.26 (0.22 to 0.3)	0.64 (0.54 to 0.75)
All Ports	0.69 (0.59 to 0.8)	43 (36 to 50)	14 (11 to 16)	57 (48 to 66)

Table 5.46 Avoided premature mortality by switching from MGO to shore power. We assume that electricity in this case is supplied through solar panels and is emissions free. The growth in shipping is assumed to be 3% each year. 89,90

Port	PM _{2.5}	SO ₂	NO _x	Avoided Premature Mortality
Chennai	0.01 (0.0089 to 0.012)	0.36 (0.3 to 0.42)	0.91 (0.76 to 1)	1.3 (1.1 to 1.5)
Cochin	0.015 (0.013 to 0.017)	1.1 (0.94 to 1.3)	1.4 (1.2 to 1.7)	2.6 (2.2 to 3)
Deendayal	0.0083 (0.007 to 0.0095)	0.45 (0.38 to 0.53)	0.64 (0.54 to 0.74)	1.1 (0.92 to 1.3)
JNPT	0.043 (0.037 to 0.05)	2 (1.7 to 2.3)	3.3 (2.8 to 3.8)	5.3 (4.5 to 6.2)

136

Kamarajar	0.0028 (0.0024 to 0.0033)	0.1 (0.086 to 0.12)	0.25 (0.21 to 0.29)	0.36 (0.3 to 0.41)
Kolkata	0.0063 (0.0054 to 0.0073)	0.31 (0.26 to 0.37)	0.78 (0.66 to 0.91)	1.1 (0.93 to 1.3)
Haldia	0.00014 (0.00012 to	0.0067 (0.0056 to	0.017 (0.014 to	0.024 (0.02 to
	0.00016)	0.0078)	0.019)	0.027)
Mormugao	0.0034 (0.0029 to 0.0039)	0.55 (0.46 to 0.63)	0.43 (0.36 to 0.5)	0.98 (0.82 to 1.1)
Mumbai	0.055 (0.047 to 0.063)	2.6 (2.2 to 3)	4.2 (3.5 to 4.8)	6.8 (5.7 to 7.9)
New				
Mangalore	0.0044 (0.0038 to 0.0051)	0.36 (0.31 to 0.42)	0.43 (0.36 to 0.5)	0.8 (0.67 to 0.92)
Paradip		0.007 (0.0059 to		
	0.0017 (0.0014 to 0.0019)	0.0081)	0.24 (0.2 to 0.28)	0.25 (0.21 to 0.29)
VOC	0.00085 (0.00072 to		0.065 (0.055 to	0.085 (0.071 to
	0.00098)	0.019 (0.016 to 0.022)	0.076)	0.098)
Vizag	0.002 (0.0017 to 0.0023)	0.067 (0.056 to 0.078)	0.24 (0.21 to 0.28)	0.31 (0.26 to 0.36)
All Ports	0.15 (0.13 to 0.18)	7.9 (6.7 to 9.2)	13 (11 to 15)	21 (18 to 24)

5.10.4 Switchover Analysis

We conduct an analysis to estimate the switchover point at which the vessel operator is indifferent between using marine fuel oil and grid electricity. While we don't know what the exact emission factors are for each of the coal power plants in the respective states, we can at the very least determine the percentage change required in those emission factors to an extent where it doesn't matter whether a ship uses shore-based electricity or fuel oil to power their auxiliary engines at berth. The results from this calculation are included in **Table 5.47**.

Table 5.47 % difference in emission factors at which the vessel operator becomes indifferent in burning diesel oil in ships' on-board generator versus using grid-electricity. The *green* values show that the electricity grid is cleaner. The value in the cell indicates the percentage change in the grid emission factor for in-situ electricity generation using ships' on-board generators to be the cleaner option. The *red* values show that in-situ electricity generation using ships' on-board generators is cleaner. The numbers indicate the proportional change in grid electricity emission factors needed for shore power to be the cleaner alternative.

State	RO (2.7% S	RO (2.7% S; High Sulfur Fuel)			MGO (0.5% S; Low Sulfur Fuel)			
	% Diff	% Diff	% Diff	% Diff	% Diff	% Diff	% Diff	% Diff
	$PM_{2.5}$	SO_2	NO_x	CO_2	$PM_{2.5}$	SO_2	NO_x	CO_2
Gujarat	980%	70%	1,100%	28%	140%	-70%	1,000%	23%
Maharashtra	1,900%	480%	1,000%	58%	330%	2%	970%	51%
Andhra	2,200%	520%	1,300%	140%	410%	9%	1,300%	130%
Pradesh								
Tamil Nadu	570%	-29%	930%	42%	48%	-88%	870%	36%
West Bengal	440%	76%	300%	-48%	19%	-69%	280%	-51%
Odisha	250%	-6%	100%	-70%	-23%	-83%	89%	-71%
Kerala	66,000%	18,000%	39,000%	5,500%	14,000%	3,200%	36,000%	5,300%

Karnataka	1,500%	360%	810%	43%	250%	-18%	760%	37%
Goa	1,300%	160%	1,000%	42%	210%	-53%	980%	35%
Min. Diff	250%	-29%	100%	-70%	-23%	-88%	89%	-71%
Max. Diff	66,000%	18,000%	39,000%	5,500%	14,000%	3,200%	36,000%	5,300%

6 Appendix B: Supplementary Information for Chapter 3

6.1 Extracting freight trucking emissions from the National Emissions Inventory (NEI), 2017

In our study, we assume that a dominant share of US freight tonnage is carried by diesel freight trucks. According to the Transportation Energy Databook, we observe that long-haul heavy-duty trucks (class 7 or above) account for ~86% of all energy use in the US.²³⁸ Also, we use National Emissions Inventory (NEI), 2017 ¹²⁷ as a reference for our results.

To estimate percentage freight trucking air pollutant and GHG contributions from the NEI, we consider emissions from all sources included in the NEI: point, non-point, on-road, non-road, and wildfire events. We exclude non-contiguous US states (Alaska, Hawaii, Puerto Rico, Virgin Islands, American Samoa, Guam, and other non-contiguous territories). Next, we merge the NEI with the source classification codes (SCCs) that the US EPA uses to classify different activities that contribute to emissions. SCC provide "a unique source category-specific process or function that emits air pollutants."²³⁹ Within the on-road sources, there are 16 vehicle categories included in the "SCC level three description" where the fuel used is "diesel fuel". These are, (1) passenger truck, (2) light commercial truck, (3) single unit short-haul truck, (4) single unit long-haul truck, (5) refuse truck, (6) combination short-haul truck, (7) combination long-haul truck, (8) truck (9), tank cars and trucks, (10) automobiles/truck assembly operations, (11) automobiles and light trucks, (12) tank truck cleaning, (13) intercity bus, (14) transit bus, (15) school bus, and (16) motor home. Out of these, we only include 5 truck categories (i.e. (3) single unit short-haul truck, (4) single unit long-haul truck, (5) refuse truck, (6) combination short-haul truck, (7) combination long-haul truck) that are relevant for diesel freight trucking. We include these five truck categories that are relevant for medium and heavy-duty freight trucking and exclude the

others such as passenger truck, tank cars and trucks, automobiles/truck assembly operations, automobiles and light trucks, and tank truck cleaning. The excluded truck categories belong either to the passenger vehicle fleet or are involved in other local operations and don't engage in freight trucking on the road network. **Table 6.1** below provides emissions for pollutants and greenhouse gas (GHG) from the NEI, 2017.

Table 6.1 Freight trucking emissions from the NEI, 2017 data. 127

Pollutant	NEI total emissions, 2017	NEI trucking emissions, 2017	% of total US emissions
PM _{2.5}	5,241,695	51,043	1.0%
SO ₂	2,473,626	3,672	0.10%
NOx	10,941,637	1,274,074	12%
CO ₂	5,257,719,247	432,404,593	8.2%

6.2 Freight Analysis Framework 4 (FAF4) Road Network

FAF4 data consists of ~450k miles of roads consisting of interstate highways, urban and rural principal arterials. **Table 6.2** provides percentage distribution of vehicle miles travelled (VMT) by single unit and combination trucks on roads in the FAF4 dataset.

Table 6.2 VMT by single unit and combination trucks by type of road in the FAF4 dataset. A major share of combination truck VMT is traversed on the interstate highways whereas the VMT is more distributed for SU trucks.

Road Type	% Combination truck	% Single unit
	VMT	truck VMT
1: Interstate	80%	32%
2: Other Freeways and Expressways	4%	13%
3: Other Principal Arterial	13%	38%
4: Minor Arterial	3%	13%
5: Major Collector	1%	4%
6: Minor Collector	0%	0%

6.3 Emission factors for single unit and combination trucks

We use emission factors for single unit and combination trucks from the Greenhouse gases,

Regulated Emissions, and Energy use in Technologies (GREET) Model. 141 **Table 6.3** reproduces

the emission factors for PM_{2.5}, SO₂, NO_x, and CO₂ for single unit (class-6 trucks) and combination trucks (class 8 or above) that we use in our study.

Table 6.3 Lifetime mileage weighted emission factors (in g/mile) for single unit and combination trailer freight diesel trucks for model year (MY) 2017. The values are from Table A16 and Table A22 as reported in the GREET study. 141

Pollutant/ GHG	Emission Factor for combination trailer truck (in g/mile)	Emission Factor for single unit truck (in g/mile)
PM _{2.5}	0.086	0.0467
SO ₂	0.0149	0.0070
NO _x	4.585	0.9383
CO ₂	1588	1414

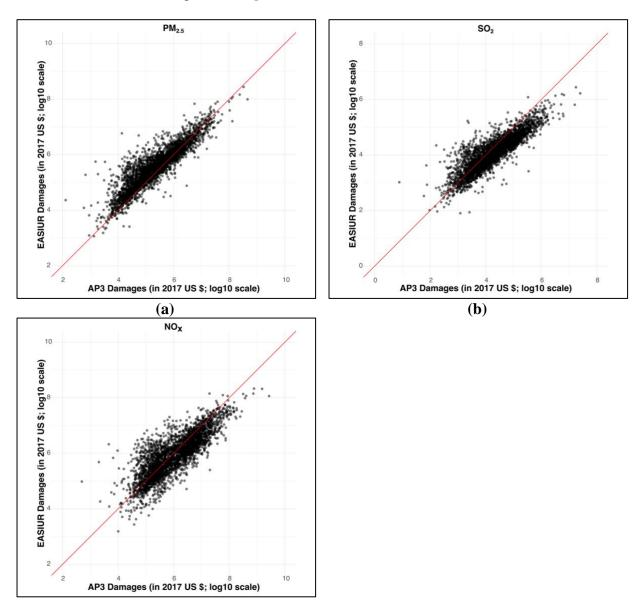
We use emission factors (expressed in g/kg-fuel) for long-haul freight trucking reported in Table S8 of Tong et al.²⁴⁰ Using an average fuel economy of 6.3 miles per diesel gallon equivalent²⁴¹ for long-haul freight trucking, we convert the emission factors to g/mile. Next, we weight the emission factors using lifetime miles for a combination tractor (Table 2-28)²⁴² to estimate lifetime mileage weighted emission factors. Tong et al.'s ²⁴⁰ method is different than ours in that they estimate tail pipe emissions profiles using empirical data, literature, and GREET model. ¹⁴¹ They use a mass-balance approach and harmonize emissions from literature for different air pollutants and greenhouse gases. **Table 6.4** reports emissions comparison for long-haul freight trucking using Tong et al.²⁴⁰ emission factors and GREET model emission factors. ¹⁴¹

Table 6.4 Comparison of long-haul freight trucking emissions (in tons) using lifetime mileage weighted emission factors reported in Tong et al. 240 and GREET model. 141

emission factors reported in Tong e	emission factors reported in Tong et al. and GREET model.				
Pollutant/ GHG	Long-haul trucking emissions	Long-haul trucking emissions			
	(in tons) using Tong et al.	(in tons) using GREET			
	emission factors	emission factors.			
PM _{2.5}	5.5K	17K			
SO_2	80	3K			
NO_x	108K	920K			
CO_2	32M	31M			

6.4 Comparison of freight trucking air pollution related public health damages from different models

In this section, we compare the results of freight trucking air pollution related social costs for two reduced complexity models (RCMs): Estimating Air pollution Social Impact Using Regression (EASIUR)^{133,134} and Air Pollution Emission Experiments and Policy Version 3 (AP3). While these social costs are broadly consistent, we see a slight deviation from the y-x line for SO_2 and NO_x damages (see **Figure 6.1**).



(c)
Figure 6.1 Comparison of freight trucking air pollution related public health social costs (in log10 tons) from EASIUR and AP3. We observe that social costs from both the models roughly lie on the y=x line.

Figure 6.2 provides map of counties that are net exporters and net importers of freight trucking air pollution related human health damages in the contiguous US.

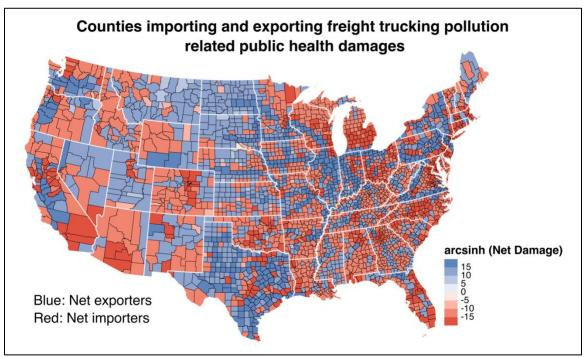


Figure 6.2 Net exporter and importer counties of freight trucking pollution based on social costs from the EASIUR model. Blue indicates counties that are net exporters of trucking pollution related health damages whereas red indicates counties that are net importers of trucking pollution related health damages. The map indicates damages in arcsinh scale, and the unit is US \$.

6.5 Modal shift: Shifting tonnage from freight trucks to railroads

To conduct the modal shift analysis, we rely on a set of assumptions. Firstly, we only account for modal shifts for class-1 freight rail and ignore other categories of railroads such as passenger and commuter rail, class-2 and class-3 railroads. Secondly, we use an approximation for adjusting freight rail emission factors. Usually, the US EPA reports locomotive emission factors in g/gal instead of g/ton-mile. While it is desirable to have emission factors for rail in g/ton-mile of freight hauled, it has its own limitations. Depending on the terrain where the railroad is

operating, the useful work done to haul a ton-mile of freight varies.²⁴³ We can adjust emission rates expressed in g/gal to reflect equivalent g/ton-mile emission factor by dividing the emission factor in g/gal by the freight rail fuel efficiency. We discuss the approach adopted to estimate emission factors for different pollutant and GHG in the subsequent sections.

6.5.1 Emission factors for Class-1 railroad

<u>PM2.5 emission factor:</u> For locomotives, particulate matter (PM) emissions are expressed as PM₁₀ (i.e., particles that are up to 10 microns in diameter) or PM_{2.5} (i.e., particles that are up to 2.5 microns in diameter). According to the US EPA guidance, we assume that for class-1 rail, PM_{2.5} emissions are nearly 97% of all PM₁₀ emissions.²⁴³ From Table 4 in 2017 US rail national emissions inventory (NEI), we find that the weighted PM₁₀ emission factor after accounting for locomotives fleet mix in 2017 is 3.944 g/gal. Thus, the PM_{2.5} emission factor is 3.82568 g/gal. <u>NOx emission factor:</u> The NOx emission factor is 134.770 g/gal and is the same as used in the 2017 US rail NEI.

<u>SO₂ and CO₂ emission factor:</u> These are independent of the railroad engine characteristics and largely dependent on the amount of sulfur and carbon present in the diesel fuel. For SO₂ and CO₂, we use the following equation from the US EPA guidance document²⁴³ to estimate emission factor.

Equation 6.1

$$SO_{2}\left(\frac{g}{gal}\right) = (fuel\ density)*(conversion\ factor)*(64\ g\ SO_{2}/32\ g\ S)*(S\ content\ of\ fuel)$$

We assume that the fuel used is ultra-low sulfur diesel (ULSD) with sulfur content of 15 ppm and the density of the diesel fuel is 3,200 g/gal. Further, the fraction of fuel sulfur converted to SO_2 is assumed to be $97.8 \%.^{243}$ Using these numbers, the SO_2 emission factor comes out to be

$$SO_2\left(\frac{g}{gal}\right) = (3,200)*(0.978)*(2)*(15*10^{-6}) = 0.093888 \, g/gal$$

144

Similarly, we estimate the CO₂ emission factor using the following equation:

Equation 6.2

$$CO_2\left(\frac{g}{gal}\right) = (fuel\ density)*(44\ g\ CO_2/12\ g\ C)*(C\ content\ of\ fuel)$$

The density of the diesel fuel is assumed to be 3,200 g/gal and the carbon content of the fuel is 87 % on a mass basis.²⁴³ Therefore, the CO₂ emission factor is

$$CO_2\left(\frac{g}{gal}\right) = (3,200) * (3.67) * (0.87) = 10,217 \ g/gal$$

According to the Association of American Railroads (AAR), in 2019, class-1 rail roads had a freight rail fuel efficiency of 472 ton-miles per gallon (see **Figure 6.3**). We divide the g/gal emission rates by 472 ton-miles/gal provides a rough measure of g/ton-mile of emission rates for class-1 rail. **Table 6.5** provides the emission factors for railroad expressed in g/ton-mile.

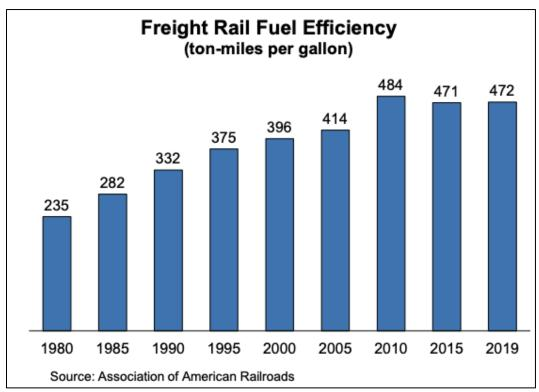


Figure 6.3 Freight rail fuel efficiency of freight railroads from 1980-2019. The figure is from AAR report. 146

Table 6.5 Emission factors for class-1 railroad expressed in g/ton-mile for 2017.

Pollutant/ GHG	EF rail (in g/ton-mile)
PM _{2.5}	0.1575
SO ₂	0.0049
NOx	0.0001
CO ₂	10.6427

Finally, we estimate the emissions change if a certain proportion of the freight ton-miles were shifted from diesel freight trucks to class-1 railroads. **Figure 6.4** shows percentage change in emissions by shifting part of the freight tonnage to rail. We find that this strategy reduces SO₂ and CO₂ emissions considerably.

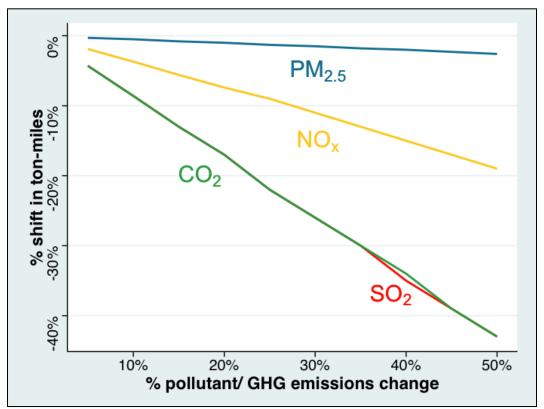


Figure 6.4 % change in $PM_{2.5}$, SO_2 , NO_x , and CO_2 emissions if a percentage of the total freight ton-miles are shifted from diesel freight trucks to Class-1 railroads.

6.6 Distributional effects of freight trucking air pollution

The following are preliminary results from an analysis that we run to estimate distributional impacts and explore environmental justice implications of freight trucking air pollution on minority groups. These results are subject to change as we get the manuscript ready for publishing owing to adjustments and other changes owing to missing value treatment and changes to how we extract the US census bureau data.

6.6.1 Satisfying linear regression assumptions

In order to use linear least squared regression, we satisfy the Gauss-Markov assumptions in our analysis. These are:

(1) Linearity in parameters

In this case, we have to be able to write a model such that $y_i = X_i \beta_i$ for y_i and X_i but the variables themselves can have non-linear transformations. Our model specifications satisfy this requirement and the only non-linear transformation we apply is the log transform to all dependent variables and some independent variables.

(2) Random sampling

This condition allows us to take the results of our sample regression specification and be able to apply it to the true population regression. To the best of our ability and knowledge, we have attempted to satisfy this condition while collating data and avoided introducing any bias in the data.

(3) Zero conditional mean of errors

This is popularly known as the omitted variable bias. This means that anything that is not in the model specification but potentially related with the independent and dependent variable could bias our estimates. In our modeling, we take great care in ensuring that we satisfy this

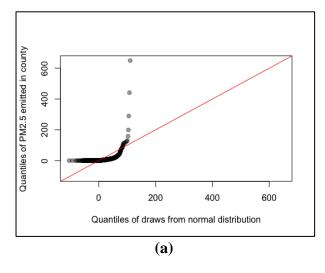
requirement by including census relevant variables that could influence freight trucking emissions.

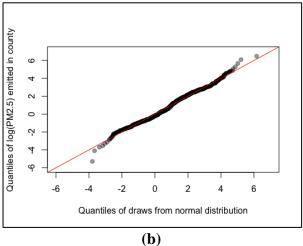
(4) No perfect collinearity

In our analysis, we ensure that we exclude variables that are linear functions of each other because it results in poor specification of the regression model.

6.6.2 Distribution of dependent variables

We hypothesize that the errors in our regression relationship function $y_i = \beta_0 + \beta_i x_i + \epsilon_i$ are normally distributed such that $\epsilon_i \sim N(0, \sigma^2)$. Next, we look at plot the quantiles of our dependent variables against quantiles of normal distribution. The plot of the quantiles of two distributions against each other is called a quantile-quantile plot (Q-Q plot). The advantage of using a Q-Q plot is that it allows us to simulate as many draws from the normal distribution as possible to satisfactorily represent the distribution. **Figure 6.5** shows Q-Q plots for dependent variables. We see that the log-transformed variables are much closer to the normal distribution.





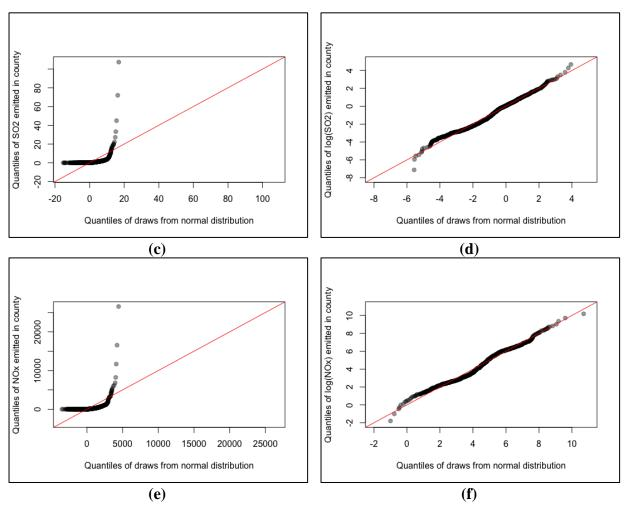


Figure 6.5 Q-Q plot of untransformed dependent variables ($PM_{2.5}$, SO_2 , and NO_x emissions). The untransformed variables are non-linear (a,c,e; left panel) whereas the log transformed dependent variables, i.e., $log(PM_{2.5})$, $log(SO_2)$, and $log(NO_x)$ emissions (b,d,f; right panel) are distributed normally.

We run three different model specifications for PM_{2.5}, SO₂, and NO_x emissions from freight trucking.

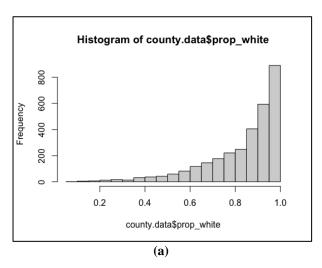
6.6.3 Distribution of independent variables

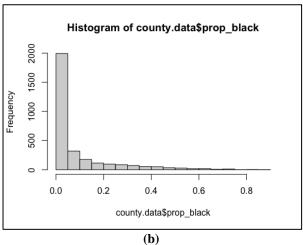
Table 6.6 provides a summary of dependent and independent variables that we use in our analysis. We calculate proportions of different racial and ethnic sub-groups at the county level from the total population provided in the census data. Additionally, we log transform the area of the county, median county level household income, and the total population of the county.

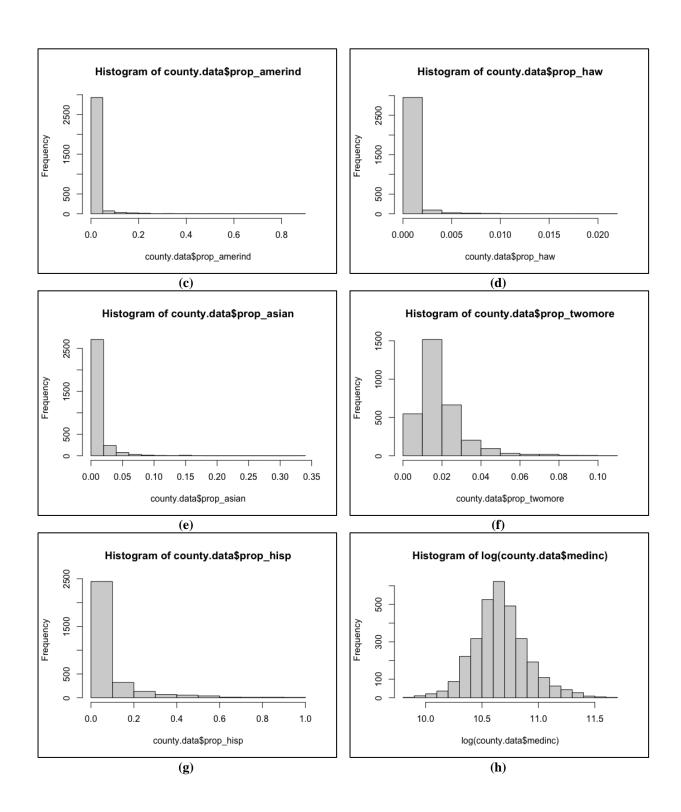
Table 6.6 Description of independent variables used in the regression analysis.

Variables	Description
	log of freight trucking emissions for pollutant $p \in (PM_{2.5}, SO_2, and NO_x)$ in
$Y_{p,c}(X)$	county c
X_c^{area}	area of the county c
X_c^{black}	proportion of the total population in the county c that is black
$X_c^{amerind}$	proportion of the total population in the county c that is American Indian and Alaska native
X_c^{haw}	proportion of the total population in the county c that is Hawaiian and other Pacific Islanders
Xasian C	proportion of the total population in the county c that is Asian
X_c^{hisp}	proportion of the total population in the county c identifying as Hispanic or Latino
$X_c^{twomore}$	proportion of the total population in the county c that identifies as having two or more races
X_c^{totpop}	total population in county c
X_c^{medinc}	median household income in county c

Figure 6.6 shows the histograms of independent variables included in the analysis.







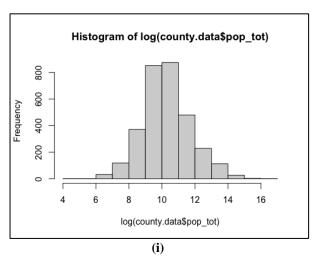
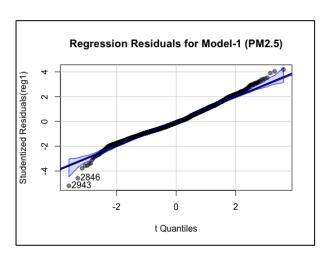
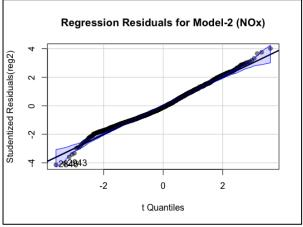


Figure 6.6 Distribution of independent variables that are included in the model specification.

6.6.4 Studentized Regression Residual Plots

Another method to evaluate conditional distribution of dependent variables is to look at the distribution of the regression residuals. If our regression relationship is such that $y_i = \beta_0 + \beta_i x_i + \epsilon_i$ and the errors are normally distributed $\epsilon_i \sim N(0, \sigma^2)$, then the residuals are also normally distributed. Thus, if we assume that our errors come from a normal distribution, then we can compare the studentized residuals to a standard normal distribution. We notice that the distribution of residuals looks tame for the three model specifications (see **Figure 6.7**).





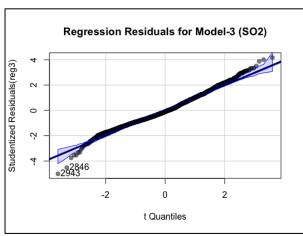


Figure 6.7 Regression residual plots for the three model specifications.

7 Appendix C: Environmental Impacts of Electrification and Automation of Freight Trucking in the United States (Future Work Chapter)

Abstract

Freight trucks are a major source of CAPs and GHG emissions. In this analysis, we explore the environmental impacts of electrification and automation on short distance and long-distance freight trucking in the US. Based on government data, we outline how to quantify the environmental impacts and cost savings of electrifying short-haul (<300 miles) freight trucking in the US. We also describe a benefit-cost analysis (BCA) on the impact of electrifying last mile journeys of long-haul freight trips while automating the highway leg of the long-haul freight trips in the US. The results of this future work will allow policy makers to understand the effects of automation and electrification for long and short distance shippers while enabling them to design targeted freight decarbonization policies in the near future.

7.1 Introduction

The transportation sector is a critical element of the US economy and contributed ~9% of US gross domestic product (GDP) in 2018.²⁴⁴ Pressures from increasing globalization and economic activity have led to a significant increase in road freight activity. Between 1975 and 2015, road freight activity increased "2.5-fold"14 in the U.S. and this trend is projected to continue due to growth in freight demand and developments such as e-commerce.

Increased freight vehicle miles traveled (VMT) corresponds to an increased concentration of criteria air pollutants (CAPs) and damaging impacts of negative air pollution externalities. In the past, emissions control regulations such as the Clean Air Act (CAA) in the 1970s and ultra-low sulfur diesel (ULSD) in 2006 have tried to limit the extent of these damages by successfully reducing concentrations of ambient air pollutants. For instance, under the CAA, hourly sulfur dioxide (SO₂) and oxides of nitrogen (NO_x) concentrations have fallen by 89% and 50%. Instead of a cross-sector overarching regulation, the approach to achieving the next wave of emissions reductions could focus on a series of sector specific strategies based on technological advances to reduce the emissions intensity of the fuels.

This holds true for the freight transportation sector as well and in order to reduce the emissions footprint of shipped goods, it would be wise to experiment with different strategies while accounting for the costs and tradeoffs involved. Electrification is of particular interest because of its potential to decarbonize other sectors such as the passenger vehicles sector.²⁴⁵ In fact, there is a lot of interest in electrifying and automating operations in the trucking industry. This proposition is particularly attractive because it comes with twin benefits. Electrification allows us to reduce freight trucking emissions by switching to electricity instead of burning diesel and gasoline for trucking operations. Automation can help to improve the economics of tracking for

shippers and large trucking companies. Furthermore, this strategy may improve supply chain productivity since automation allows freight shippers to operate continuously even during the time intervals when freight trucks with human drivers are idle in order to allow drivers sufficient rest to operate safely. In fact, many companies are trying to implement the "transfer hub" model wherein part of the journey in the urban areas is completed by a driver behind the wheel and the highway leg of the journey is automated.²⁴⁶

7.2 Methods

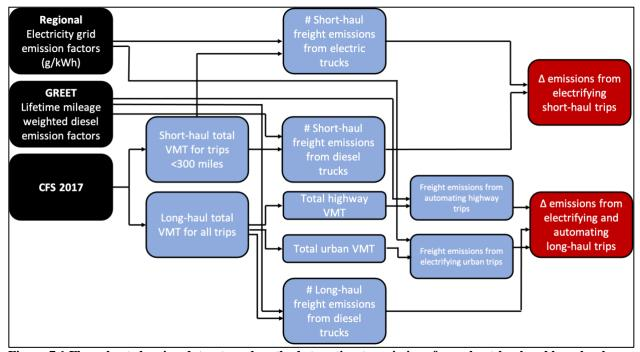


Figure 7.1 Flow chart showing datasets and methods to estimate emissions from short-haul and long-haul freight trucking.

Figure 7.1 shows a flow chart to help the reader better understand our approach. To estimate the environmental impacts of automating and electrifying trucks, we use the latest available Commodities Flow Survey (CFS) dataset from the US government for the year 2017. The CFS 2017 dataset provides origin and destinations of long and short distance trips conducted by freight trucks along with relevant conversion factors to estimate the route lengths of the freight

trips. To conduct the analysis for short distance freight trucks, we filter the dataset for records where the travel distance for shipments was less than 300 miles, which constitute about 17% of the ton-miles traveled by heavy trucks (see **Figure 7.2**).

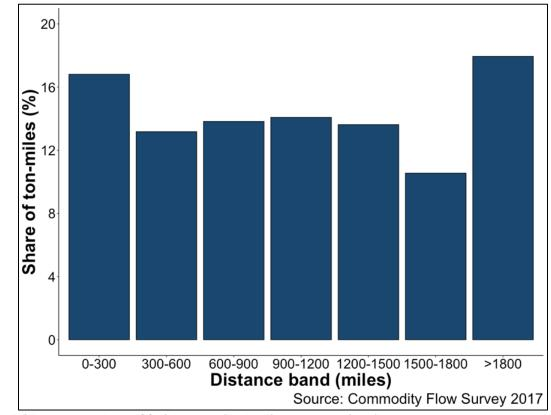


Figure 7.2 Percentage share of freight ton-miles by distance range in miles.

We plan two analyses. In the **first** analysis, we will assess the health and environmental benefits of shifting to electric Class 8 trucks for all trips that are shorter than 300 miles. We choose 300 miles as an initial threshold, because this is about the maximum range that an electric semi-truck can attain without an unacceptable reduction in payload carrying capacity, assuming current lithium-ion battery technology.²⁴⁷ Roughly ~61% of the freight trips in the CFS data are less than 300 miles. Next, we will use the regional electricity generation mix at the origin of the trip to estimate the magnitude of emissions generated by the grid for charging the truck. We will also estimate the emissions from using diesel fuel for short haul trucks over the same trip length. The

difference between the emissions from electrifying the trip and conducting the same journey with diesel trucks will provide us with emissions change for the trips. We will aggregate these emissions reductions for all shipments for all US states to arrive at net environmental benefit or cost from electrifying short distance freight trucking.

In the **second** analysis, we will assess the potential benefits of the automation of long-haul trucking. One way in which this could occur is by the adoption of the freight transfer hub model, illustrated in **Figure 7.3** from Viscelli (2020).²⁴⁸ In this model, at the origin, human-driven prime movers haul loaded trailers from urban centers to transfer hubs at the edge of interstate highways. At the transfer hub, the trailers are transferred to autonomous prime movers, which haul them along the interstate to another transfer hub close to the destination. At the destination transfer hub, the trailer is detached from the autonomous prime-mover and attached to a human-driven prime mover for the "last mile" of the journey.

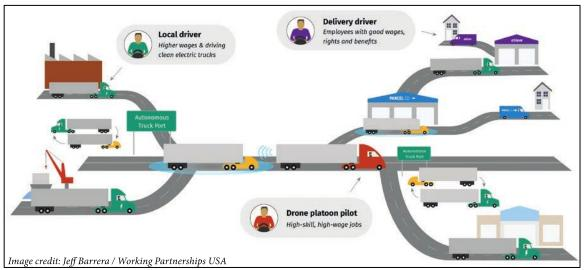


Figure 7.3 Schematic of the transfer hub model for autonomous long-haul trucking. From Viscelli (2020).²⁴⁸

We assess the benefits, in terms of reduced CO₂ emissions and local air quality, of electrifying the short haul legs at the start and end of the interstate journey. We will apportion the length of the road segment in various counties while providing us with other details of the journey such as

the travel time for the trip, the permissible speed limit on the road network, share of miles traveled on highways, urban, and rural areas. From the CFS data, we find that ~6% of the trip journey is performed within urban and densely populated areas and this portion of the trip can be electrified. For the remainder of the long-distance part of the journey, we assume that it can be automated. We estimate emissions from the electricity grid for electrifying the short distance legs of the long-haul trip. Under this scenario, there may be environmental benefits in the urban leg of the trip of emitting less CAPs in a densely populated cites which have adverse human health impacts. For the highway leg of the trip, the economic benefits may be in terms of time and cost savings. We estimate the change in emissions from electrifying and automating the long-distance trip relative to the scenario when this journey is undertaken by a diesel-powered long-distance freight truck (class 8 or above).

8 Chapter 8: References

- (1) United Nations. Paris Agreement; 2015.
- (2) Abbafati, C.; Abbas, K. M.; Abbasi-Kangevari, M.; Abd-Allah, F.; Abdelalim, A.; Abdollahi, M.; Abdollahpour, I.; Abegaz, K. H.; Abolhassani, H.; Aboyans, V.; Abreu, L. G.; Abrigo, M. R. M.; Abualhasan, A.; Abu-Raddad, L. J.; Abushouk, A. I.; Adabi, M.; Adekanmbi, V.; Adeoye, A. M.; Adetokunboh, O. O.; Adham, D.; Advani, S. M.; Afshin, A.; Agarwal, G.; Aghamir, S. M. K.; Agrawal, A.; Ahmad, T.; Ahmadi, K.; Ahmadi, M.; Ahmadieh, H.; Ahmed, M. B.; Akalu, T. Y.; Akinyemi, R. O.; Akinyemiju, T.; Akombi, B.; Akunna, C. J.; Alahdab, F.; Al-Aly, Z.; Alam, K.; Alam, S.; Alam, T.; Alanezi, F. M.; Alanzi, T. M.; Alemu, B. W.; Alhabib, K. F.; Ali, M.; Ali, S.; Alicandro, G.; Alinia, C.; Alipour, V.; Alizade, H.; Aljunid, S. M.; Alla, F.; Allebeck, P.; Almasi-Hashiani, A.; Al-Mekhlafi, H. M.; Alonso, J.; Altirkawi, K. A.; Amini-Rarani, M.; Amiri, F.; Amugsi, D. A.; Ancuceanu, R.; Anderlini, D.; Anderson, J. A.; Andrei, C. L.; Andrei, T.; Angus, C.; Anjomshoa, M.; Ansari, F.; Ansari-Moghaddam, A.; Antonazzo, I. C.; Antonio, C. A. T.; Antony, C. M.; Antriyandarti, E.; Anvari, D.; Anwer, R.; Appiah, S. C. Y.; Arabloo, J.; Arab-Zozani, M.; Aravkin, A. Y.; Ariani, F.; Armoon, B.; Ärnlöv, J.; Arzani, A.; Asadi-Aliabadi, M.; Asadi-Pooya, A. A.; Ashbaugh, C.; Assmus, M.; Atafar, Z.; Atnafu, D. D.; Atout, M. M. d. W.; Ausloos, F.; Ausloos, M.; Ayala Quintanilla, B. P.; Ayano, G.; Ayanore, M. A.; Azari, S.; Azarian, G.; Azene, Z. N.; Badawi, A.; Badiye, A. D.; Bahrami, M. A.; Bakhshaei, M. H.; Bakhtiari, A.; Bakkannavar, S. M.; Baldasseroni, A.; Ball, K.; Ballew, S. H.; Balzi, D.; Banach, M.; Banerjee, S. K.; Bante, A. B.; Baraki, A. G.; Barker-Collo, S. L.; Bärnighausen, T. W.; Barrero, L. H.; Barthelemy, C. M.; Barua, L.; Basu, S.; Baune, B. T.; Bayati, M.; Becker, J. S.; Bedi, N.; Beghi, E.; Béjot, Y.; Bell,

M. L.; Bennitt, F. B.; Bensenor, I. M.; Berhe, K.; Berman, A. E.; Bhagavathula, A. S.; Bhageerathy, R.; Bhala, N.; Bhandari, D.; Bhattacharyya, K.; Bhutta, Z. A.; Bijani, A.; Bikbov, B.; bin Sayeed, M. S.; Biondi, A.; Birihane, B. M.; Bisignano, C.; Biswas, R. K.; Bitew, H.; Bohlouli, S.; Bohluli, M.; Boon-Dooley, A. S.; Borges, G.; Borzì, A. M.; Borzouei, S.; Bosetti, C.; Boufous, S.; Braithwaite, D.; Brauer, M.; Breitborde, N. J. K.; Breitner, S.; Brenner, H.; Briant, P. S.; Briko, A. N.; Briko, N. I.; Britton, G. B.; Bryazka, D.; Bumgarner, B. R.; Burkart, K.; Burnett, R. T.; Burugina Nagaraja, S.; Butt, Z. A.; Caetano Dos Santos, F. L.; Cahill, L. E.; Cámera, L. A.; Campos-Nonato, I. R.; Cárdenas, R.; Carreras, G.; Carrero, J. J.; Carvalho, F.; Castaldelli-Maia, J. M.; Castañeda-Orjuela, C. A.; Castelpietra, G.; Castro, F.; Causey, K.; Cederroth, C. R.; Cercy, K. M.; Cerin, E.; Chandan, J. S.; Chang, K. L.; Charlson, F. J.; Chattu, V. K.; Chaturvedi, S.; Cherbuin, N.; Chimed-Ochir, O.; Cho, D. Y.; Choi, J. Y. J.; Christensen, H.; Chu, D. T.; Chung, M. T.; Chung, S. C.; Cicuttini, F. M.; Ciobanu, L. G.; Cirillo, M.; Classen, T. K. D.; Cohen, A. J.; Compton, K.; Cooper, O. R.; Costa, V. M.; Cousin, E.; Cowden, R. G.; Cross, D. H.; Cruz, J. A.; Dahlawi, S. M. A.; Damasceno, A. A. M.; Damiani, G.; Dandona, L.; Dandona, R.; Dangel, W. J.; Danielsson, A. K.; Dargan, P. I.; Darwesh, A. M.; Daryani, A.; Das, J. K.; das Gupta, R.; das Neves, J.; Dávila-Cervantes, C. A.; Davitoiu, D. V.; de Leo, D.; Degenhardt, L.; DeLang, M.; Dellavalle, R. P.; Demeke, F. M.; Demoz, G. T.; Demsie, D. G.; Denova-Gutiérrez, E.; Dervenis, N.; Dhungana, G. P.; Dianatinasab, M.; Dias da Silva, D.; Diaz, D.; Dibaji Forooshani, Z. S.; Djalalinia, S.; Do, H. T.; Dokova, K.; Dorostkar, F.; Doshmangir, L.; Driscoll, T. R.; Duncan, B. B.; Duraes, A. R.; Eagan, A. W.; Edvardsson, D.; el Nahas, N.; el Sayed, I.; el Tantawi, M.; Elbarazi, I.; Elgendy, I. Y.; El-Jaafary, S. I.; Elyazar, I. R. F.; Emmons-Bell, S.; Erskine, H. E.; Eskandarieh, S.;

Esmaeilnejad, S.; Esteghamati, A.; Estep, K.; Etemadi, A.; Etisso, A. E.; Fanzo, J.; Farahmand, M.; Fareed, M.; Faridnia, R.; Farioli, A.; Faro, A.; Faruque, M.; Farzadfar, F.; Fattahi, N.; Fazlzadeh, M.; Feigin, V. L.; Feldman, R.; Fereshtehnejad, S. M.; Fernandes, E.; Ferrara, G.; Ferrari, A. J.; Ferreira, M. L.; Filip, I.; Fischer, F.; Fisher, J. L.; Flor, L. S.; Foigt, N. A.; Folayan, M. O.; Fomenkov, A. A.; Force, L. M.; Foroutan, M.; Franklin, R. C.; Freitas, M.; Fu, W.; Fukumoto, T.; Furtado, J. M.; Gad, M. M.; Gakidou, E.; Gallus, S.; Garcia-Basteiro, A. L.; Gardner, W. M.; Geberemariyam, B. S.; Ayalew Gebreslassie, A. A.; Geremew, A.; Gershberg Hayoon, A.; Gething, P. W.; Ghadimi, M.; Ghadiri, K.; Ghaffarifar, F.; Ghafourifard, M.; Ghamari, F.; Ghashghaee, A.; Ghiasvand, H.; Ghith, N.; Gholamian, A.; Ghosh, R.; Gill, P. S.; Ginindza, T. G.; Giussani, G.; Gnedovskaya, E. v.; Goharinezhad, S.; Gopalani, S. V.; Gorini, G.; Goudarzi, H.; Goulart, A. C.; Greaves, F.; Grivna, M.; Grosso, G.; Gubari, M. I. M.; Gugnani, H. C.; Guimarães, R. A.; Guled, R. A.; Guo, G.; Guo, Y.; Gupta, R.; Gupta, T.; Haddock, B.; Hafezi-Nejad, N.; Hafiz, A.; Haj-Mirzaian, A.; Haj-Mirzaian, A.; Hall, B. J.; Halvaei, I.; Hamadeh, R. R.; Hamidi, S.; Hammer, M. S.; Hankey, G. J.; Haririan, H.; Haro, J. M.; Hasaballah, A. I.; Hasan, M. M.; Hasanpoor, E.; Hashi, A.; Hassanipour, S.; Hassankhani, H.; Havmoeller, R. J.; Hay, S. I.; Hayat, K.; Heidari, G.; Heidari-Soureshjani, R.; Henrikson, H. J.; Herbert, M. E.; Herteliu, C.; Heydarpour, F.; Hird, T. R.; Hoek, H. W.; Holla, R.; Hoogar, P.; Hosgood, H. D.; Hossain, N.; Hosseini, M.; Hosseinzadeh, M.; Hostiuc, M.; Hostiuc, S.; Househ, M.; Hsairi, M.; Hsieh, V. C. R.; Hu, G.; Hu, K.; Huda, T. M.; Humayun, A.; Huynh, C. K.; Hwang, B. F.; Iannucci, V. C.; Ibitoye, S. E.; Ikeda, N.; Ikuta, K. S.; Ilesanmi, O. S.; Ilic, I. M.; Ilic, M. D.; Inbaraj, L. R.; Ippolito, H.; Iqbal, U.; Irvani, S. S. N.; Irvine, C. M. S.; Islam, M. M.; Islam, S. M. S.; Iso, H.; Ivers, R. Q.; Iwu, C. C. D.; Iwu, C. J.; Iyamu, I. O.;

Jaafari, J.; Jacobsen, K. H.; Jafari, H.; Jafarinia, M.; Jahani, M. A.; Jakovljevic, M.; Jalilian, F.; James, S. L.; Janjani, H.; Javaheri, T.; Javidnia, J.; Jeemon, P.; Jenabi, E.; Jha, R. P.; Jha, V.; Ji, J. S.; Johansson, L.; John, O.; John-Akinola, Y. O.; Johnson, C. O.; Jonas, J. B.; Joukar, F.; Jozwiak, J. J.; Jürisson, M.; Kabir, A.; Kabir, Z.; Kalani, H.; Kalani, R.; Kalankesh, L. R.; Kalhor, R.; Kanchan, T.; Kapoor, N.; Matin, B. K.; Karch, A.; Karim, M. A.; Kassa, G. M.; Katikireddi, S. V.; Kayode, G. A.; Kazemi Karyani, A.; Keiyoro, P. N.; Keller, C.; Kemmer, L.; Kendrick, P. J.; Khalid, N.; Khammarnia, M.; Khan, E. A.; Khan, M.; Khatab, K.; Khater, M. M.; Khatib, M. N.; Khayamzadeh, M.; Khazaei, S.; Kieling, C.; Kim, Y. J.; Kimokoti, R. W.; Kisa, A.; Kisa, S.; Kivimäki, M.; Knibbs, L. D.; Knudsen, A. K. S.; Kocarnik, J. M.; Kochhar, S.; Kopec, J. A.; Korshunov, V. A.; Koul, P. A.; Koyanagi, A.; Kraemer, M. U. G.; Krishan, K.; Krohn, K. J.; Kromhout, H.; Kuate Defo, B.; Kumar, G. A.; Kumar, V.; Kurmi, O. P.; Kusuma, D.; la Vecchia, C.; Lacey, B.; Lal, D. K.; Lalloo, R.; Lallukka, T.; Lami, F. H.; Landires, I.; Lang, J. J.; Langan, S. M.; Larsson, A. O.; Lasrado, S.; Lauriola, P.; Lazarus, J. v.; Lee, P. H.; Lee, S. W. H.; Legrand, K. E.; Leigh, J.; Leonardi, M.; Lescinsky, H.; Leung, J.; Levi, M.; Li, S.; Lim, L. L.; Linn, S.; Liu, S.; Liu, S.; Liu, Y.; Lo, J.; Lopez, A. D.; Lopez, J. C. F.; Lopukhov, P. D.; Lorkowski, S.; Lotufo, P. A.; Lu, A.; Lugo, A.; Maddison, E. R.; Mahasha, P. W.; Mahdavi, M. M.; Mahmoudi, M.; Majeed, A.; Maleki, A.; Maleki, S.; Malekzadeh, R.; Malta, D. C.; Mamun, A. A.; Manda, A. L.; Manguerra, H.; Mansour-Ghanaei, F.; Mansouri, B.; Mansournia, M. A.; Mantilla Herrera, A. M.; Maravilla, J. C.; Marks, A.; Martin, R. v.; Martini, S.; Martins-Melo, F. R.; Masaka, A.; Masoumi, S. Z.; Mathur, M. R.; Matsushita, K.; Maulik, P. K.; McAlinden, C.; McGrath, J. J.; McKee, M.; Mehndiratta, M. M.; Mehri, F.; Mehta, K. M.; Memish, Z. A.; Mendoza, W.; Menezes, R.

G.; Mengesha, E. W.; Mereke, A.; Mereta, S. T.; Meretoja, A.; Meretoja, T. J.; Mestrovic, T.; Miazgowski, B.; Miazgowski, T.; Michalek, I. M.; Miller, T. R.; Mills, E. J.; Mini, G. K.; Miri, M.; Mirica, A.; Mirrakhimov, E. M.; Mirzaei, H.; Mirzaei, M.; Mirzaei, R.; Mirzaei-Alavijeh, M.; Misganaw, A. T.; Mithra, P.; Moazen, B.; Mohammad, D. K.; Mohammad, Y.; Mohammad Gholi Mezerji, N.; Mohammadian-Hafshejani, A.; Mohammadifard, N.; Mohammadpourhodki, R.; Mohammed, A. S.; Mohammed, H.; Mohammed, J. A.; Mohammed, S.; Mokdad, A. H.; Molokhia, M.; Monasta, L.; Mooney, M. D.; Moradi, G.; Moradi, M.; Moradi-Lakeh, M.; Moradzadeh, R.; Moraga, P.; Morawska, L.; Morgado-Da-Costa, J.; Morrison, S. D.; Mosapour, A.; Mosser, J. F.; Mouodi, S.; Mousavi, S. M.; Khaneghah, A. M.; Mueller, U. O.; Mukhopadhyay, S.; Mullany, E. C.; Musa, K. I.; Muthupandian, S.; Nabhan, A. F.; Naderi, M.; Nagarajan, A. J.; Nagel, G.; Naghavi, M.; Naghshtabrizi, B.; Naimzada, M. D.; Najafi, F.; Nangia, V.; Nansseu, J. R.; Naserbakht, M.; Nayak, V. C.; Negoi, I.; Ngunjiri, J. W.; Nguyen, C. T.; Nguyen, H. L. T.; Nguyen, M.; Nigatu, Y. T.; Nikbakhsh, R.; Nixon, M. R.; Nnaji, C. A.; Nomura, S.; Norrving, B.; Noubiap, J. J.; Nowak, C.; Nunez-Samudio, V.; Oancea, B.; Odell, C. M.; Ogbo, F. A.; Oh, I. H.; Okunga, E. W.; Oladnabi, M.; Olagunju, A. T.; Olusanya, B. O.; Olusanya, J. O.; Omer, M. O.; Ong, K. L.; Onwujekwe, O. E.; Orpana, H. M.; Ortiz, A.; Osarenotor, O.; Osei, F. B.; Ostroff, S. M.; Otoiu, A.; Otstavnov, N.; Otstavnov, S. S.; Øverland, S.; Owolabi, M. O.; Mahesh, P. A.; Padubidri, J. R.; Palladino, R.; Panda-Jonas, S.; Pandey, A.; Parry, C. D. H.; Pasovic, M.; Pasupula, D. K.; Patel, S. K.; Pathak, M.; Patten, S. B.; Patton, G. C.; Toroudi, H. P.; Peden, A. E.; Pennini, A.; Pepito, V. C. F.; Peprah, E. K.; Pereira, D. M.; Pesudovs, K.; Pham, H. Q.; Phillips, M. R.; Piccinelli, C.; Pilz, T. M.; Piradov, M. A.; Pirsaheb, M.; Plass, D.; Polinder, S.;

Polkinghorne, K. R.; Pond, C. D.; Postma, M. J.; Pourjafar, H.; Pourmalek, F.; Poznañska, A.; Prada, S. I.; Prakash, V.; Pribadi, D. R. A.; Pupillo, E.; Syed, Z. Q.; Rabiee, M.; Rabiee, N.; Radfar, A.; Rafiee, A.; Raggi, A.; Rahman, M. A.; Rajabpour-Sanati, A.; Rajati, F.; Rakovac, I.; Ram, P.; Ramezanzadeh, K.; Ranabhat, C. L.; Rao, P. C.; Rao, S. J.; Rashedi, V.; Rathi, P.; Rawaf, D. L.; Rawaf, S.; Rawal, L.; Rawassizadeh, R.; Rawat, R.; Razo, C.; Redford, S. B.; Reiner, R. C.; Reitsma, M. B.; Remuzzi, G.; Renjith, V.; Renzaho, A. M. N.; Resnikoff, S.; Rezaei, N.; Rezaei, N.; Rezapour, A.; Rhinehart, P. A.; Riahi, S. M.; Ribeiro, D. C.; Ribeiro, D.; Rickard, J.; Rivera, J. A.; Roberts, N. L. S.; Rodríguez-Ramírez, S.; Roever, L.; Ronfani, L.; Room, R.; Roshandel, G.; Roth, G. A.; Rothenbacher, D.; Rubagotti, E.; Rwegerera, G. M.; Sabour, S.; Sachdev, P. S.; Saddik, B.; Sadeghi, E.; Sadeghi, M.; Saeedi, R.; Saeedi Moghaddam, S.; Safari, Y.; Safi, S.; Safiri, S.; Sagar, R.; Sahebkar, A.; Sajadi, S. M.; Salam, N.; Salamati, P.; Salem, H.; Salem, M. R.; Salimzadeh, H.; Salman, O. M.; Salomon, J. A.; Samad, Z.; Samadi Kafil, H.; Sambala, E. Z.; Samy, A. M.; Sanabria, J.; Sánchez-Pimienta, T. G.; Santomauro, D. F.; Santos, I. S.; Santos, J. V.; Santric-Milicevic, M. M.; Saraswathy, S. Y. I.; Sarmiento-Suárez, R.; Sarrafzadegan, N.; Sartorius, B.; Sarveazad, A.; Sathian, B.; Sathish, T.; Sattin, D.; Saxena, S.; Schaeffer, L. E.; Schiavolin, S.; Schlaich, M. P.; Schmidt, M. I.; Schutte, A. E.; Schwebel, D. C.; Schwendicke, F.; Senbeta, A. M.; Senthilkumaran, S.; Sepanlou, S. G.; Serdar, B.; Serre, M. L.; Shadid, J.; Shafaat, O.; Shahabi, S.; Shaheen, A. A.; Shaikh, M. A.; Shalash, A. S.; Shams-Beyranvand, M.; Shamsizadeh, M.; Sharafi, K.; Sheikh, A.; Sheikhtaheri, A.; Shibuya, K.; Shield, K. D.; Shigematsu, M.; Shin, J. il; Shin, M. J.; Shiri, R.; Shirkoohi, R.; Shuval, K.; Siabani, S.; Sierpinski, R.; Sigfusdottir, I. D.; Sigurvinsdottir, R.; Silva, J. P.; Simpson, K. E.; Singh, J. A.; Singh, P.; Skiadaresi, E.;

Skou, S. T.; Skryabin, V. Y.; Smith, E. U. R.; Soheili, A.; Soltani, S.; Soofi, M.; Sorensen, R. J. D.; Soriano, J. B.; Sorrie, M. B.; Soshnikov, S.; Soyiri, I. N.; Spencer, C. N.; Spotin, A.; Sreeramareddy, C. T.; Srinivasan, V.; Stanaway, J. D.; Stein, C.; Stein, D. J.; Steiner, C.; Stockfelt, L.; Stokes, M. A.; Straif, K.; Stubbs, J. L.; Sufiyan, M. B.; Suleria, H. A. R.; Suliankatchi Abdulkader, R.; Sulo, G.; Sultan, I.; Tabarés-Seisdedos, R.; Tabb, K. M.; Tabuchi, T.; Taherkhani, A.; Tajdini, M.; Takahashi, K.; Takala, J. S.; Tamiru, A. T.; Taveira, N.; Tehrani-Banihashemi, A.; Temsah, M. H.; Tesema, G. A.; Tessema, Z. T.; Thurston, G. D.; Titova, M. V.; Tohidinik, H. R.; Tonelli, M.; Topor-Madry, R.; Topouzis, F.; Torre, A. E.; Touvier, M.; Tovani-Palone, M. R.; Tran, B. X.; Travillian, R.; Tsatsakis, A.; Tudor Car, L. T.; Tyrovolas, S.; Uddin, R.; Umeokonkwo, C. D.; Unnikrishnan, B.; Upadhyay, E.; Vacante, M.; Valdez, P. R.; van Donkelaar, A.; Vasankari, T. J.; Vasseghian, Y.; Veisani, Y.; Venketasubramanian, N.; Violante, F. S.; Vlassov, V.; Vollset, S. E.; Vos, T.; Vukovic, R.; Waheed, Y.; Wallin, M. T.; Wang, Y.; Wang, Y. P.; Watson, A.; Wei, J.; Wei, M. Y. W.; Weintraub, R. G.; Weiss, J.; Werdecker, A.; West, J. J.; Westerman, R.; Whisnant, J. L.; Whiteford, H. A.; Wiens, K. E.; Wolfe, C. D. A.; Wozniak, S. S.; Wu, A. M.; Wu, J.; Wulf Hanson, S.; Xu, G.; Xu, R.; Yadgir, S.; Yahyazadeh Jabbari, S. H.; Yamagishi, K.; Yaminfirooz, M.; Yano, Y.; Yaya, S.; Yazdi-Feyzabadi, V.; Yeheyis, T. Y.; Yilgwan, C. S.; Yilma, M. T.; Yip, P.; Yonemoto, N.; Younis, M. Z.; Younker, T. P.; Yousefi, B.; Yousefi, Z.; Yousefinezhadi, T.; Yousuf, A. Y.; Yu, C.; Yusefzadeh, H.; Moghadam, T. Z.; Zamani, M.; Zamanian, M.; Zandian, H.; Zastrozhin, M. S.; Zhang, Y.; Zhang, Z. J.; Zhao, J. T.; Zhao, X. J. G.; Zhao, Y.; Zheng, P.; Zhou, M.; Ziapour, A.; Zimsen, S. R. M.; Lim, S. S.; Murray, C. J. L. Global Burden of 87 Risk Factors in 204 Countries and Territories, 1990–2019: A

- Systematic Analysis for the Global Burden of Disease Study 2019. *The Lancet* **2020**, *396* (10258), 1223–1249. https://doi.org/10.1016/S0140-6736(20)30752-2.
- (3) Lelieveld, J.; Klingmüller, K.; Pozzer, A.; Burnett, R. T.; Haines, A.; Ramanathan, V. Effects of Fossil Fuel and Total Anthropogenic Emission Removal on Public Health and Climate. *Proceedings of the National Academy of Sciences of the United States of America* **2019**, *116* (15), 7192–7197. https://doi.org/10.1073/pnas.1819989116.
- (4) Axsen, J.; Plötz, P.; Wolinetz, M. Crafting Strong, Integrated Policy Mixes for Deep CO2 Mitigation in Road Transport. *Nature Climate Change* 2020, 10 (9), 809–818. https://doi.org/10.1038/s41558-020-0877-y.
- (5) Greene, S.; Façanha, C. Carbon Offsets for Freight Transport Decarbonization. *Nature Sustainability* **2019**, *2* (11), 994–996. https://doi.org/10.1038/s41893-019-0413-0.
- (6) The Carbon Footprint of Global Trade: Tackling Emissions from International Freight Transport. *International Transport Forum*.
- (7) Transport sector CO2 emissions by mode in the Sustainable Development Scenario, 2000-2030 Charts Data & Statistics IEA https://www.iea.org/data-and-statistics/charts/transport-sector-co2-emissions-by-mode-in-the-sustainable-development-scenario-2000-2030 (accessed Oct 23, 2020).
- (8) International Energy Agency. Trucks and Buses Analysis IEA https://www.iea.org/reports/trucks-and-buses#tracking-progress (accessed Sep 23, 2020).
- (9) Kaack, L. H.; Vaishnav, P.; Morgan, M. G.; Azevedo, I. L.; Rai, S. Decarbonizing Intraregional Freight Systems with a Focus on Modal Shift. *Environmental Research Letters* **2018**, *13* (8), 083001. https://doi.org/10.1088/1748-9326/aad56c.

- (10) Davis, S. J.; Lewis, N. S.; Shaner, M.; Aggarwal, S.; Arent, D.; Azevedo, I. L.; Benson, S. M.; Bradley, T.; Brouwer, J.; Chiang, Y.-M.; Clack, C. T. M.; Cohen, A.; Doig, S.; Edmonds, J.; Fennell, P.; Field, C. B.; Hannegan, B.; Hodge, B.-M.; Hoffert, M. I.; Ingersoll, E.; Jaramillo, P.; Lackner, K. S.; Mach, K. J.; Mastrandrea, M.; Ogden, J.; Peterson, P. F.; Sanchez, D. L.; Sperling, D.; Stagner, J.; Trancik, J. E.; Yang, C.-J.; Caldeira, K. Net-Zero Emissions Energy Systems. *Science* 2018, 360 (6396), eaas9793. https://doi.org/10.1126/science.aas9793.
- (11) The Future of Trucks Analysis IEA https://www.iea.org/reports/the-future-of-trucks (accessed Jun 28, 2021).
- (12) ITF Transport Outlook 2021 | ITF https://www.itf-oecd.org/itf-transport-outlook-2021 (accessed Jun 26, 2021).
- (13) On-Road Freight Complexities. *Nature Sustainability* **2019**, *2* (2), 77–77. https://doi.org/10.1038/s41893-019-0241-2.
- Mulholland, E.; Teter, J.; Cazzola, P.; McDonald, Z.; Ó Gallachóir, B. P. The Long Haul towards Decarbonising Road Freight A Global Assessment to 2050. *Applied Energy* 2018, 216, 678–693. https://doi.org/10.1016/j.apenergy.2018.01.058.
- (15) Morgan, M. G. Climate Policy Needs More than Muddling. Proceedings of the National Academy of Sciences of the United States of America. National Academy of Sciences March 1, 2016, pp 2322–2324. https://doi.org/10.1073/pnas.1601167113.
- (16) Liu, L.; Hwang, T.; Lee, S.; Ouyang, Y.; Lee, B.; Smith, S. J.; Tessum, C. W.; Marshall, J. D.; Yan, F.; Daenzer, K.; Bond, T. C. Health and Climate Impacts of Future United States Land Freight Modelled with Global-to-Urban Models. *Nature Sustainability* 2019, 2 (2), 105–112. https://doi.org/10.1038/s41893-019-0224-3.

- (17) Bickford, E.; Holloway, T.; Karambelas, A.; Johnston, M.; Adams, T.; Janssen, M.; Moberg, C. Emissions and Air Quality Impacts of Truck-to-Rail Freight Modal Shifts in the Midwestern United States. *Environmental Science and Technology* 2013, 48 (1), 446– 454. https://doi.org/10.1021/ES4016102.
- (18) Basic Information about NO2 | Nitrogen Dioxide (NO2) Pollution | US EPA https://www.epa.gov/no2-pollution/basic-information-about-no2#Effects (accessed Jun 29, 2021).
- (19) Health Effects of Ozone Pollution | Ground-level Ozone Pollution | US EPA https://www.epa.gov/ground-level-ozone-pollution/health-effects-ozone-pollution (accessed Jun 29, 2021).
- (20) Sulfur Dioxide Basics | Sulfur Dioxide (SO2) Pollution | US EPA

 https://www.epa.gov/so2-pollution/sulfur-dioxide-basics#effects (accessed Jul 10, 2021).
- (21) Particulate Matter (PM) Basics | Particulate Matter (PM) Pollution | US EPA https://www.epa.gov/pm-pollution/particulate-matter-pm-basics#PM (accessed Jun 29, 2021).
- (22) Health and Environmental Effects of Particulate Matter (PM) | Particulate Matter (PM) | Pollution | US EPA https://www.epa.gov/pm-pollution/health-and-environmental-effects-particulate-matter-pm (accessed Jun 29, 2021).
- (23) Laden, F.; Neas, L. M.; Dockery, D. W.; Schwartz, J. Association of Fine Particulate Matter from Different Sources with Daily Mortality in Six U.S. Cities. *Environmental Health Perspectives* **2000**, *108* (10), 941–947. https://doi.org/10.1289/ehp.00108941.
- (24) Krewski, D.; Burnett, R.; Jerrett, M.; Pope, C. A.; Rainham, D.; Calle, E.; Thurston, G.; Thun, M. Mortality and Long-Term Exposure to Ambient Air Pollution: Ongoing

- Analyses Based on the American Cancer Society Cohort. *Journal of Toxicology and Environmental Health Part A.* July 9, 2005, pp 1093–1109. https://doi.org/10.1080/15287390590935941.
- (25) Pope, C. A.; Burnett, R. T.; Thun, M. J.; Calle, E. E.; Krewski, D.; Ito, K.; Thurston, G. D. Lung Cancer, Cardiopulmonary Mortality, and Long-Term Exposure to Fine Particulate Air Pollution. *Journal of the American Medical Association* **2002**, 287 (9), 1132–1141. https://doi.org/10.1001/jama.287.9.1132.
- (26) Explore the Data | State of Global Air https://www.stateofglobalair.org/data/#/air/plot (accessed Aug 18, 2021).
- (27) Health Impacts of PM2.5 | State of Global Air https://www.stateofglobalair.org/health/pm (accessed Jun 26, 2021).
- (28) McKinnon, A. Freight Transport in a Low-Carbon World.
- (29) Lathwal, P.; Vaishnav, P.; Morgan, M. G. Environmental and Health Consequences of Shore Power for Vessels Calling at Major Ports in India. *Environmental Research Letters* 2021, 16 (6), 064042. https://doi.org/10.1088/1748-9326/abfd5b.
- (30) Roberts, D. The key to tackling climate change: electrify everything Vox https://www.vox.com/2016/9/19/12938086/electrify-everything (accessed Apr 21, 2020).
- (31) Holland, S. P.; Mansur, E. T.; Muller, N. Z.; Yates, A. J. Are There Environmental Benefits from Driving Electric Vehicles? The Importance of Local Factors. *American Economic Review* **2016**, *106* (12), 3700–3729. https://doi.org/10.1257/aer.20150897.
- (32) Holland, S. P.; Mansur, E. T.; Muller, N. Z.; Yates, A. J. Distributional Effects of Air Pollution from Electric Vehicle Adoption. *Journal of the Association of Environmental and Resource Economists* **2019**, *6* (S1), S65–S94. https://doi.org/10.1086/701188.

- (33) Eyring, V.; Isaksen, I. S. A.; Berntsen, T.; Collins, W. J.; Corbett, J. J.; Endresen, O.; Grainger, R. G.; Moldanova, J.; Schlager, H.; Stevenson, D. S. Transport Impacts on Atmosphere and Climate: Shipping. *Atmospheric Environment* 2010, 44 (37), 4735–4771. https://doi.org/10.1016/j.atmosenv.2009.04.059.
- (34) Endresen, Ø. Emission from International Sea Transportation and Environmental Impact.
 Journal of Geophysical Research 2003, 108 (D17), 4560.
 https://doi.org/10.1029/2002JD002898.
- (35) Dalsøren, S. B.; Eide, M. S.; Endresen, Ø.; Mjelde, A.; Gravir, G.; Isaksen, I. S. A. Update on Emissions and Environmental Impacts from the International Fleet of Ships: The Contribution from Major Ship Types and Ports. *Atmospheric Chemistry and Physics* **2009**, 9 (6), 2171–2194. https://doi.org/10.5194/acp-9-2171-2009.
- (36) Liu, H.; Fu, M.; Jin, X.; Shang, Y.; Shindell, D.; Faluvegi, G.; Shindell, C.; He, K. Health and Climate Impacts of Ocean-Going Vessels in East Asia. *Nature Climate Change* **2016**, 6 (11), 1037–1041. https://doi.org/10.1038/nclimate3083.
- (37) Hassellöv, I.-M.; Turner, D. R.; Lauer, A.; Corbett, J. J. Shipping Contributes to Ocean Acidification. *Geophysical Research Letters* **2013**, *40* (11), 2731–2736. https://doi.org/10.1002/grl.50521.
- (38) Corbett, J. J.; Winebrake, J. J.; Green, E. H.; Kasibhatla, P.; Eyring, V.; Lauer, A. Mortality from Ship Emissions: A Global Assessment. *Environmental Science and Technology* **2007**, *41* (24), 8512–8518. https://doi.org/10.1021/es071686z.
- (39) Sofiev, M.; Winebrake, J. J.; Johansson, L.; Carr, E. W.; Prank, M.; Soares, J.; Vira, J.; Kouznetsov, R.; Jalkanen, J.-P.; Corbett, J. J. Cleaner Fuels for Ships Provide Public

- Health Benefits with Climate Tradeoffs. *Nature Communications* **2018**, *9* (1), 406. https://doi.org/10.1038/s41467-017-02774-9.
- (40) International Council on Clean Transportation. Silent but deadly: The case of shipping emissions https://theicct.org/blog/staff/silent-deadly-case-shipping-emissions (accessed Aug 22, 2020).
- (41) Smith, T. W. P.; Jalkanen, J. P.; Anderson, B. A.; Corbett, J. J.; Faber, J.; Hanayama, S.; O'Keeffe, E.; Parker, S.; Johansson, L.; Aldous, L.; Raucci, C.; Traut, M.; Ettinger, S.; Nelissen, D.; Lee, D. S.; Ng, S.; Agrawal, A.; Winebrake, J. J.; Hoen, M., A. *Third IMO Greenhouse Gas Study 2014, Executive Summary and Final Report*; 2014.
- (42) Kim, J.; Rahimi, M.; Newell, J. Life-Cycle Emissions from Port Electrification: A Case Study of Cargo Handling Tractors at the Port of Los Angeles. *International Journal of Sustainable Transportation* 2012, 6 (6), 321–337. https://doi.org/10.1080/15568318.2011.606353.
- (43) Iris, Ç.; Lam, J. S. L. A Review of Energy Efficiency in Ports: Operational Strategies, Technologies and Energy Management Systems. *Renewable and Sustainable Energy Reviews* **2019**, *112*, 170–182. https://doi.org/10.1016/j.rser.2019.04.069.
- (44) Edison Electric Institute. Utilities Take Transportation Electrification to Nation's Ports https://www.eei.org/resourcesandmedia/energynews/Pages/Utilities Take Transportation Electrification to Nation's Ports.aspx (accessed Apr 21, 2020).
- (45) Hall, W. J. Assessment of CO2 and Priority Pollutant Reduction by Installation of Shoreside Power. *Resources, Conservation and Recycling* 2010, 54 (7), 462–467. https://doi.org/10.1016/j.resconrec.2009.10.002.

- (46) International Council on Clean Transportation. *Costs and Benefits of Shore Power at the Port of Shenzhen*; 2015.
- (47) Vaishnav, P.; Fischbeck, P. S.; Morgan, M. G.; Corbett, J. J. Shore Power for Vessels Calling at U.S. Ports: Benefits and Costs. *Environmental Science & Technology* **2016**, *50* (3), 1102–1110. https://doi.org/10.1021/acs.est.5b04860.
- (48) Winkel, R.; Weddige, U.; Johnsen, D.; Hoen, V.; Papaefthimiou, S. Shore Side Electricity in Europe: Potential and Environmental Benefits. *Energy Policy* **2016**, 88, 584–593. https://doi.org/10.1016/j.enpol.2015.07.013.
- (49) California Air Resources Board. Shore Power for Ocean-Going Vessels https://ww3.arb.ca.gov/ports/shorepower/shorepower.htm (accessed Apr 21, 2020).
- (50) Government of India. Shore Power Supply at Indian Ports to Visiting Ship https://www.dgshipping.gov.in/writereaddata/ShippingNotices/202002100559222431579

 Shore_power_supply_eng.pdf (accessed Jun 11, 2020).
- (51) Wan, Z.; Zhu, M.; Chen, S.; Sperling, D. Pollution: Three Steps to a Green Shipping Industry. *Nature* **2016**, *530* (7590), 275–277. https://doi.org/10.1038/530275a.
- (52) UNCTAD. Handbook of Statistics 2019, World Seaborne Trade https://stats.unctad.org/handbook/MaritimeTransport/WorldSeaborneTrade.html (accessed Mar 3, 2020).
- (53) UNCTAD. Review of Maritime Transport 2019; 2019.
- (54) Natural Resources Defense Council. China Taking Further Steps to Clean Up Shipping Pollution https://www.nrdc.org/experts/barbara-finamore/china-taking-further-steps-clean-shipping-pollution (accessed Oct 26, 2019).

- (55) International Council on Clean Transportation. Technical and Economic Analysis of the Transition to Ultra-Low Sulfur Fuels in Brazil, China, India, and Mexico. Prepared for the International Council on Clean Transportation; 2012.
- (56) International Council on Clean Transportation. *Technical Background on India BS VI Fuel Specifications*; 2016.
- (57) Assocham India https://www.assocham.org/newsdetail.php?id=6632 (accessed Oct 18, 2019).
- (58) Government of India. Developing Ports: Sagarmala Project

 http://www.makeinindia.com/article/-/v/developing-ports-sagarmala-project (accessed

 Dec 13, 2019).
- (59) Bankes-Hughes, L. India begins roll-out of countrywide on-shore power programme https://www.bunkerspot.com/asia/46495-asia-pacific-india-begins-roll-out-of-countrywide-on-shore-power-programme (accessed Feb 2, 2020).
- (60) Maritime Executive. First for Shore Power in India https://www.maritime-executive.com/editorials/first-for-shore-power-in-india (accessed Oct 27, 2019).
- (61) World Population Review. Los Angeles Population 2019
 http://worldpopulationreview.com/us-cities/los-angeles-population/ (accessed Aug 23, 2019).
- (62) Li, R.; Wu, H.; DIng, J.; Fu, W.; Gan, L.; Li, Y. Mercury Pollution in Vegetables, Grains and Soils from Areas Surrounding Coal-Fired Power Plants. *Scientific Reports* **2017**, *7* (1), 1–9. https://doi.org/10.1038/srep46545.
- (63) Corbett, J. Shipping Emissions in East Asia. *Nature Climate Change* **2016**, *6* (11), 983–984. https://doi.org/10.1038/nclimate3091.

- (64) Fu, M.; Liu, H.; Jin, X.; He, K. National- to Port-Level Inventories of Shipping Emissions in China. *Environmental Research Letters* 2017, 12 (11), 114024.
 https://doi.org/10.1088/1748-9326/aa897a.
- Zhang, Y.; Yang, X.; Brown, R.; Yang, L.; Morawska, L.; Ristovski, Z.; Fu, Q.; Huang,
 C. Shipping Emissions and Their Impacts on Air Quality in China. *Science of The Total Environment* 2017, 581–582, 186–198. https://doi.org/10.1016/j.scitotenv.2016.12.098.
- (66) Liu, H.; Jin, X.; Wu, L.; Wang, X.; Fu, M.; Lv, Z.; Morawska, L.; Huang, F.; He, K. The Impact of Marine Shipping and Its DECA Control on Air Quality in the Pearl River Delta, China. Science of The Total Environment 2018, 625, 1476–1485.
 https://doi.org/10.1016/j.scitotenv.2018.01.033.
- (67) Joseph, J.; Patil, R. S.; Gupta, S. K. Estimation of Air Pollutant Emission Loads from Construction and Operational Activities of a Port and Harbour in Mumbai, India. *Environmental monitoring and assessment* 2009, 159 (1–4), 85–98. https://doi.org/10.1007/s10661-008-0614-x.
- (68) Mandal, A.; Biswas, J.; Roychowdhury, S.; Farooqui, Z. M. Appraisal of Emissions from Ocean-Going Vessels Coming to Kolkata Port, India. *Journal of The Institution of Engineers (India): Series A* 2017, 98 (4), 387–395. https://doi.org/10.1007/s40030-017-0238-7.
- (69) Indian Ports Association. Cargo Traffic at Major Ports http://www.ipa.nic.in/index1.cshtml?lsid=155 (accessed Oct 28, 2019).
- (70) Government of India. Report No. 269, Cargo Handling at the Major Ports; 2018.

- (71) Ministry of Shipping Government of India. Ports

 http://shipmin.gov.in/index1.php?lang=1&level=0&linkid=16&lid=64 (accessed Aug 23, 2019).
- (72) Indian Ports Association. Cargo Traffic at Major Ports http://www.ipa.nic.in/index1.cshtml?lsid=155 (accessed Nov 6, 2020).
- (73) Port of Los Angeles. Port of Los Angeles Facts and Figures https://www.portoflosangeles.org/business/statistics/facts-and-figures (accessed Aug 23, 2019).
- (74) Environmental Protection Agency. Current Methodologies in Preparing Mobile Source

 Port-Related Emission Inventories Final Report April 2009: Prepared for US

 Environmental Protection Agency (EPA); 2009.
- (75) Goldsworthy, B.; Goldsworthy, L. Assigning Machinery Power Values for Estimating Ship Exhaust Emissions: Comparison of Auxiliary Power Schemes. *Science of The Total Environment* **2019**, *657*, 963–977. https://doi.org/10.1016/j.scitotenv.2018.12.014.
- (76) Starcrest Consulting Group. The Port of Los Angeles Inventory of Air Emissions for Calendar Year 2016; 2017.
- (77) Starcrest Consulting Group. The Port of Long Beach 2016 Air Emissions Inventory; 2017.
- (78) World Bank. Electric power transmission and distribution losses data (% of output) https://data.worldbank.org/indicator/EG.ELC.LOSS.ZS (accessed Sep 6, 2019).
- (79) Nirula, A. India's Power Distribution Sector India's Power Distribution Sector: An Assessment of Financial and Operational Sustainability India's Power Distribution Sector: An Assessment of Financial and Operational Sustainability; 2019.
- (80) Central Electricity Authority. *Growth of Electricity Sector in India from 1947-2018*; 2018.

- (81) Oberschelp, C.; Pfister, S.; Raptis, C. E.; Hellweg, S. Global Emission Hotspots of Coal Power Generation. *Nature Sustainability* **2019**, *2* (2), 113–121. https://doi.org/10.1038/s41893-019-0221-6.
- (82) Central Electricity Authority. *Highlights of India's Power Sector*, 2012; 2012.
- (83) Entec. Quantification of Emissions from Ships Associated with Ship Movements between Ports in the European Community; 2002.
- (84) Starcrest Consulting Group. Port of Long Beach Air Emissions Inventory, 2013; 2013.
- (85) Petrol Bunkering & Trading. Price information for Petrol Bunkering https://www.petrolbunkering.com/price-information/ (accessed Sep 6, 2019).
- (86) Currency Converter. USD to INR Currency Converter http://currencyconverter.io/68.96-usd-inr (accessed Nov 30, 2019).
- (87) Joint Research Centre. EDGAR EDGAR v5.0 Global Air Pollutant Emissions European Commission https://edgar.jrc.ec.europa.eu/overview.php?v=50_AP (accessed Feb 26, 2021).
- (88) OECD. Economic Outlook No 103 (Long-term Baseline GDP Projections)

 https://stats.oecd.org/Index.aspx?DataSetCode=EO103_LTB (accessed Dec 14, 2019).
- (89) Government of India. Traffic Handled at Major Ports in India

 https://data.gov.in/catalog/traffic-handled-major-portsindia?filters%5Bfield_catalog_reference%5D=316621&format=json&offset=0&limit=6&
 sort%5Bcreated%5D=desc (accessed Feb 9, 2020).
- (90) IndiaStat. Traffic Handled at Indian Ports (1955-2020) https://www.indiastat.com/transport-data/30/shipping-and-ports/253/traffic-handled-at-ports-1955-2020/449979/stats.aspx (accessed Apr 4, 2020).

- (91) Government of India. India Transport Report: Moving India to 2032; 2014.
- (92) Center for Study of Science Technology and Policy. *Benefit Cost Analysis of Emission Standards for Coal-Based Thermal Power Plants in India*; 2018.
- (93) Sahil, A.; Tongia, R. The future of Indian electricity supply: Scenarios of coal use by 2030 https://www.brookings.edu/research/the-future-of-indian-electricity-supply-scenarios-of-coal-use-by-2030/ (accessed Dec 14, 2019).
- (94) Lee, C. J.; Martin, R. v.; Henze, D. K.; Brauer, M.; Cohen, A.; Donkelaar, A. van.
 Response of Global Particulate-Matter-Related Mortality to Changes in Local Precursor
 Emissions. Environmental Science & Technology 2015, 49 (7), 4335–4344.
 https://doi.org/10.1021/acs.est.5b00873.
- (95) POSOCO. POSOCO National Load Despatch Center https://posoco.in/ (accessed Nov 10, 2020).
- (96) Central Electricity Authority. Guidelines for Distribution Utilities for Development of Distribution Infrastructure; 2018.
- (97) Central Electricity Regulatory Commission. *Petition No. 173/TT/2016*; New Delhi, 2017.
- (98) Central Electricity Regulatory Commission. *Terms and Conditions of Tariff Regulations* for 01.04.2014 to 31.03.2019; 2013.
- (99) California Air Resources Board. Carl Moyer Memorial Air Quality Standards Attainment Program, Chapter 7; 2020.
- (100) Central Electricity Authority. Standard Technical Specification For Retrofit Of Wet Limestone Based Flue Gas Desulphurisation (FGD) System In A Typical 2*500 MW Thermal Power Plant; New Delhi, 2017.

- (101) Kerala State Electricity Board Limited. Generation

 http://www.kseb.in/index.php?option=com_content&view=article&id=45&Itemid=553&I

 ang=en (accessed Mar 23, 2020).
- (102) NLC India Limited. NLC India Limited https://www.nlcindia.com/new_website/index.htm.
- (103) Coal India Limited. *Mahanadi Coalfields Limited Monthly Production Report, February* 2020; 2020.
- (104) NTPC. Coal Based Power Stations https://www.ntpc.co.in/en/power-generation/coal-based-power-stations (accessed Mar 22, 2020).
- (105) V.O. Chidambaranar Port. Citizen Charter; 2018.
- (106) PTI. India-China Bilateral Trade Hits Historic High of \$84.44 Billion in 2017. *Times of India*. 2018.
- (107) Mao, X. Action Plan for Establishing China's National Emission Control Area.

 International Council on Clean Transportation. 2019.
- (108) Port of Los Angeles. Port of Los Angeles Container TEU Statistics for 2013 https://www.portoflosangeles.org/business/statistics/container-statistics/historical-teustatistics-2013 (accessed Dec 13, 2019).
- (109) U.S. Energy Information Administration EIA Independent Statistics and Analysis https://www.eia.gov/outlooks/aeo/data/browser/#/?id=45-AEO2021&cases=ref2021&sourcekey=0 (accessed Jun 12, 2021).
- (110) Environmental Protection Agency. Fast Facts on Transportation Greenhouse Gas

 Emissions https://www.epa.gov/greenvehicles/fast-facts-transportation-greenhouse-gasemissions (accessed Nov 19, 2019).

- (111) Liu, X.; Elgowainy, A.; Vijayagopal, R.; Wang, M. Well-to-Wheels Analysis of Zero-Emission Plug-In Battery Electric Vehicle Technology for Medium- And Heavy-Duty Trucks. *Environmental Science and Technology* 2021, 55 (1), 538–546. https://doi.org/10.1021/acs.est.0c02931.
- (112) Bickford, E.; Holloway, T.; Karambelas, A.; Johnston, M.; Adams, T.; Janssen, M.; Moberg, C. Emissions and Air Quality Impacts of Truck-to-Rail Freight Modal Shifts in the Midwestern United States. *Environmental Science & Technology* 2014, 48 (1), 446– 454. https://doi.org/10.1021/es4016102.
- (113) US Department of Transportation. 2017 CFS Preliminary Data Bureau of Transportation

 Statistics https://www.bts.gov/surveys/commodity-flow-survey/2017-cfs-preliminary-data
 (accessed Nov 15, 2020).
- (114) Federal Highway Administration. FHWA Forecasts of Vehicle Miles Traveled (VMT): Spring 2019; 2019.
- (115) Overview of the Clean Air Act and Air Pollution | US EPA https://www.epa.gov/clean-air-act-overview (accessed Jun 30, 2021).
- (116) Diesel Fuel Standards and Rulemakings | Diesel Fuel Standards | US EPA https://19january2017snapshot.epa.gov/diesel-fuel-standards/diesel-fuel-standards-and-rulemakings_.html (accessed Jun 30, 2021).
- (117) GBD Results Tool | GHDx http://ghdx.healthdata.org/gbd-results-tool (accessed Jun 12, 2021).
- (118) Burnett, R.; Chen, H.; Szyszkowicz, M.; Fann, N.; Hubbell, B.; Pope, C. A.; Apte, J. S.; Brauer, M.; Cohen, A.; Weichenthal, S.; Coggins, J.; Di, Q.; Brunekreef, B.; Frostad, J.; Lim, S. S.; Kan, H.; Walker, K. D.; Thurston, G. D.; Hayes, R. B.; Lim, C. C.; Turner, M.

- C.; Jerrett, M.; Krewski, D.; Gapstur, S. M.; Diver, W. R.; Ostro, B.; Goldberg, D.; Crouse, D. L.; Martin, R. v.; Peters, P.; Pinault, L.; Tjepkema, M.; van Donkelaar, A.; Villeneuve, P. J.; Miller, A. B.; Yin, P.; Zhou, M.; Wang, L.; Janssen, N. A. H.; Marra, M.; Atkinson, R. W.; Tsang, H.; Thach, T. Q.; Cannon, J. B.; Allen, R. T.; Hart, J. E.; Laden, F.; Cesaroni, G.; Forastiere, F.; Weinmayr, G.; Jaensch, A.; Nagel, G.; Concin, H.; Spadaro, J. v. Global Estimates of Mortality Associated with Longterm Exposure to Outdoor Fine Particulate Matter. *Proceedings of the National Academy of Sciences of the United States of America* **2018**, *115* (38), 9592–9597.
- (119) Tessum, C. W.; Paolella, D. A.; Chambliss, S. E.; Apte, J. S.; Hill, J. D.; Marshall, J. D.
 PM2.5 Polluters Disproportionately and Systemically Affect People of Color in the United States. *Science Advances* 2021, 7 (18), 4491–4519.
 https://doi.org/10.1126/sciadv.abf4491.
- (120) Marshall, J. D.; Swor, K. R.; Nguyen, N. P. Prioritizing Environmental Justice and Equality: Diesel Emissions in Southern California. *Environmental Science and Technology* **2014**, *48* (7), 4063–4068. https://doi.org/10.1021/es405167f.
- (121) Colmer, J.; Hardman, I.; Shimshack, J.; Voorheis, J. Disparities in PM2.5 Air Pollution in the United States. *Science* 2020, 369 (6503), 575–578. https://doi.org/10.1126/science.aaz9353.
- (122) Bullard, R. D. Solid Waste Sites and the Black Houston Community. *Sociological Inquiry* **1983**, *53* (2–3), 273–288. https://doi.org/10.1111/j.1475-682X.1983.tb00037.x.

- (123) Brender, J. D.; Maantay, J. A.; Chakraborty, J. Residential Proximity to Environmental Hazards and Adverse Health Outcomes. *American Journal of Public Health* **2011**, *101* (SUPPL. 1), 37–52. https://doi.org/10.2105/AJPH.2011.300183.
- (124) Mohai, P.; Saha, R. Which Came First, People or Pollution? A Review of Theory and Evidence from Longitudinal Environmental Justice Studies. *Environmental Research Letters* **2015**, *10* (12), 125011. https://doi.org/10.1088/1748-9326/10/12/125011.
- (125) Mohai, P.; Pellow, D.; Roberts, J. T. Environmental Justice. *Annual Review of Environment and Resources* **2009**, *34*, 405–430. https://doi.org/10.1146/annurev-environ-082508-094348.
- (126) Hajat, A.; Hsia, C.; O'Neill, M. S. Socioeconomic Disparities and Air Pollution Exposure:

 A Global Review. *Current environmental health reports*. Springer December 1, 2015, pp

 440–450. https://doi.org/10.1007/s40572-015-0069-5.
- (127) US EPA. 2017 National Emissions Inventory (NEI) Data https://www.epa.gov/air-emissions-inventories/2017-national-emissions-inventory-nei-data (accessed Aug 11, 2020).
- (128) US EPA. 2017 National Emissions Inventory (NEI) Technical Support Document; 2020.
- (129) Johnston, M.; Bickford, E.; Holloway, T.; Dresser, C.; Adams, T. M. Impacts of Biodiesel Blending on Freight Emissions in the Midwestern United States. *Transportation Research Part D: Transport and Environment* **2012**. https://doi.org/10.1016/j.trd.2012.05.001.
- (130) Bickford, E. Emissions and Air Quality Impacts of Freight Transportation; 2012.
- (131) Freight Analysis Framework FHWA Freight Management and Operations https://ops.fhwa.dot.gov/freight/freight_analysis/faf/ (accessed Oct 3, 2020).

- (132) Heo, J.; Adams, P. J.; Gao, H. O. Public Health Costs Accounting of Inorganic PM2.5
 Pollution in Metropolitan Areas of the United States Using a Risk-Based Source-Receptor
 Model. Environment International 2017. https://doi.org/10.1016/j.envint.2017.06.006.
- (133) Heo, J.; Adams, P. J.; Gao, H. O. Reduced-Form Modeling of Public Health Impacts of Inorganic PM2.5 and Precursor Emissions. *Atmospheric Environment* **2016**, *137*, 80–89. https://doi.org/10.1016/j.atmosenv.2016.04.026.
- (134) Heo, J.; Adams, P. J.; Gao, H. O. Public Health Costs of Primary PM2.5 and Inorganic PM2.5 Precursor Emissions in the United States. *Environmental Science and Technology* **2016**, *50* (11), 6061–6070. https://doi.org/10.1021/acs.est.5b06125.
- (135) Epa, U.; of Policy Analysis, O. The Benefits and Costs of the Clean Air Act from 1990 to 2020, Final Report, Revision A, April 2011; 2011.
- (136) Freight Analysis Framework Frequently Asked Questions | Bureau of Transportation Statistics https://www.bts.gov/faf/faqs (accessed Jun 12, 2021).
- (137) Explore Census Data https://data.census.gov/cedsci/ (accessed Jul 1, 2021).
- (138) Bus Registrations 2012

 https://www.fhwa.dot.gov/policyinformation/statistics/2012/mv10.cfm (accessed Jul 26, 2020).
- (139) FHWA. Truck Registrations 2012 https://www.fhwa.dot.gov/policyinformation/statistics/2012/mv9.cfm (accessed Jul 26, 2020).
- (140) U.S. Vehicle-Miles | Bureau of Transportation Statistics https://www.bts.gov/content/us-vehicle-miles (accessed Sep 29, 2020).
- (141) Argonne GREET Model https://greet.es.anl.gov/ (accessed Sep 30, 2020).

- (142) Tong, F.; Azevedo, I. M. L. What Are the Best Combinations of Fuel-Vehicle Technologies to Mitigate Climate Change and Air Pollution Effects across the United States? *Environmental Research Letters* 2020, 15 (7), 74046. https://doi.org/10.1088/1748-9326/ab8a85.
- (143) United States Government. Technical Support Document:-Technical Update of the Social Cost of Carbon for Regulatory Impact Analysis-Under Executive Order 12866; 2013.
- (144) CPI Inflation Calculator https://www.bls.gov/data/inflation_calculator.htm (accessed Jun 13, 2021).
- (145) APModel https://public.tepper.cmu.edu/nmuller/APModel.aspx (accessed Jul 2, 2021).
- (146) Association of American Railroads. *The Positive Environmental Effects of Increased*Freight by Rail Movements in America; 2020.
- (147) 2017 Commodity Flow Survey Datasets https://www.census.gov/data/datasets/2017/econ/cfs/historical-datasets.html (accessed Jul 7, 2021).
- (148) TIGER/Line Shapefiles https://www.census.gov/geographies/mapping-files/time-series/geo/tiger-line-file.html (accessed Jul 2, 2021).
- (149) Where Does EPA Obtain Default Vehicle Miles Traveled (VMT)? | MOVES and Other

 Mobile Source Emissions Models | US EPA https://www.epa.gov/moves/where-does-epaobtain-default-vehicle-miles-traveled-vmt (accessed Nov 15, 2020).
- (150) Mapping Inequality https://dsl.richmond.edu/panorama/redlining/#loc=13/40.491/-80.01&city=pittsburgh-pa (accessed Jul 2, 2021).

- (151) The Color of Law: A Forgotten History of How Our Government Segregated America |

 Economic Policy Institute https://www.epi.org/publication/the-color-of-law-a-forgotten-history-of-how-our-government-segregated-america/ (accessed Aug 17, 2021).
- (152) Tschofen, P.; Azevedo, I. L.; Muller, N. Z. Fine Particulate Matter Damages and Value Added in the US Economy. *Proceedings of the National Academy of Sciences* 2019, 116 (40), 19857–19862. https://doi.org/10.1073/pnas.1905030116.
- (153) FACT SHEET: President Biden Sets 2030 Greenhouse Gas Pollution Reduction Target
 Aimed at Creating Good-Paying Union Jobs and Securing U.S. Leadership on Clean
 Energy Technologies | The White House https://www.whitehouse.gov/briefingroom/statements-releases/2021/04/22/fact-sheet-president-biden-sets-2030-greenhousegas-pollution-reduction-target-aimed-at-creating-good-paying-union-jobs-and-securing-us-leadership-on-clean-energy-technologies/ (accessed Aug 14, 2021).
- (154) Biden and Senators Reach Broad Infrastructure Deal The New York Times https://www.nytimes.com/2021/06/24/us/politics/biden-bipartisan-infrastructure.html (accessed Jul 11, 2021).
- (155) The trucking industry is in the midst of upheaval—and hype | The Economist https://www.economist.com/business/2020/08/06/the-trucking-industry-is-in-the-midst-of-upheaval-and-hype (accessed Jul 11, 2021).
- (156) International Maritime Organization. GISIS: Status of Treaties https://gisis.imo.org/Public/ST/Treaties.aspx (accessed Nov 13, 2019).
- (157) NOx, SOx, & PM | World Shipping Council http://www.worldshipping.org/industry-issues/environment/air-emissions/nox-sox-pm (accessed Nov 13, 2019).
- (158) International Maritime Organization. Frequently Asked Questions; 2017.

- (159) China Dialogue Ocean. Should China Create an Emissions Control Area Through IMO? https://www.maritime-executive.com/editorials/should-china-create-an-emissions-control-area-through-imo (accessed Nov 14, 2019).
- (160) Special Areas Under MARPOL
 http://www.imo.org/en/OurWork/Environment/SpecialAreasUnderMARPOL/Pages/Defau
 lt.aspx (accessed Nov 13, 2019).
- (161) Chennai Population 2019 http://worldpopulationreview.com/world-cities/chennai-population/ (accessed Aug 22, 2019).
- (162) Poverty Reduction https://cochinmunicipalcorporation.kerala.gov.in/web/guest/poverty-reduction (accessed Aug 22, 2019).
- (163) The most densely populated cities the world: Mumbai, India tops list https://www.usatoday.com/story/news/world/2019/07/11/the-50-most-densely-populated-cities-in-the-world/39664259/ (accessed Nov 13, 2019).
- (164) Kolkata Population 2019 https://worldpopulationreview.com/world-cities/kolkata-population/ (accessed Mar 21, 2020).
- (165) Haldia subdivision Wikipedia https://en.wikipedia.org/wiki/Haldia_subdivision (accessed Apr 3, 2020).
- (166) Population of Mangalore 2019 https://indiapopulation2019.com/population-of-mangalore-2019.html (accessed Aug 22, 2019).
- (167) Population of Mormugao 2019 https://indiapopulation2019.com/population-of-mormugao-2019.html (accessed Aug 22, 2019).
- (168) Population of Thoothukkudi 2019 https://indiapopulation2019.com/population-of-thoothukkudi-2019.html (accessed Aug 22, 2019).

- (169) Population of Visakhapatnam 2019 https://indiapopulation2019.com/population-of-visakhapatnam-2019.html (accessed Aug 22, 2019).
- (170) Gandhidham Municipality https://indikosh.com/city/533587/gandhidham (accessed Nov 13, 2019).
- (171) Paradip Municipality https://indikosh.com/city/414810/paradip (accessed Nov 13, 2019).
- (172) Ports IBEF June 2019 https://www.ibef.org/download/Ports-June-2019.pdf (accessed Feb 17, 2021).
- (173) Government of India. Indian Shipping Statistics 2018; 2018.
- (174) Central Pollution Control Board, N. D. Air Quality Assessment, Emissions Inventory and Source Apportionment Studies: Mumbai; 2010.
- (175) MarineTraffic. MarineTraffic: Global Ship Tracking Intelligence | AIS Marine Traffic https://www.marinetraffic.com/en/ais/home/centerx:-12.0/centery:25.0/zoom:4 (accessed Sep 5, 2019).
- (176) Wikipedia. MarineTraffic https://en.wikipedia.org/wiki/MarineTraffic (accessed Sep 5, 2019).
- (177) MarineTraffic. Marine Traffic Quick Guide

 https://www.marinetraffic.com/files/AmmitecQuickGuide.pdf?utm_source=landingpage&

 utm_medium=referral&utm_content=Guide&utm_campaign=Ammitec-03-2015

 (accessed Sep 5, 2019).
- (178) MarineTraffic joins Equasis as provider of AIS data MarineTraffic Blog https://www.marinetraffic.com/blog/marinetraffic-provider-ais-data-equasis/ (accessed Nov 27, 2019).

- (179) MarineTraffic. New UNCTAD report stresses the importance of port call optimisation MarineTraffic Blog https://www.marinetraffic.com/blog/new-unctad-report-stresses-the-importance-of-port-call-optimisation-2/ (accessed Sep 5, 2019).
- (180) MarineTraffic. UNCTAD Archives MarineTraffic Blog

 https://www.marinetraffic.com/blog/tag/unctad/ (accessed Sep 5, 2019).
- (181) Custom Search JSON API | Google Developers https://developers.google.com/custom-search/v1/overview (accessed Feb 25, 2020).
- (182) ENVIRON International Corporation. *Cold Ironing Cost Effectiveness Study For the Port of Long Beach-Volume 1*; 2004.
- (183) Government of India. Chennai Port Trust Administration Report 2017-2018; 2018.
- (184) Government of India. Deendayal Port Trust Annual Administration Report 2017-2018; 2018.
- (185) Kamarajar Port Limited. Vessels Handled http://www.ennoreport.gov.in/content/innerpage/vessels-handled.php (accessed Jul 4, 2020).
- (186) Government of India. Kolkata Port Trust Annual Administration Report 2017-2018; 2018.
- (187) Government of India. Mumbai Port Trust Annual Administration Report 2017-2018; 2018.
- (188) Government of India. New Mangalore Port Trust Annual Administration Report 2017-2018 http://newmangaloreport.gov.in:8080/docs/Adm Report 2017-18.pdf (accessed Jul 4, 2020).
- (189) Government of India. Paradip Port Trust Annual Administration Report 2017-2018; 2018.
- (190) Government of India. V.O. Chidambaranar Port Trust Annual Administration Report 2017-2018; 2018.

- (191) Government of India. Visakhapatnam Port Trust Annual Administration Report 2017-2018; 2018.
- (192) James Corbett http://www.ceoe.udel.edu/our-people/profiles/jcorbett (accessed Nov 27, 2019).
- (193) Professor Anthony F Molland | Engineering | University of Southampton https://www.southampton.ac.uk/engineering/about/staff/afm.page (accessed Nov 28, 2019).
- (194) Lou Browning Technical Director | ICF https://www.icf.com/company/about/our-people/b/browning-lou (accessed Nov 28, 2019).
- (195) Starcrest Consulting Group. Port of Long Beach 2017 Air Emissions Inventory; 2018.
- (196) Abhijit Aul Regulatory Affairs Lead Lloyd's Register | LinkedIn https://uk.linkedin.com/in/abhijit-aul-56624438 (accessed Nov 28, 2019).
- (197) Brett Goldsworthy | Gas Energy Australia http://gasenergyaustralia.asn.au/brett-goldsworthy/ (accessed Nov 28, 2019).
- (198) Laurie Goldsworthy | LinkedIn https://www.linkedin.com/in/laurie-goldsworthy-9a188948/?originalSubdomain=au (accessed Nov 28, 2019).
- (199) Cliatt, O.; Harbor Line Greg Peters, P.; Harbor Line Joe Gregorio, P.; Chris Morales, P.; Grant Westmoreland, P.; Tugboat Service Olenka Palomo, P.; Recycling Emile Shiff, S.; Brothers Bob Kelly, S.; Melissa Rubio, S.; Jeremy Anthony, S. *Port of Long Beach 2017 Air Emissions Inventory*; 2018.
- (200) Sahu, S. K.; Ohara, T.; Beig, G. The Role of Coal Technology in Redefining India's Climate Change Agents and Other Pollutants. *Environmental Research Letters* **2017**. https://doi.org/10.1088/1748-9326/aa814a.

- (201) Sehgal, A.; Tongia, R. Coal Requirement in 2020: A Bottom-up Analysis; 2016.
- (202) How much do ultra-supercritical coal plants reduce air pollution?

 https://energypost.eu/how-much-do-ultra-supercritical-coal-plants-really-reduce-air-pollution/ (accessed Feb 20, 2021).
- (203) Ministry of Power Government of India. Initiatives to Improve the Efficiency of Coal Based Power Plants https://pib.gov.in/newsite/PrintRelease.aspx?relid=116893 (accessed Feb 5, 2021).
- (204) 70 per cent of coal-fired power plants may not meet emission standards by 2022, says

 CSE | India News Times of India https://timesofindia.indiatimes.com/india/70-per-centof-coal-fired-power-plants-may-not-meet-emission-standards-by-2022-sayscse/articleshow/75874044.cms (accessed Feb 20, 2021).
- (205) Government of India. Growth of Electricity Sector in India from 1947-2020; 2020.
- (206) Government of Goa. Goa Electricity Department https://www.goaelectricity.gov.in/ (accessed Sep 5, 2019).
- (207) Oberschelp, C.; Pfister, S.; Raptis, C.; Hellweg, S. Global Coal Power Plant Airborne Emission Dataset. *Mendeley Data* **2019**, *1*. https://doi.org/10.17632/DM3RJB9YMC.1.
- (208) Tamil Nadu Electricity Regulatory Commission. *Determination of Tariff for Generation* and Distribution (Effective from 08-11-2017); 2017.
- (209) Kerala State Electricity Regulatory Commission. *Order No. 1007/F&T/2016/KSERC Dated 17th April*, 2017; 2017.
- (210) Gujarat Electricity Regulatory Commission. *Tariff Order for Uttar Gujarat Vij Company Limited (Case No. 1759)*; 2019.
- (211) Maharashtra Electricity Regulatory Commission. Case No. 48; 2016.

- (212) West Bengal State Electricity Distribution Company Ltd. Gist of the Tariff Order Dated 28/10/2016 for the Year 2016-17 Issued by the WB Electricity Regulatory Commission; 2016.
- (213) Joint Electricity Regulatory Commission for the Union Territories. *Tariff Order for Lakshadweep Electricity Department*; 2019.
- (214) Karnataka Electricity Regulatory Commission. *Tariff Order 2019: Determination of Retail Supply Tariff for 2020*; 2019.
- (215) Odisha Electricity Regulatory Commission. *Annual Revenue Requirement and Retail Supply Tariff for the FY 2019-20*; 2019.
- (216) Andhra Pradesh Electricity Regulatory Commission. Tariff Order http://aperc.gov.in/admin/upload/TOFY2019-20.pdf.
- (217) Kochi Population 2019 https://worldpopulationreview.com/world-cities/kochi-population/ (accessed Mar 21, 2020).
- (218) Gandhidham Population 2019 https://worldpopulationreview.com/world-cities/gandhidham-population/ (accessed Mar 21, 2020).
- (219) Haldia Population 2019 https://worldpopulationreview.com/countries/india-population/cities/ (accessed Mar 21, 2020).
- (220) Mumbai Population 2019 http://worldpopulationreview.com/world-cities/mumbai-population/ (accessed Aug 22, 2019).
- (221) Paradip Municipality City Population Census 2011-2020 Odisha https://www.census2011.co.in/data/town/801839-paradip-orissa.html (accessed Mar 21, 2020).

- (222) Global SO2 pollution map Google My Maps

 https://www.google.com/maps/d/u/0/viewer?mid=1qkTfy6jxARFtkU5MHaJv_ZA7T_pJDmv&ll=19.745931803587354%2C78.93892487833773
 &z=5 (accessed Mar 22, 2020).
- (223) Mapped: The world's coal power plants in 2019 https://www.carbonbrief.org/mapped-worlds-coal-power-plants (accessed Oct 27, 2019).
- (224) Center for International Earth Science Information Network (CIESIN) Columbia University. Gridded Population of the World, Version 4 (GPWv4): Population Density, Revision 11. Palisades, NY:NASA Socioeconomic Data and Applications Center (SEDAC) https://doi.org/10.7927/H49C6VHW (accessed Oct 27, 2019).
- (225) City Kochi, India http://www.urbanemissions.info/india-apna/kochi-india/ (accessed Mar 27, 2020).
- (226) City Chennai, India http://www.urbanemissions.info/india-apna/chennai-india/ (accessed Oct 27, 2019).
- (227) Kandla Port Trust. Integrated Environment Impact Assessment Report; 2013.
- (228) Iowa State University. Iowa Environmental Mesonet

 http://mesonet.agron.iastate.edu/sites/locate.php?network=IN__ASOS (accessed Mar 28, 2020).
- (229) Meteoblue. Climate Haldia

 https://www.meteoblue.com/en/weather/historyclimate/climatemodelled/haldia_india_134

 4377 (accessed Mar 28, 2020).

- (230) Meteoblue. Climate Paradip
 https://www.meteoblue.com/en/weather/historyclimate/climatemodelled/paradip_india_12
 60393 (accessed Mar 28, 2020).
- (231) IMO 2020 cutting sulphur oxide emissions
 https://www.imo.org/en/MediaCentre/HotTopics/Pages/Sulphur-2020.aspx (accessed Feb 4, 2021).
- (232) Solar Panel Price in India https://www.bijlibachao.com/solar/solar-panel-cell-cost-manufacturer-price-list-in-india.html (accessed Mar 9, 2020).
- (233) What would be the annual maintenance cost for a solar PV system?

 https://www.itsmysun.com/faqs/what-would-be-the-annual-maintenance-cost-for-a-solar-pv-system/ (accessed Mar 12, 2020).
- (234) Bhoir, A.; Das, S. Wary of External Risks to Projects, Banks May Hike Infrastructure Funding Rates. *The Economic Times*.
- (235) PVWatts Calculator https://pvwatts.nrel.gov/ (accessed Mar 11, 2020).
- (236) India Witnesses Sharp Fall In Solar Tariffs In 750 Megawatt Auction | CleanTechnica https://cleantechnica.com/2019/03/04/india-witnesses-sharp-fall-in-solar-tariffs-in-750-megawatt-auction/ (accessed Mar 31, 2020).
- (237) Central Electricity Regulatory Commission. *Indian Electricity Grid Code*; 2010.
- (238) Davis, S. C.; Boundy, R. G. Transportation Energy Data Book: Edition 39; 2021.
- (239) Source Classification Codes https://sor-scc-api.epa.gov/sccwebservices/sccsearch/ (accessed Jun 5, 2021).

- (240) Tong, F.; Jenn, A.; Wolfson, D.; Scown, C. D.; Auffhammer, M. Health and Climate Impacts from Long-Haul Truck Electrification. *Environmental Science & Technology* **2021**, *55* (13), 8514–8523. https://doi.org/10.1021/ACS.EST.1C01273.
- (241) AFLEET Tool https://greet.es.anl.gov/afleet_tool (accessed Aug 18, 2021).
- (242) Epa, U.; of Transportation, O.; Quality, A.; Department of Transportation, U.; Highway Traffic Safety Administration, N. Final Rulemaking to Establish Greenhouse Gas Emissions Standards and Fuel Efficiency Standards for Medium- and Heavy-Duty Engines and Vehicles:Regulatory Impact Analysis (EPA-420-R-11-901, August 2011).
- (243) US EPA. Technical Highlights Emission Factors for Locomotives

 https://nepis.epa.gov/Exe/ZyNET.exe/P100500B.TXT?ZyActionD=ZyDocument&Client

 =EPA&Index=2006+Thru+2010&Docs=&Query=&Time=&EndTime=&SearchMethod=

 1&TocRestrict=n&Toc=&TocEntry=&QField=&QFieldYear=&QFieldMonth=&QFieldD

 ay=&IntQFieldOp=0&ExtQFieldOp=0&XmlQuery=&File=D%3A%5Czyfiles%5CIndex

 %20Data%5C06thru10%5CTxt%5C00000010%5CP100500B.txt&User=ANONYMOUS

 &Password=anonymous&SortMethod=h%7C
 &MaximumDocuments=1&FuzzyDegree=0&ImageQuality=r75g8/r75g8/x150y150g16/i

 425&Display=hpfr&DefSeekPage=x&SearchBack=ZyActionL&Back=ZyActionS&Back

 Desc=Results%20page&MaximumPages=1&ZyEntry=1&SeekPage=x&ZyPURL#

 (accessed May 31, 2021).
- (244) U.S. Gross Domestic Product (GDP) Attributed to Transportation Functions | Bureau of Transportation Statistics https://www.bts.gov/content/us-gross-domestic-product-gdp-attributed-transportation-functions-billions-current-dollars (accessed Sep 28, 2020).

- (245) Needell, Z. A.; McNerney, J.; Chang, M. T.; Trancik, J. E. Potential for Widespread Electrification of Personal Vehicle Travel in the United States. *Nature Energy* **2016**. https://doi.org/10.1038/nenergy.2016.112.
- (246) How Drivers and Autonomous Trucks Could Work Together to Move Freight | Transport Topics https://www.ttnews.com/articles/how-drivers-and-autonomous-trucks-could-work-together-move-freight (accessed Sep 26, 2020).
- (247) Sripad, S.; Viswanathan, V. Performance Metrics Required of Next-Generation Batteries to Make a Practical Electric Semi Truck. ACS Energy Letters. 2017. https://doi.org/10.1021/acsenergylett.7b00432.
- (248) Viscelli, S. Will Robotic Trucks Be "Sweatshops on Wheels"? *Issues in Science and Technology* **2020**, 79–88.